Reviewer #02

In this paper, the authors analyzed aerosol optical and physical properties derived from CARSNET ground-based measurements for 7 locations in the RYD region. Ground based observations are definitely welcomed in the community. However, this paper needs major revisions. Firstly, also suggested by the first reviewer, this is a poorly written paper. Also, there are several major technical issues with the paper. The first reviewer has done a great job highlighting issues and I have added several more comments below.

Response: Thanks for the reviewer's important and constructive comments. The manuscript has been revised and re-organized carefully to make the paper more concise and focused. The major overhaul has been done in some sections which need to be rewritten and reorganized according to the helpful suggestion.

1. Aerosol radiative forcing values are computed using a radiative transfer model (Global Atmospheric ModEl, GAME). However, no details are provided on their radiative transfer modeling efforts. For example, how do they define surface (broadband) characteristics? What are the required aerosol properties such as vertical distributions? The CARSNET observations are in discrete channels, how the authors perform a narrowband to broad band conversion? A detailed uncertainty analysis is also needed but is lacking.

Response: Thanks for the important and constructive suggestions. The detail on the radiative transfer modeling has been added in sention 2 line 188-211 as "*The ARF (aerosol radiative forcing) data were calculated by the radiative transfer module used by the AERONET inversion (Dubovik et al., 2006) under the assumption of cloud-free consideration. In this code, the aerosol vertical properties have been considered into a homogeneous atmosphere layers because of the weak dependent of ground radiances on the whole atmospheric column with minor uncertainties (Dubovik et al., 2000). The fluxes from 0.20 to 4.0μm were calculated according to the radiative transfer model GAME (Global Atmospheric ModEl) (Dubuisson et al., 1996, 2006; Roger et al., 2006). While the broadband radiation was calculated based on the aerosol optical depth, single scattering albedo and asymmetry factor based on those properties at four distinct wavelengths (440, 670, 870, 1020) which were linearly interpolated and extrapolated from the retrieval of the sun/sky-radiometer measurements. The*

uncertainties have been found to about 30% including the influence of spectral and solar zenith angle in the aerosol radiative effect (Myhre et al., 2003; Zhou et al., 2005). The size distribution, complex refractive index, and spherical particles fraction has been retrieved from the almucantar plane in the measurements. The SA (surface albedo) is obtained from the MODIS albedo product (MCD43C3) with the interpolation value of 440, 670, 870, and 1020 nm. The water vapor at 940 nm has been retrieved by the sun photometer. The ozone content was obtained from NASA Total Ozone Mapping Spectrometer measurements from 1978 to 2004. And other atmospheric gaseous data came from the US standard 1976 atmosphere model. In this study, the two parameters of ARF at the surface (ARF-BOA) and at the top of the atmosphere (ARF-TOA) have been calculated to describe the aerosol direct radiation effect to account for the changes of the solar radiation by calculating the difference energy between the aerosols presentation and absentation.".

2. The authors compared CARSNET measurements with a merged MODIS Deep Blue and Dark Target product. Given that the MODIS Deep Blue and Dark Target methods are fundamentally different in their retrieval processes, I would recommend the authors evaluating each product separately.

Response: Thanks for the helpful suggestions. According to both reviewers' comments, the Aqua product has been added to validate the MODIS AOD at 550nm according to the suggestions in section 3.2. The MODIS C6 aerosol optical thickness products refined by Levy et al. (2013) were evaluated against our ground-based observations by the Deep Blue and Dark Target methods at 3km and 10km separately in section 3.2 as follows in line 400-476:

The product of MODIS/Terra and MODIS/Aqua with Deep Blue (at 10km) and Dark Target (at 3km and 10km) methods has been evaluated against by ground-based observations separately in Fig. 6-8. We use the better estimated data of Quality flag = 3 and Quality flag=2, 3 for DT and TB methods, respectively. The systematic performance of the MODIS/Terra C6 retrieval AOD values was generally more stable in the YRD region compared with the MODIS/Aqua product with the two Deep Blue and Dark Target methods, which most of the plots scattered around the 1:1 regression line.

The correlation coefficients (R) between the MODIS/Aqua and MODIS/Terra between by the Dark Target methods at 3km and sun photometer AOD (550 nm) values were about 0.84 to 0.92 and 0.85 to 0.94 in the YRD region, respectively. The linear regression fitting performed better at the suburban sites of LinAn and Jiande according to the product of MODIS/Terra by the Dark Target methods at 3km. The fitting curve was almost consistent with the 1:1 reference line, which suggests that the aerosol properties were well defined for the MODIS C6 products. A large part of the MODIS retrieval AOD value was outside the expected error envelope of ± (0.05 + 20%$\tau_{CARSNET}$), especially for AOD values<0.80 in Hangzhou and Xiaoshan. This indicates that the MODIS retrieval algorithm could still be improved, especially in urban areas. The MODIS retrieval AOD performed better at the other five sites (Fuyang, LinAn, Tonglu, Jiande and ChunAn) in the YRD; most of the retrieved AOD values for these sites fell within the expected error envelope. The MODIS/Aqua retrievals with Dark Target methods at 3km were underestimated while the MODIS/Terra retrievals with Dark Target methods at 3km were overestimated except Hangzhou, Tonglu and Jiande. The small deviation at the suburban sites suggested that the MODIS C6 retrieval using the DT method was suitable for capturing the optical properties of aerosols in suburban areas with dense vegetation coverage of the YRD. However, this method may have larger difference in the urban areas with less vegetation such as Hangzhou. The correlation coefficients (R) of the MODIS/Aqua and MODIS/Terra between sun photometer AOD (550 nm) values by the Deep Blue and Dark Target methods at 10km were about 0.81 to 0.90, 0.85 to 0.90, 0.69 to 0.91 and 0.85 to 0.93 in the YRD region, respectively. The MODIS/Aqua and MODIS/Terra retrievals with Deep Blue and Dark Target methods at 10km were underestimated except Hangzhou and Xiaoshan. In particular, the biases of the correlation coefficients (R) occurred in LinAn and Jiande has decreased from 0.94 and 0.90 to 0.87 and 0.88. The validation results indicate a good MODIS/Terra matching with better fitting correlation at 3km rather than 10km products.

The AOD overestimation retrieved using Dark Target (DT) and Deep Blue (DB) methods are more influenced by the SSA and the phase function of aerosol in eastern China with AOD >0.4 (Tao et al. 2015). Therefore, the detailed ground-based observation in this work is more helpful to the calibration of MODIS retrievals in eastern China.

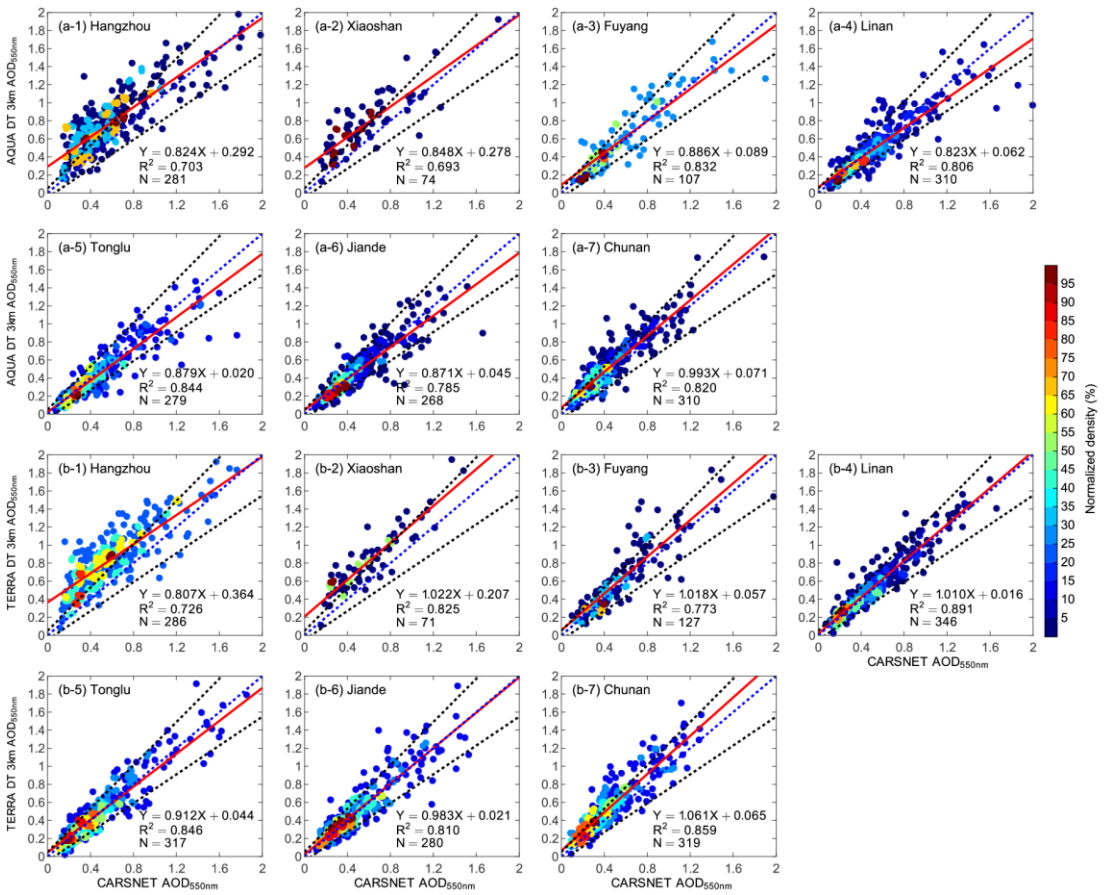

Fig.6. Comparison of MODIS/Aqua Dark Target (DT) AOD at 550 nm with the CARSNET AOD at 3km in (a-1) Hangzhou, (a-2) Xiaoshan, (a-3) Fuyang, (a-4) LinAn, (a-5) Tonglu, (a-6) Jiande, (a-7) ChunAn and MODIS/Terra DT AOD at 550 nm with the CARSNET AOD at 3km in (b-1) Hangzhou, (b-2) Xiaoshan, (b-3) Fuyang, (b-4) LinAn, (b-5) Tonglu, (b-6) Jiande, (b-7) ChunAn. The red solid line represents the linear regression. The two black dotted lines represent the expected errors in the MODIS retrievals.

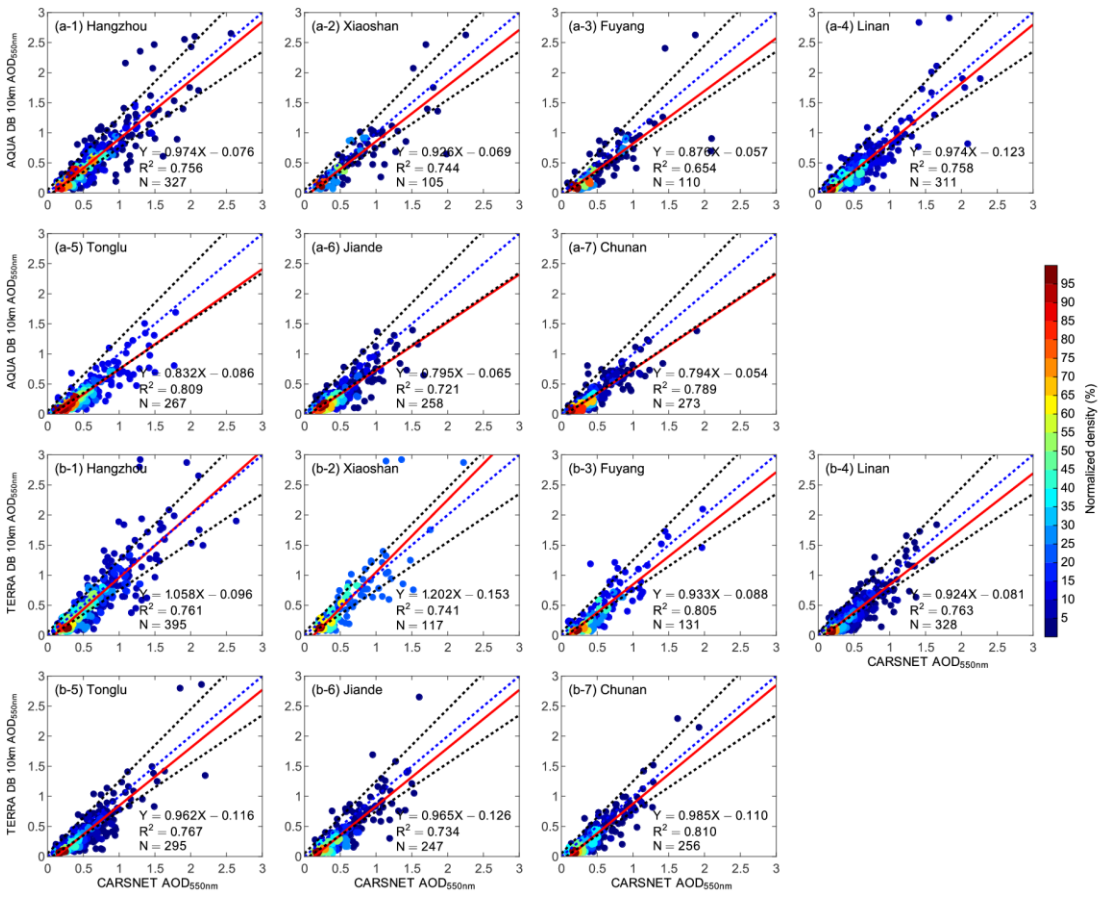

Fig.7. Comparison of MODIS/Aqua Deep Blue (DB) AOD at 550 nm with the CARSNET AOD at 10km in (a-1) Hangzhou, (a-2) Xiaoshan, (a-3) Fuyang, (a-4) LinAn, (a-5) Tonglu, (a-6) Jiande, (a-7) ChunAn and MODIS/Terra AOD DB at 550 nm with the CARSNET AOD at 10km in (b-1) Hangzhou, (b-2) Xiaoshan, (b-3) Fuyang, (b-4) LinAn, (b-5) Tonglu, (b-6) Jiande, (b-7) ChunAn. The red solid line represents the linear regression. The two black dotted lines represent the expected errors in the MODIS retrievals.

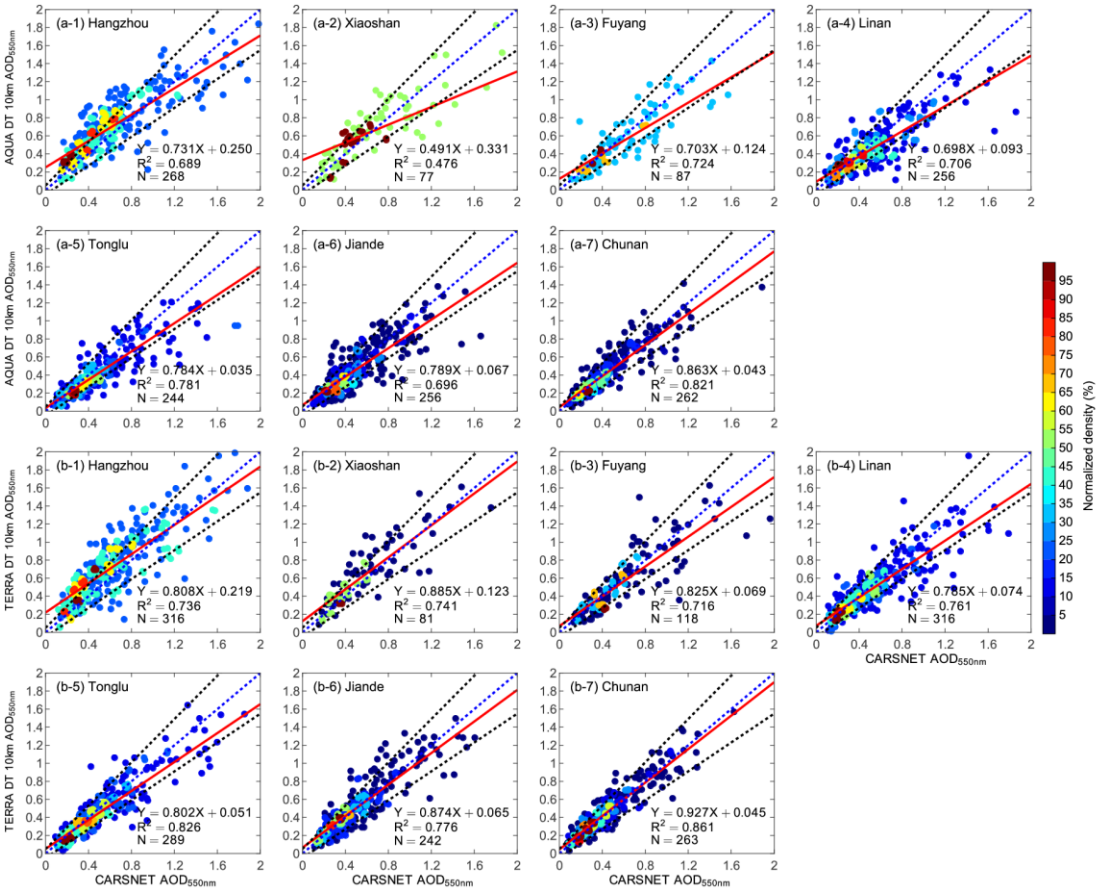

Fig.8. Comparison of MODIS/Aqua AOD DT at 550 nm with the CARSNET AOD at 10km in (a-1) Hangzhou, (a-2) Xiaoshan, (a-3) Fuyang, (a-4) LinAn, (a-5) Tonglu, (a-6) Jiande, (a-7) ChunAn and MODIS/Terra DT AOD at 550 nm with the CARSNET AOD at 10km in (b-1) Hangzhou, (b-2) Xiaoshan, (b-3) Fuyang, (b-4) LinAn, (b-5) Tonglu, (b-6) Jiande, (b-7) ChunAn. The red solid line represents the linear regression. The two black dotted lines represent the expected errors in the MODIS retrievals.

3. Also, in lines 248-249, it states “The EAE was lower in March (~1.16±0.24) and April (~1.13±0.22), which reflects the effect of mineral dust aerosols (Gong et al., 2003).” This seems to contradict to a later conclusion (Table 2) that the dust aerosol presence is insignificant for the region. This actually brings up an issue, as the authors try to compare mean properties of the 7 sites and try to provide explanations for the differences. Some explanations are weak with little or no supporting evidence. In addition, the differences in some

of the mean properties are actually way smaller than variations (numbers after ± sign) of the data, and thus some statistical methods are needed to back up the authors' comments with consideration of data spreads.

Response: Both reviewers mentioned this question. Though the dust aerosol presence is not insignificant for this region but the particle size was larger in spring with small EAE in March (~1.16±0.24) and April (~1.13±0.22). Some dusts cases can be observed in YRD region that transported from north/northwest China during 2012-2015 reflect the effect of mineral dust aerosols as follow cases:

As can be seen in the figure below, the PM10 mass concentration is higher in March to May than the value in February and June. This pattern clearly indicates the influence of dust in spring of Hangzhou. The Eastern China has been affected by a wide range of dust event in North China. These dust events across the northwest to the northeast area of China, then continue keep going south and east China. The higher PM10 mass concentration is obviously affected by the dust come from the northwest.

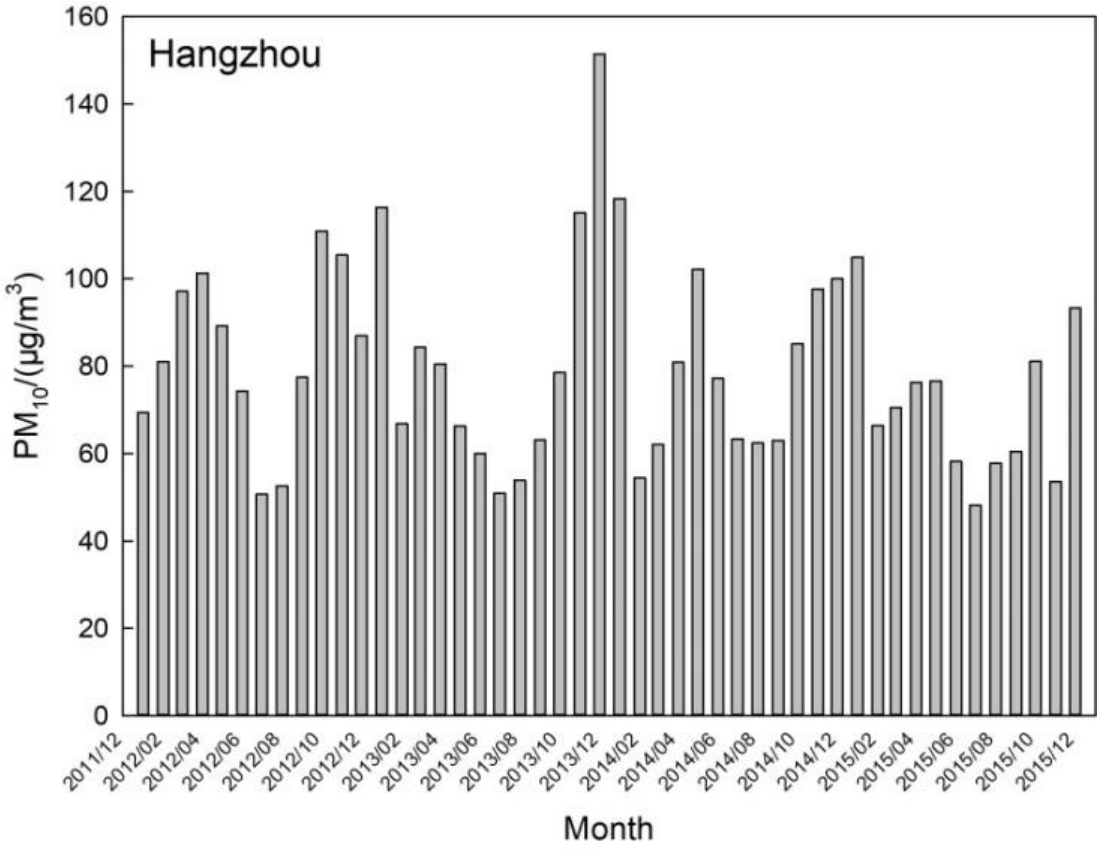

For example, there is a dust transportation event occurred in Hangzhou on 05-09 March, 2013. A series of transported aerosol masses over Hangzhou are monitored by MPL shown through time-height cross section of extinction coefficient at 527nm. Referring to CALIPSO L2 retrieval results of vertical feature mask and aerosol subtypes illustrated in Fig. 9(b), the northwestern upwind areas of Hangzhou exists an aerosol layer mixed of “dust” and “polluted dust” about 3km thick from the surface in 5 March 2015, since when a thin external layer is detected concurrently. Therefore, the higher AOD in spring descripted in this study is significantly affected by dust process.

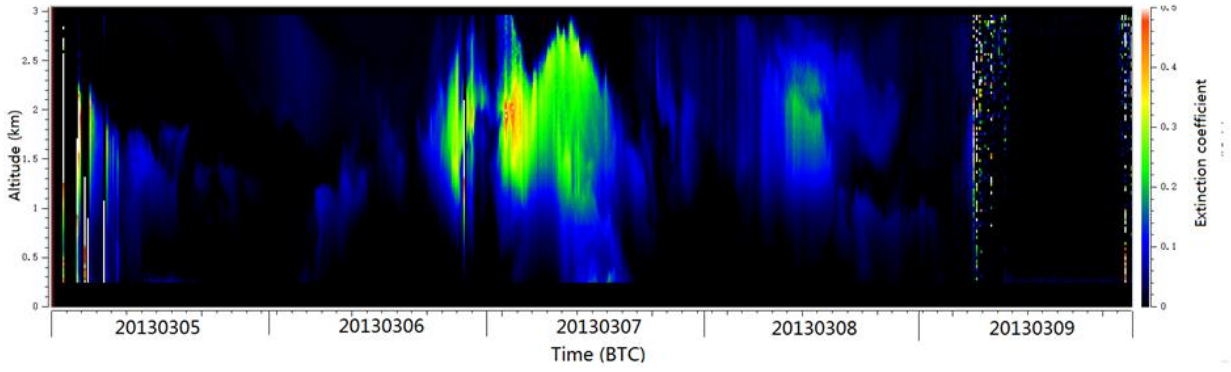

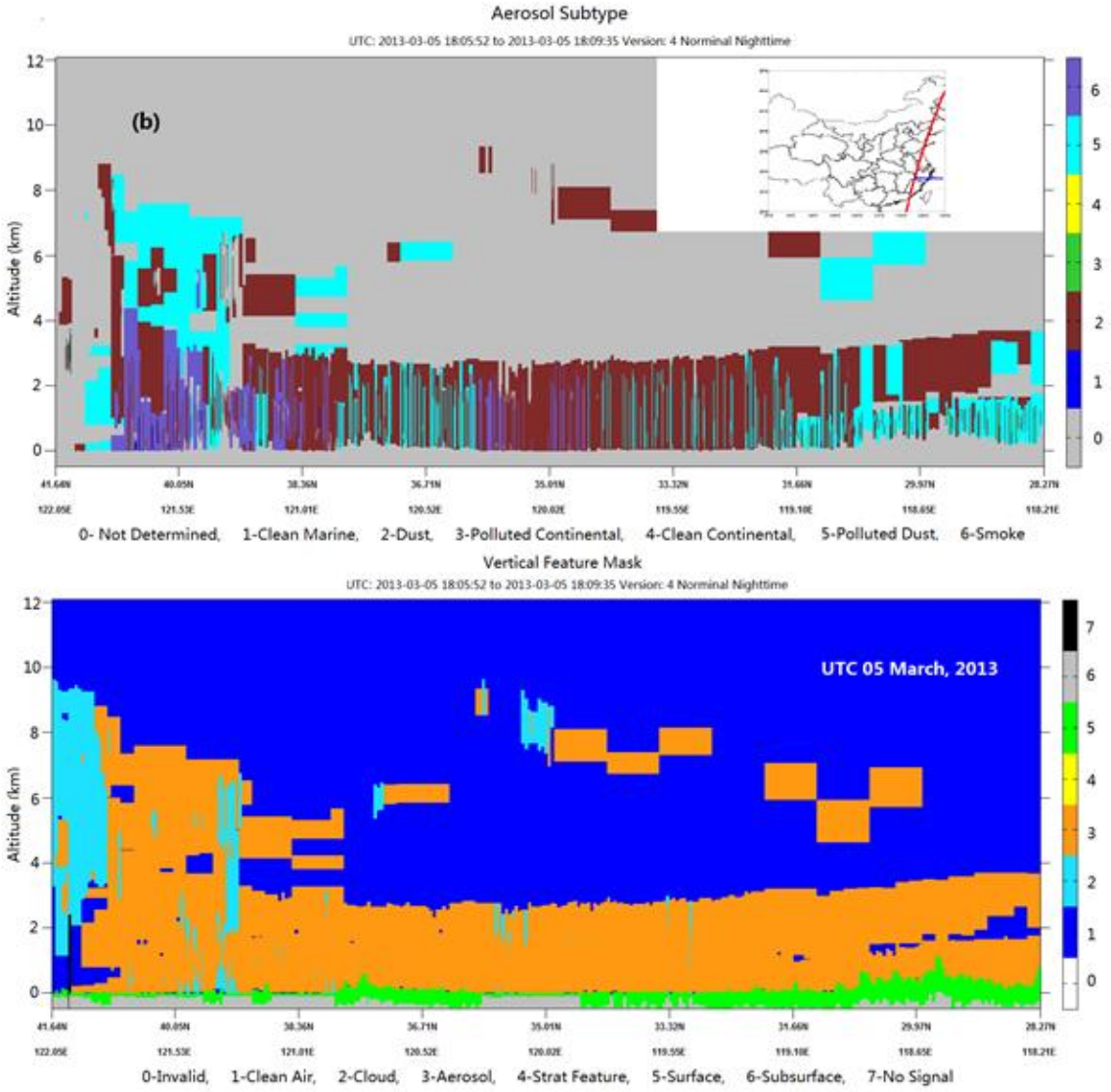

4. Line 108-109, I am not sure what the authors mean by “Levy et al. (2013) refined the MODIS Collection 6 (C6) aerosol retrieval process to provide better AOD retrievals”. What is “better AOD retrieval”? May be the authors referring to more accurate AOD retrievals?

Response: Thank for the reviewer’s suggestion. The “Levy et al. (2013) refined the MODIS Collection 6 (C6) aerosol retrieval process to provide better AOD retrievals” has been modified as “Levy et al. (2013) refined the MODIS Collection 6 (C6) aerosol retrieval process to provide more accurate AOD retrievals”. in the revised manuscript on line 124-125.

5. Line 135 “Jiande, Xiaoshan Tonglu and Xiaoshan” should be “Jiande, Xiaoshan, Tonglu and

Xiaoshan"?

Response: The "Jiande, Xiaoshan Tonglu and Xiaoshan" in line 135 has been changed as "Jiande, Xiaoshan and Tonglu" in revised manuscript on line150.

6. Lines 143-144, "Instantaneous direct data for the AOD were selected at least ten times each day at temporal resolution of about three minutes" Define "direct data". Also, what are the section criteria? Details need to be provided.

Response: Thank for the useful suggestion. The direct data means AOD calculated by the direct solar measurements at each wavelength. This selection is to increase the representability of the aerosol optical characteristics. This criterion is also used in previous studies such as Che et al. (2015). The sentence is line 143-144 has been modified as "*Instantaneous AOD measurements more than ten times at each day were selected for daily average calculation and statistical analysis to increase the representability of the aerosol optical characteristics (Che et al., 2015).*" in revised manuscript in line 158-162.

7. Line 156, define EAOD.

Response: According to the reviewer's suggestion, the EAOD has been defined in line 183-184 as "*The EAOD in this study has been defined as extinction aerosol optical depth calculated by the direct solar measurements at the wavelengths of 440, 500,670, 870, 1020nm*".

8. Lines 169-171, "The AOD data from Terra-MODIS were validated by matching the CARSNET AODs within 30 minutes of the MODIS overpass within the 3×3 pixels surrounding the CARSNET site." Are both CARSNET and MODIS data averaged for the process? Need some details.

Response: Yes. Both the CARSNET and MODIS data are averaged in the process. The details has been descript as "*The AOD averaged data from Terra-MODIS and Aqua-MODIS were validated by matching the averaged CARSNET AODs within 30 minutes of the MODIS overpass within the 5×5 pixels surrounding the CARSNET site (Tao et al., 2015)*." in line 220-222.

9. Lines 180-182, “The AOD at the urban site of Hangzhou was the highest of all the study sites as a result of high local anthropogenic activity in this urban area compared with the other suburban and rural sites.” Results do not support this comment, as the three sites, including Handzou, Xiaoshan and Fuyang, have mean AOD of 0.76. Also, as I mentioned before, variations in data are larger than differences in mean values. Some statistical analyses are needed to back up their conclusions.

Response: The authors agree with the reviewer’s opinion. To decrease the misunderstanding, This sentence has been rewritten as “*The AOD440nm at Hangzhou Xiaoshan and Fuyang was higher as a result of the more industrial activity and high resident density in the eastern part metropolis region resulting in larger aerosol emissions compared with the other suburban and rural sites.*” in line 260-270.

10. Lines 189-197, the authors compared AOD values from the 7 sites to other regions in China as reported from other papers. However, the authors should also take the temporal variation into consideration (e.g., mean values change from year to year, right?).

Response: The reviewer’s suggestions are right. The mean values could change from year to year. In this paper, we did not take the temporal variation into consideration because of the different observation periods. So we just compared the multi-year averaged AOD values from the 7 sites in this study to other regions.

11. Line 241, what is extinction Angström exponent?

Response: Thank for the suggestion. The extinction Angström exponent has been defined in 309-310 as “*As Fig.3 shown, the monthly average value of the extinction Angström exponent (EAE, -dln[EAOD(λ)]/dln(λ)).*”

12. Lines 311-314, “The characteristics of the SSA at these seven sites gradually increased from the east coast (0.91±0.06 at Hangzhou) inland toward the west (0.94±0.03 at ChunAn). These results indicate the emissions caused by human activity affect the absorption of aerosols in urban areas.” Again, the authors need to consider other possibilities and worry

about data varibility. How about meteorological conditions? What about hygroscopic growth? Again, the authors need to back up their comments with evidence.

Response: Thanks for the important suggestions. The sites in this study are in the city scale about 10 km apart from each other over adjacent urban, suburban and rural areas in the YRD region. Therefore the same weather system can be regarded as weak effect of meteorological elements. The discussion has been added in line 512-518 as "*The seven observation sites are usually controlled by the same weather system that indicates a weak effect of meteorological elements in each site to the change of aerosol optical characteristics. These results indicate the emissions caused by human activity affect the absorption of aerosols in urban areas. The SSA was higher at LinAn and ChunAn than at the other sites, which may reflect the presence of a larger number of scattering aerosols (e.g. particles from urban/industrial activities) over the clear rural sites than over urban or suburban sites.*" in section 3.3. Furthermore, we added the discussion of hygroscopic growth in line 529-531as "*The increased level of scattering aerosols with higher SSA in June may be influenced by the hygroscopic growth in favor of the interaction between aerosols from different emissions sources (Xia et al., 2007)*."

13. Figure 10, what do the colors represent?

Response: Figure 10 has been changed as Figure 14 in the revised manuscript. The blue dot represent the sphericity fraction of particles and the red dot represent the AAE (α_{abs}) values (AAE = −dln[AAOD(λ)]/dln(λ)).

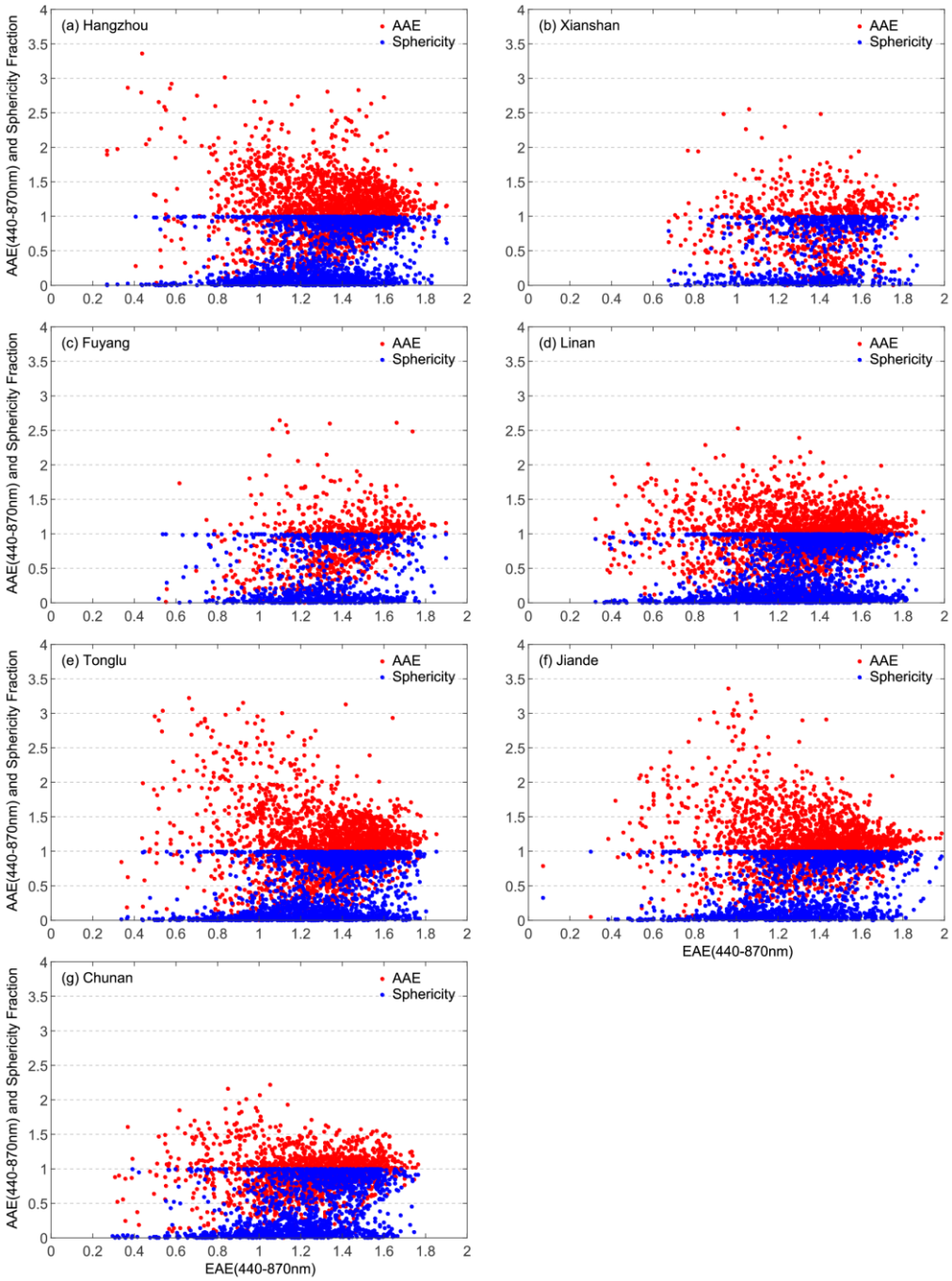

Fig.14.The AAE (red dot) and the sphericity fraction (blue dot) as a function of the EAE at 440–870 nm over (a) Hangzhou, (b) Xiaoshan, (c) Fuyang, (d), LinAn, (e) Tonglu, (f) Jiande and (g) ChunAn.

Aerosol optical properties and ~~instantaneous~~ radiative forcing based on synchronous measurements of China Aerosol Remote Sensing Network (CARSNET) over eastern China~~hightemporospatial spatiotemporal resolution of China Aerosol Remote Sensing Network (CARSNET) ground-based measurements over eastern China~~

Huizheng Che[1*], Bing Qi[2], Hujia Zhao[1], Xiangao Xia[3,4], Philippe Goloub[5], Oleg Dubovik[5], Victor Estelles[6], Emilio Cuevas-Agulló[7], Luc Blarel[3], Yunfei Wu[8], Jun Zhu[9], Rongguang Du[2], Yaqiang WANG[1], Hong Wang[1], Ke Gui[1], Jie Yu[1], Yu Zheng[9], Tianze Sun[1], Quanliang Chen[10], Guangyu Shi[11], Xiaoye Zhang[1*]

1 State Key Laboratory of Severe Weather (LASW) and Institute of Atmospheric Composition, Chinese Academy of Meteorological Sciences, CMA, Beijing, 100081, China

2 Hangzhou Meteorological Bureau, Hangzhou, 310051, China

3 Laboratory for Middle Atmosphere and Global Environment Observation (LAGEO), Institute of Atmospheric Physics, Chinese Academy of Sciences, Beijing, 100029, China

4 School of Geoscience University of Chinese Academy of Science, Beijing, 100049, China

5 Laboratoire d'Optique Amosphérique, Université des Sciences et Technologies de Lille, 59655, Villeneuve d'Ascq, France

6 Dept. Fisica de la Terra i Termodinamica, Universitat de Valencia, C/ Dr. Moliner 50, 46100 Burjassot, Spain

7 Centro de Investigación Atmosférica de Izaña, AEMET, 38001 Santa Cruz de Tenerife , Spain

8 Key Laboratory of Regional Climate-Environment for Temperate East Asia, Institute of Atmospheric Physics, Chinese Academy of Sciences, Beijing 100029, China

9 Collaborative Innovation Center on Forecast and Evaluation of Meteorological Disasters, Nanjing University of Information Science & Technology, Nanjing 210044, China

10 Plateau Atmospheric and Environment Key Laboratory of Sichuan Province, College of Atmospheric Sciences, Chengdu University of Information Technology, Chengdu, 610225, China

11 State Key Laboratory of Numerical Modeling for Atmospheric Sciences and Geophysical Fluid Dynamics (LASG), Institute of Atmospheric Physics, Chinese Academy of Sciences, Beijing, 100029, China

Corresponding author: chehz@camscma.cn & xiaoye@camscma.cn

Abstract

Variations in the optical properties of aerosols and their radiative forcing were investigated based on long-term synchronous observations made at three-minute intervals from 2011 to 2015 over seven adjacent CARSNET (China Aerosol Remote Sensing NETwork) urban (Hangzhou), suburban (Xiaoshan, Fuyang, LinAn, Tonglu, Jiande) and rural (ChunAn) stations in the Yangtze River Delta region, eastern China. The fine-mode radii in the Yangtze River Delta region were ~0.2–0.3 μm with a volume fraction of 0.10–0.12 μm^3 and the coarse-mode radii were ~2.0 μm with a volume fraction close to 0.07 μm^3.~~The radii of fine volume fraction in the Yangtze River Delta region were ~0.2–0.3 μm with a volume of 0.10–0.12 μm^3 and the radii of coarse volume fraction were ~2.0 μm with a volume close to 0.07 μm^3.~~ The fine-mode aerosols were obviously larger in June and September than in other months at almost the sites. The aerosol optical depth (AOD at 440nm) varied from 0.68 to 0.76, with two peaks in June and September, and decreased from the eastern coast to western inland areas. The ~~ratio of the AODof fine-mode particles~~fine mode fraction to the total AOD was >0.90 and the extinction Angström exponent was >1.20 throughout the year at all seven sites. The AOD at 500nm has also been studied because of the wavelength dependent of optical properties to show the monthly and diurnal cycle. ~~ against~~The Moderate Resolution Imaging Spectroradiometer (MODIS) C6 retrieval AOD was validated by comparisonwith ground-based observations.The correlation coefficients (R^2 *R*) between the MODIS C6 AODdata and the values measuredon the ground were ~0.73–0.89. The MODIS/Terra C6 retrieval AOD values was generally more stable in the YRD region compared with the MODIS/Aqua product with the two Deep Blue (10km) and Dark Target (3km and 10km) methods against ground-based observations. The single-scattering albedo varied from 0.91 to 0.94, indicating that scattering aerosol particles are dominant in this region. ~~The real parts of the refractive index were ~1.41–1.43, with no significant difference among the seven urban, suburban and rural sites.~~ Large imaginary parts of the refractive index were seen in August at all urban, suburban and rural sites. ~~The fine-moderadii in the Yangtze River Delta region were ~0.2–0.3 μm with a volume of 0.10–0.12 μm^3 and the coarse-mode radii were ~2.0 μm with a volume close to 0.07 μm^3. The fine-mode aerosols were obviously larger in June and September than in other months at almost the sites.~~

The absorption AOD was low in the winter. The absorption Angström exponent and the extinction Angström exponent ~~were used to classify the different types of aerosol and the components of mixtures.~~shows that the “mostly dust” category was very low in the suburban and rural sites (<0.01%) and also less in the urban site (~0.24%). The aerosols caused negative radiative forcing both at the Earth’s surface and at the top of the atmosphere all year round in the Yangtze River Delta region ~~of eastern China~~ with the lower surface albedo ~~–~~in a unique geographical climate condition of better vegetation in the YRD region than in north/northeast China.

1. Introduction

Aerosols have important effects on the Earth's climate at both global and regional scales, although there are still great uncertainties in assessing their impact (Hansen et al.2000; Solomon et al., 2007; Schwartz and Andreae, 1996). Aerosols affect not only the radiative balance of the Earth–atmosphere system by directly scattering and absorbing solar radiation (Charlson et al., 1992; Ackerman and Toon, 1981), but also indirectly affect the climate through aerosol – cloud interactions (Twomey et al., 1984; Albrecht et al., 1989; Li et al., 2016).

The optical properties of aerosols influence the aerosol radiative balance and can be used to predict and assess global and regional changes in the Earth's climate (Eck et al., 2005; Myhre et al., 2009; IPCC, 2013; Panicker et al., 2013). Long-term, ground-based observations are crucial to our understanding of the global and regional variations in the optical properties of aerosols and their effects on the Earth's climate (Holben et al., 2001; Kaufman et al., 2002; Sanap and Pandithurai, 2014; Li et al., 2016). Ground-based monitoring networks have been established worldwide—for instance, AERONET (Aerosol Robotic Network) (Holben et al.,1998; Goloub et al., 2007), SKYNET (SKYrad Network) (Takamura et al., 2004), EARLINET (European aerosol Lidar network) (Pappalardo et al.,2014) and the GAW-PFR Network (Global Atmosphere Watch Programmer-Precision Filter Radiometers) (Wehrli, 2002; Estelles et al., 2012~~),~~).The above networks exclude EARLINET~~which~~ include~~s~~ several automated sites in China. CARSNET (the China Aerosol Remote Sensing NETwork) (Che et al., 2009a, 2015b) and CSHNET (the Chinese Sun Hazemeter Network) were established to obtain data on aerosol optical characteristics in China (Xin et al., 2007).

Most of the ground-based studies of the optical properties of aerosols in China have been concentrated in urban regions undergoing rapid economic development, which have high aerosol loadings and serious environmental problems (Cheng et al., 2015; Pan et al., 2010; Xia et al., 2013; Wang et al., 2015; Che et al., 2015a). Analyses of the aerosol optical depth (AOD), the types of aerosol ~~present~~s and the classification of ambient aerosol populations based on their size and absorption properties(Giles et al., 2011) are needed to understand their effects on the Earth's climate and environment (Che et al., 2009b; Wang et al., 2010; Zhu

et al., 2014).

The Yangtze River Delta (YRD) region in eastern China has undergone rapid economic growth and has high emissions of aerosols (Fu et al., 2008; Zhang et al., 2009).There have been many studies of the optical properties of aerosols in eastern China and these are important in our understanding of both the local air quality and regional climate change (Duan and Mao, 2007; Pan et al., 2010; Ding et al., 2016). Basic investigations of the variation in the optical characteristics of aerosols over the YRD region have been carried out at Nanjing, Hefei, Shanghai, Shouxian and Taihu (Zhuang et al. 2014; Li et al., 2015; Wang et al., 2015; He et al., 2012; Lee et al., 2010; Cheng et al., 2015; Xia et al., 2007). These studies in the YRD region have mostly been single-site and/or short-period investigations. The study sites are ~100 km apart from each other, which makes high spatial resolution satellite and modeling validations difficult. Thus there is still a lack of long-term, continuous and synchronous observations of the optical characteristics of aerosols, especially over adjacent urban, suburban and rural areas in the YRD region.

High-frequency ground-based observations of the variations in the optical characteristics of aerosols are necessary to our understanding of the processes involved in air pollution (e.g. the source, transport and diurnal variations of the pollution) and their effect on the regional climate. Ground-based observations are also important in the validation and improvement of satellite retrieval data (Holben et al., 2017; Xie et al., 2011). A high density of ground-based sun-and sky-scanning spectral radiometers within a local or meso-scale region is required to capture small-scale variations in aerosols for the accurate validation of satellite observations and to compare in situ versus remote sensing observations (Xiao et al., 2016; Holben et al., 2017). The MODIS (Moderate Resolution Imaging Spectroradiometer) retrieval AOD has a high accuracy with a wide spectral coverage (Tanré et al., 1997; Kaufman, et al. 1997) and the algorithm has been validated and improved based on AERONET data (Chu et al., 2002; Ichoku et al., 2002; Remer et al., 2005; Levy et al., 2010~~;~~). Levy et al. (2013) refined the MODIS Collection 6 (C6) aerosol retrieval process to provide ~~better~~ more accurate AOD retrievals. Some validations of satellite aerosol retrievals have been carried out in China with

ground-based observations from CSHNET (Li, et al., 2007; Wang, et al., 2007; Xin, et al., 2007) and CARSNET (Che et al., 2009a, ~~Che et al., 2011a~~; Tao et al., 2015).

We investigated the variation in the optical properties of aerosols and aerosol radiative forcing (ARF) using three-minute intervals of sunphotometer measurements from 2011 to 2015 at seven adjacent CARSNET (~10–40 km) urban, suburban and rural sites over eastern China. The aims of this study were: (1) to investigate the synchronous variations and differences in the optical properties of aerosols over urban, suburban and rural areas of the YRD megacity, eastern China; (2) to analyze the type and dominant distribution pattern of aerosols in the YRD via the extinction and absorption properties of aerosols; (3) to understand the difference in the ARF calculated from ground-based measurements of the optical properties of aerosols over urban, suburban and rural areas in eastern China; and (4) to evaluate the MODIS AOD retrieval data using the CARSNET AOD for the YRD. The results of this study will help the satellite and modeling communities to improve future aerosol retrieval data and simulations.

2. Site descriptions, measurements and data

Fig. 1 shows the geographical locations of the seven CARSNET sites in the YRD; these locations are described in Table 1.

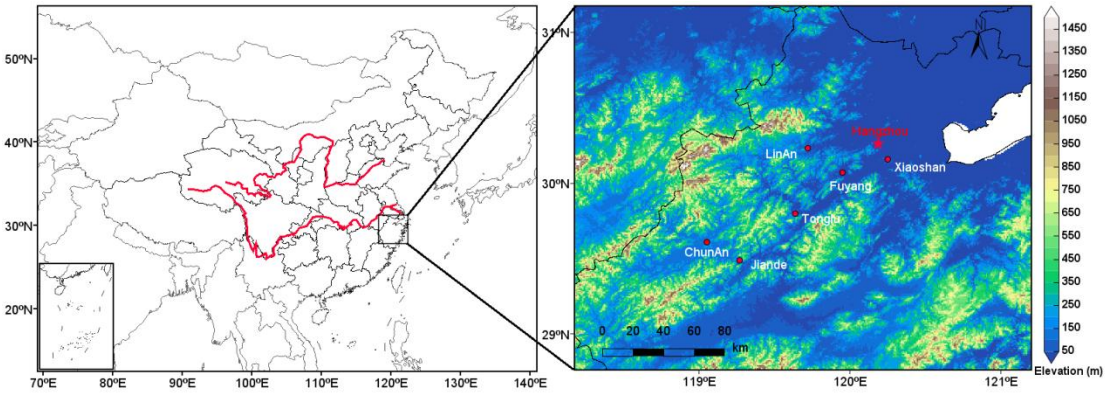

Fig. 1. Geographical location and elevation map for the seven CARSNET sites in the YRD.

The rural site of ChunAn can be regarded as a representative ~~background location~~clean~~r~~ site less ~~un~~affected by local and regional pollution. The site has a small population and a good

ecological environment, although there is some agricultural activity and burning of biomass from crop residues. Hangzhou is a densely populated urban site with a large volume of vehicular traffic and is therefore more affected by anthropogenic activity. LinAn, Fuyang, Jiande, Xiaoshan, and Tonglu are suburban sites and are all affected by both anthropogenic activity and pollution from industrial and agricultural production.

CE-318 sun photometers (Cimel Electronique, Paris, France) were installed at these seven sites in the YRD from 2011 to 2015. The instruments were standardized and calibrated annually according to the protocols reported by Che et al. (2009a). The instruments in this study were made inter-comparison calibration by the CARSNET reference instruments, which were periodically calibrated at Izaña in Spain. The cloud-screened AOD at different wavelengths was obtained using ASTPwin software (Cimel Electronique) (Smirnov et al.,2000). Instantaneous AOD measurements more than ten times at each day were selected for daily average calculation and statistical analysis to increase the representability of the aerosol optical characteristics (Che et al., 2015). The large AOD were checked by MODerate-resolution Imaging Spectroradiometer (MODIS) images (http://modis-atmos.gsfc.nasa.gov/IMAGES/) to further determine the cloud contamination. The corresponding values of Angström exponent (α) were calculated by instantaneous AOD values at 440 and 870 nm.

The aerosol microphysical properties of the volume size distribution and aerosol optical properties—including the single-scattering albedo (SSA), the complex refractive index, the absorption AOD (AAOD), the absorption Angström exponent (AAE) and the fraction of spherical particles—were retrieved from the almucantar irradiance measurements according to the methods of Dubovik and King (2000) and Dubovik et al. (2002, 2006). The inversion algorithm is under an assumption of homogeneous nonsphericity aerosol particles distribution according to Dubovik and King (2006) and has been applied in many different types of areas world widely. The accuracies of SSA is~0.03, and the errors are about 30%–50%/0.04 for the imaginary/real part of the complex refractive index under the

conditions of AOD at 440nm larger than 0.4 with the solar zenith angle more than 50°. The SSA was retrieved using only AOD_{440nm}>0.40 measurements to avoid the large uncertainties inherent in a low AOD (Dubovik et al. 2002, 2006). Real and imaginary parts of refractive index at 4 wavelengths (440, 675, 870, and 1020 nm) were retrieved from sky radiance and were confined in the range of ~~The complex refractive index was also retrieved by sky irradiance measurements in the range~~ 1.33–1.60 and 0.0005–0.50, respectively ~~for the real part and in the range 0.0005–0.50 for the imaginary part~~ (Dubovik and King, 2000; Che et al., 2015b). Also retrieved were aerosol volumes of 22 size bins within the 0.05 - 15 um radius range.~~In the volume size distribution, the radius range is selected from 0.05–15μm.~~ The EAOD in this study has been defined as extinction aerosol optical depth, and t~~T~~he AAOD and the AAE were calculated as described in equations (1) and (2):

$$AAOD(\lambda) = [1 - SSA(\lambda)] \times EAOD(\lambda) \quad (1)$$

$$AAE = -d\ln[AAOD(\lambda)]/d\ln(\lambda) \quad (2)$$

The ARF (~~arosol~~aerosol radiative forcing) data were calculated by the radiative transfer module used by the AERONET inversion (García et al., 2012) under the assumption of cloud-free consideration. In this code, the aerosol vertical properties have been considered into a homogeneous atmosphere layers because of the weak dependent of ground radiances on the whole atmospheric column with minor uncertainties (Dubovik et al., 2000). The ~~broadband~~ fluxes from 0.20 to 4.0μm were calculated according to the radiative transfer model GAME (Global Atmospheric ModEl) (Dubuisson et al., 1996, 2006; Roger et al., 2006). While the broadband radiation was calculated based on the aerosol optical depth, single scattering albedo and asymmetry factor based on those properties at four distinct wavelengths (440, 670, 870, 1020) which were linearly interpolated and extrapolated from the retrieval of the sun/sky-radiometer measurements. The uncertainties have been found to about 30% including the influence of spectral and solar zenith angle in the aerosol radiative effect (Myhre et al., 2003; Zhou et al., 2005). The size distribution, complex refractive index, and spherical particles fraction has been retrieved from the almucantar plane in the measurements. The SA (surface albedo) is obtained from the MODIS albedo product (MCD43C3) with the interpolation

value of 440, 670, 870, and 1020 nm. The water vapor at 940 nm ~~data~~ has been retrieved ~~in the 940 nm channel of~~by the sun photometer. The ozone content was ~~fixed using the monthly climatological values of the total ozone content~~ obtained from NASA Total Ozone Mapping Spectrometer measurements from 1978 to 2004. And o~~O~~ther atmospheric gaseous ~~profiles~~data ~~were~~came ~~obtained~~ from the US standard 1976 atmosphere model. In this study, ~~weused~~ the two parameters of ARF at the surface (ARF-BOA) and at the top of the atmosphere (ARF-TOA) have been calculated to describe~~s~~ the aerosol direct radiation effect to account for the changes of the solar radiation by calculating the difference energy between the aerosols presentation and absentation.~~.~~

The MODIS C6 aerosol optical thickness products refined by Levy et al. (2013) were ~~used to compare the MODIS AOD retrievals with~~ evaluated against our ground-based observations~~. The MODIS C6 AOD retrievals were formed into a merged dataset combining~~ by the Deep Blue (at 10km) and Dark Target ~~methods~~ (at 3km and 10km) methods separately. This version of MODIS includes some important changes from earlier versions—such as the central wavelength assumptions, Rayleigh scattering and the gas absorption performance (Levy et al., 2013)—and improvements in the radiometric calibration (Lyapustin et al., 2014). All cloud- and snow-free land surfaces have been expanded in the MODIS C6 aerosol products (Hsu et al., 2013). The AOD averaged data from Terra-MODIS and Aqua-MODIS were validated by matching the averaged CARSNET AODs within 30 minutes of the MODIS overpass within the ~~3~~5×5 ~~3~~pixels surrounding the CARSNET site (Tao et al., 2015). The AOD at 550 nm was interpolated between two wavelengths of the ground-based AOD measurements at 440 and 675 nm~~.~~.

3. Results and discussion

3.1 Aerosol microphysical properties of radius and volume size distributions

Fig.2 shows the monthly aerosol size distribution (d*V*/dln*r*) in the YRD for all sites. The volumes of fine-mode aerosols were obviously higher than those of coarse-mode aerosols over all sites. The ~~radii of fine volume fraction~~fine-mode radii were ~0.2–0.3 μm in the YRD

with a volume fraction of 0.10–0.12 μm^3 and the coarse-mode radii were ~2.0 μm with a volume fraction close to 0.07 μm^3. The amount of fine-mode aerosols was higher in June and September than in other months at almost sites, except for Xiaoshan. This could be caused by aerosol humidification (Eck et al., 2012; Li et al., 2010, 2014; Huang et al., 2016). This phenomenon is also found over Beijing and Shenyang in north/northeast China, suggesting that hygroscopic growth occurs over many regions of China (Li et al., 2011; Che et al., 2015c).

The coarse-mode radius in spring at all sites was smaller than in other cities in north and northeast China affected by frequent dust transport events in spring (Kong et al., 2011; Zhao et al., 2015). The coarse-mode particles showed a larger effective radius at all seven urban, suburban and rural sites in the summer, which may due to the adhesion of new particles onto larger particles (such as fly ash).

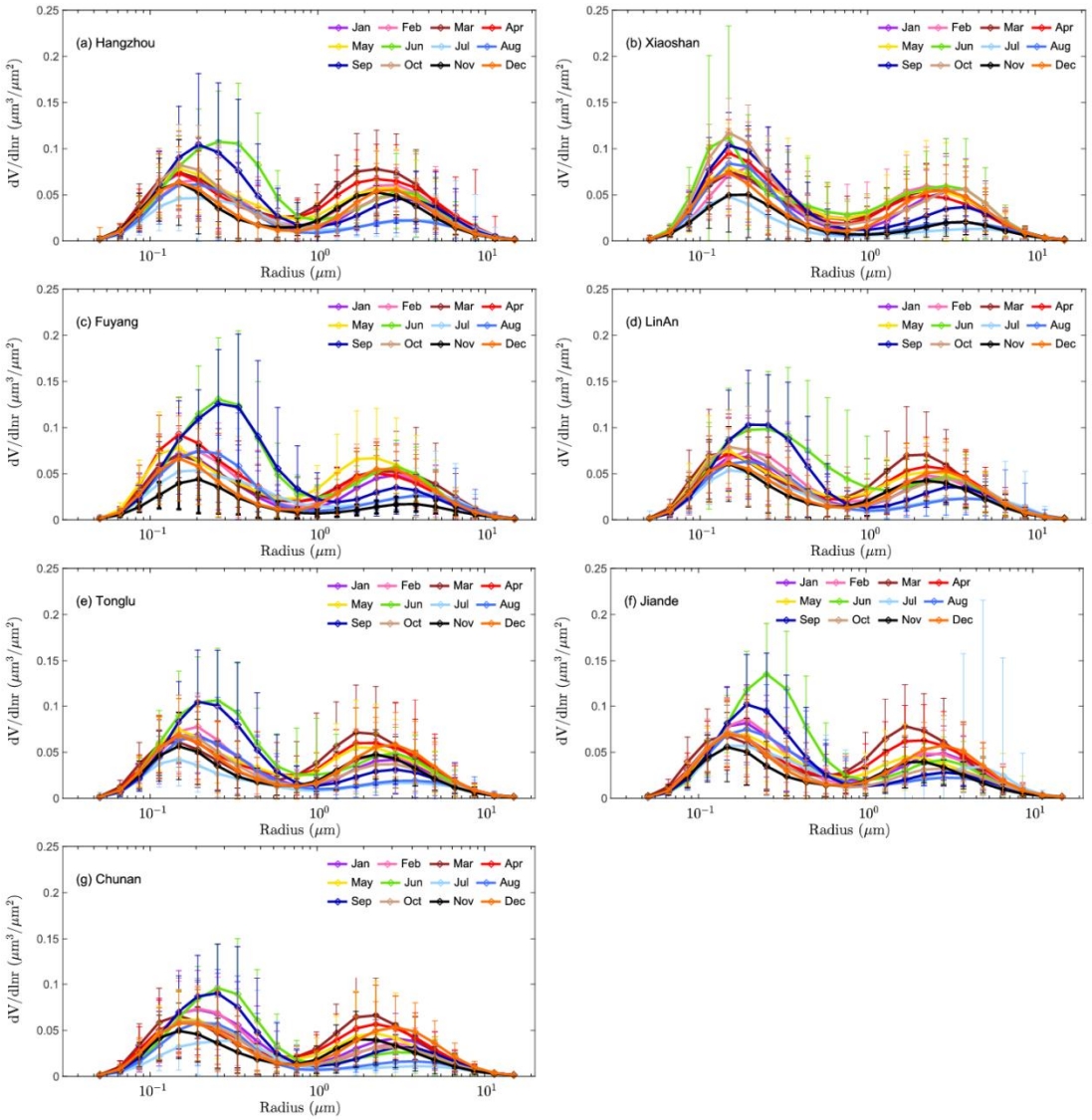

Fig.2.Variation in the annual volume size distribution over (a) Hangzhou, (b) Xiaoshan, (c) Fuyang, (d) LinAn, (e) Tonglu, (f) Jiande and (g) ChunAn.

3.~~1~~ 2 Aerosol optical properties of Aerosol optical depth and Angström exponent

The annual mean of AOD at 440nm over the seven urban, suburban and rural sites in this study ~~varied~~ ranges from 0.68 to 0.76 (Table 1). ~~Smaller observation samples has~~Smaller observation sample~~s~~ has~~ve~~ been found in Xiaoshan and Fuyang with 180 and 217 available observation days, respectively. The number of 180 observation days in Xiaoshan is less than half of the year may have less representative and need further data accumulation, while the ~~the~~ observation days of 217 in Fuyang was more than half of the year may not affect the

comparability between the other sites. The annual values of the AOD_{440nm} at Hangzhou, Xiaoshan, Fuyang, LinAn, Tonglu, Jiande and ChunAn were about 0.76±0.42, 0.76±0.43, 0.76±0.45, 0.73±0.44, 0.71±0.41, 0.73±0.40 and 0.68±0.38, respectively, which suggests that column aerosol loading is at a high level at all seven urban, suburban and rural sites in the YRD ~~. This suggests thataerosol pollution is~~on the regional rather than the local scale ~~in the YRD region~~. The AOD_{440nm} decreased from the eastern coast to the inland areas towards the west (from ~0.76±0.42 at Hangzhou to ~0.68±0.38 at ChunAn) due to the high aerosol loading from economic development and anthropogenic influences. The ~~anuual~~annual AOD_{440nm} shows that the aerosol loading has similar level in Hangzhou, Xiaoshan and Fuyang, and with the 4%-10% decrease in LinAn, Tonglu, Jiande and ChunAn, respectively. The AOD_{440nm} at the urban site of Hangzhou was ~~the~~ highe~~r~~st ~~ofall the study sites~~as a result of ~~high local anthropogenic activityin this urban area comparedwith the other suburban and rural sites.~~the more industrial activity and high resident density in the eastern part ~~of the Hangzhou~~ metropolis region resulting in larger aerosol emissions compared with the other suburban and rural sites. ~~The AOD at the rural site of ChunAn was lowerthan at the urban and suburban sites due to lower levels of anthropogenic activity.The AOD decreased from the eastern coast to the inlandareas towards the west (from ~0.76±0.42at Hangzhou to ~0.68±0.38 at ChunAn). Thisis due to the high aerosol loading from economic development and anthropogenic influences.There ismore industrial activityand high residentdensity in the eastern part of the Hangzhou metropolis region, resulting inhigheraerosol emissions.~~

~~The AOD in Hangzhou in urban eastern China was similar to that in Shenyang (0.75) in urban northeast China (Zhao et al., 2013), and in Beijing (0.76) and Tianjin (0.74) in urban north China (Che et al., 2015b), indicating that the aerosol extinction pollutionis both common and at a similar level throughout most urban areas of China. The AOD values at the urban and suburban sites of Hangzhou were slightly higher than at Pudong (0.70) and Hefei (0.69), other urban areas in eastern China, suggesting that higher aerosol extinction ability loadingswere emittedhere observed here (He et al., 2012; Liu et al., 2017). However, the AOD at all seven sites was lower than that obtained at Wuhan (1.05), Nanjing (0.88), Dongtan (0.85), Taihu(0.77) and Xuzhou (0.92) in previous studies in eastern China (Wang et al., 2015; Li et al., 2015; Pan~~

et al., 2010; Xia et al., 2007; Wu et al., 2016). This indicates that the aerosol loading caused by anthropogenic activities is very high in both urban and suburban areas in eastern China. The site at LinAn is regarded as the regional backgroundclean site in eastern China andis representative of thebackground atmospheric characteristics of this region (Che et al., 2009c). Thewith an average AOD at LinAnwas about 0.73±0.44, which is higher than that at the other regional background stations of China, such as Longfengshan (0.35; northeastern China), Mt Waliguan (0.14, inland Asia), Xinglong (0.28, northern China), Akedala (0.20, northwestern China) and Shangri-La (0.11, southwestern China) (Wang et al., 2010; Che et al., 2011; Zhu et al., 2014; Che et al., 2015b). The aerosol loading in eastern China (especially in the YRD region) is at least twice as high as in other regions of China which indicate the strong aerosol extinction.

Table1.Geographical location and annual mean optical parameters of aerosols at the seven observation sites in the YRD.

	Hangzhou	Xiaoshan	Fuyang	LinAn	Tonglu	Jiande	C
Site type	Urban	Suburban	Suburban	Suburban	Suburban	Suburban	R
Longitude (°E)	120.19	120.25	119.95	119.72	119.64	119.27	1
Latitude (°N)	30.26	30.16	30.07	30.23	29.80	29.49	2
Altitude (m)	41.9	14.0	17.0	139	46.1	88.9	1
[a]N_{day}	485	180	217	562	498	480	4
[b]$N_{inst.}$	2052	752	906	2410	2255	1952	1
[c]AOD_{500nm}	0.68±0.46	0.67±0.43	0.66±0.43	0.60±0.42	0.60±0.41	0.63±0.38	0
[e]~~AOD~~[d]AOD_{440nm}	0.76±0.42	0.76±0.43	0.76±0.45	0.73±0.44	0.71±0.41	0.73±0.40	0
[e]~~AOD_{fine}~~ [d]$AOD_{fine(440nm)}$	0.68±0.42	0.69±0.41	0.69±0.44	0.66±0.43	0.64±0.41	0.66±0.40	0
[e]~~AOD_{coarse}~~ [d]$AOD_{coarse(440nm)}$	0.08±0.06	0.07±0.06	0.07±0.06	0.07±0.07	0.07±0.06	0.07±0.07	0
[d]~~EAE~~[e]EAE	1.29±0.26	1.37±0.24	1.32±0.24	1.29±0.27	1.30±0.26	1.32±0.28	1
[e]~~SSA~~[d]SSA_{440nm}	0.91±0.06	0.93±0.04	0.94±0.04	0.93±0.05	0.92±0.04	0.92±0.05	0
[e]~~SSA_{fine}~~ [df]$SSA_{670nmfine}$	0.923±0.065	0.915±0.064	0.935±0.064	0.924±0.054	0.934±0.054	0.924±0.075	0
[e]~~SSA_{coarse}~~ [dg]$SSA_{870nmcoarse}$	0.9082±0.079	0.9083±0.078	0.9184±0.08	0.981±0.068	0.981±0.068	0.9082±0.089	0
[h]SSA_{1020nm}	0.89±0.08	0.89±0.08	0.89±0.09	0.90±0.07	0.90±0.07	0.90±0.09	0
[e]~~Real~~[d]Real	1.43±0.07	1.41±0.06	1.41±0.06	1.42±0.06	1.43±0.06	1.41±0.05	1
[e]~~Imaginary~~[d]Imaginary	0.011±0.010	0.008±0.006	0.007±0.006	0.009±0.007	0.009±0.007	0.010±0.009	0
[e]~~AAOD~~[d]AAOD	0.06±0.05	0.05±0.04	0.04±0.04	0.05±0.04	0.05±0.04	0.06±0.04	0
[d]~~AAE~~[e]AAE	1.13±0.46	0.88±0.42	0.85±0.43	0.98±0.35	1.11±0.49	1.16±0.44	0
[e]~~$Rmeas_t$~~ [d]$Rmeas_t$(μm)	0.70±0.34	0.65±0.31	0.66±0.33	0.66±0.33	0.65±0.33	0.62±0.24	0
[e]~~$Rmea_{fine}$~~ [d]$Rmea_{fine}$(μm)	0.18±0.05	0.18±0.04	0.19±0.05	0.19±0.05	0.19±0.05	0.19±0.05	0
[e]~~$Rmea_{coarse}$~~ [d]$Rmea_{coarse}$(μm)	2.67±0.47	2.73±0.42	2.75±0.45	2.71±0.52	2.66±0.48	2.63±0.47	2
[e]~~Reff~~[d]Reff(μm)	0.30±0.10	0.29±0.09	0.30±0.09	0.29±0.10	0.29±0.10	0.29±0.09	0

[e]~~Reff~~$_{fine}$ [d]Reff$_{fine}$(μm)	0.16±0.04	0.16±0.03	0.17±0.04	0.16±0.04	0.16±0.04	0.17±0.04	0
[e]~~Reff~~$_{coarse}$ [d]Reff$_{coarse}$(μm)	2.21±0.40	2.26±0.35	2.30±0.39	2.24±0.44	2.19±0.41	2.16±0.39	2
[e]~~Volume~~[d]Volume(μm^3)	0.19±0.09	0.19±0.09	0.19±0.09	0.18±0.09	0.17±0.09	0.18±0.09	0
[e]~~Volume~~$_{fine}$ [d]Volume$_{fine}$(μm^3)	0.10±0.06	0.11±0.06	0.11±0.07	0.10±0.06	0.10±0.06	0.10±0.06	0
[e]~~Volume~~$_{coarse}$ [d]Volume$_{coarse}$(μm^3)	0.09±0.06	0.08±0.05	0.08±0.06	0.08±0.05	0.08±0.06	0.08±0.07	0
[e]~~ARF~~[d]ARF-BOT(W/m^2)	−93±44	−84±41	−80±40	−81±39	−79±39	−82±40	−
[e]~~ARF~~[d]ARF-TOA(W/m^2)	−35±20	−36±21	−37±21	−36±21	−35±20	−35±21	−

[a] Number of available observation days.

[b] Number of instantaneous observations.

[c] Optical parameters at a wavelength of ~~440~~ 500nm.

[d] Optical parameters at a wavelength of 440 nm.

[d]~~Ångström~~ [e]Ångström exponents between 440 and 870 nm.

[f] Optical parameters at a wavelength of 670 nm.

[g] Optical parameters at a wavelength of 870 nm.

[h] Optical parameters at a wavelength of 1020 nm.

Ding et al. (2013a,b) showed that plumes from agricultural burning in June may significantly and seriously affect the radiation balance and air quality of the YRD region. In this study, the monthly averaged AODs at most sites showed two peaks in June and September (Fig~~.~~ ~~2~~3) with values of ~1.26±0.50 and ~1.03±0.57, respectively. This may be attributed to the accumulation of fine-mode particles via hygroscopic growth in the summer season and the burning of crop residue biomass under a continental high-pressure system with good atmospheric stability and frequent temperature inversions. These conditions lead to the poor diffusion of pollutants (Xia et al., 2007). As F~~f~~ig.3 shown, t~~T~~he monthly average value of the extinction Angström exponent (EAE, -$d$ln[EAOD(λ)]/$d$ln(λ)) ~~EAE~~ in Hangzhou was higher in January (~1.40±0.23) and September (~1.43±0.24). This conclusion is also indicated the dominance of small particles from anthropogenic emissions and agricultural activity in autumn and winter (Tan et al., 2009).

The annual fine-mode AOD values at Hangzhou, Xiaoshan, Fuyang, LinAn, Tonglu, Jiande and ChunAn were about 0.68±0.42, 0.69±0.41, 0.69±0.44, 0.66±0.43, 0.64±0.41, 0.66±0.40 and 0.61±0.38, respectively (Fig.~~2~~3). The seasonal variation in the AOD was similar to the total AOD at these urban, suburban and rural sites. The fine-mode fraction of AOD~~ratio AOD$_f$/AOD$_t$~~ consistently exceeded 0.90 ~~at all sites,~~which indicates ~~thatfine mode particles make~~ a major contribution of fine mode fraction to the total AOD in the YRD.

Moreover, the f~~F~~igure 3 shows that the ~~annualextinction Angström exponent(EAE)~~EAE at Hangzhou, Xiaoshan, Fuyang, LinAn, Tonglu, Jiande and ChunAn was about 1.29±0.26, 1.37±0.24, 1.32±0.24, 1.29±0.27, 1.30±0.26, 1.32±0.28 and 1.22±0.25, respectively. Values of EAE >1.20 were found in all months throughout the year, indicating that small particle size distributions were favored in the YRD region. The annual coarse-mode AOD values at Hangzhou, Xiaoshan, Fuyang, LinAn, Tonglu, Jiande and ChunAn were between about 0.06 and 0.08~~.The~~ with the ~~ratio~~ coarse mode fraction of AOD~~AOD$_c$/AOD$_t$~~ ~~was~~ about 0.10~~,~~ which indicates ~~that about 10% of~~ the 10% contribution of coarse mode fraction to the AOD in the YRD~~. regionis from coarse particles~~ ~~.The variation in the coarse-mode AOD (Fig. 2) also showed a significant increase in Marchatallseven sites of about 0.14±0.08, 0.08±0.04, 0.09±0.09, 0.13±0.11, 0.13±0.11, 0.14±0.08 and0.11±0.07at Hangzhou, Xiaoshan, Fuyang, LinAn, Tonglu, Jiande and ChunAn, respectively.The monthly average value of the EAEin Hangzhou was higher in January (~1.40±0.23) and September (~1.43±0.24). This indicated the dominance of small particles from anthropogenic emissions and agricultural activity in autumn and winter (Tan et al., 2009).The lower EAE was lower in March (~1.16±0.24) and April (~1.13±0.22)~~Though~~The less coarse mode fraction indicated that there is no obvious effect of the coarse particles in the YRD region than that contributed to the higher aerosol loading in other north/northeast China~~that contributedtothe higher aerosol loading~~ (Zhang et al., 2012)~~,s~~. Some ~~dust~~dusts cases ~~has also~~can be~~en~~ observed ~~found~~in YRD region that transported from north/northwest China during 2012-2015 reflect the effect of mineral dust aerosols (Gong et al., 2003). ~~,I suspect that~~The fugitive dust from road traffic ~~or~~and construction activity is another more persistent and significant source for China's cities as well as these eastern megacities~~., which reflectsthe effect ofmineral dust aerosols (Gong et al., 2003).However, this effect is not as obvious in the YRD region as other regions in north or northeast China whichcontributedtothe opticalpropertiesof aerosolsin this region(Zhang et al., 2012).~~ ~~.~~

~~This was mainly caused by dust episodes fromnorth/northwest China, whichcontributedtothe opticalpropertiesof aerosolsin this region(Zhang et al., 2012).~~

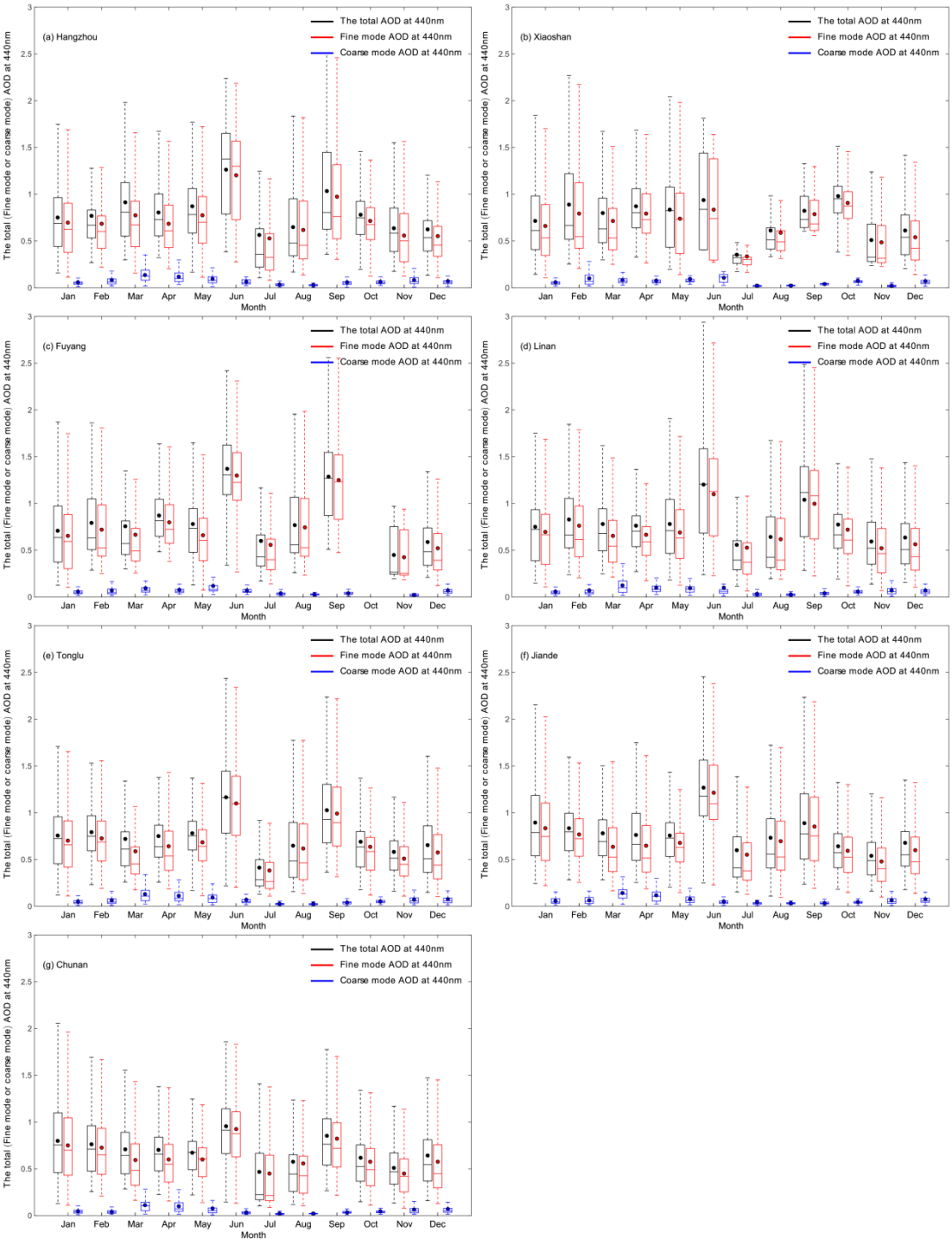
(a) Hangzhou
(b) Xiaoshan
(c) Fuyang
(d) Linan
(e) Tonglu
(f) Jiande
(g) Chunan
The total AOD at 440nm
Fine mode AOD at 440nm
Coarse mode AOD at 440nm
The total (Fine mode or coarse mode) AOD at 440nm
Month
Jan
Feb
Mar
Apr
May
Jun
Jul
Aug
Sep
Oct
Nov
Dec

349

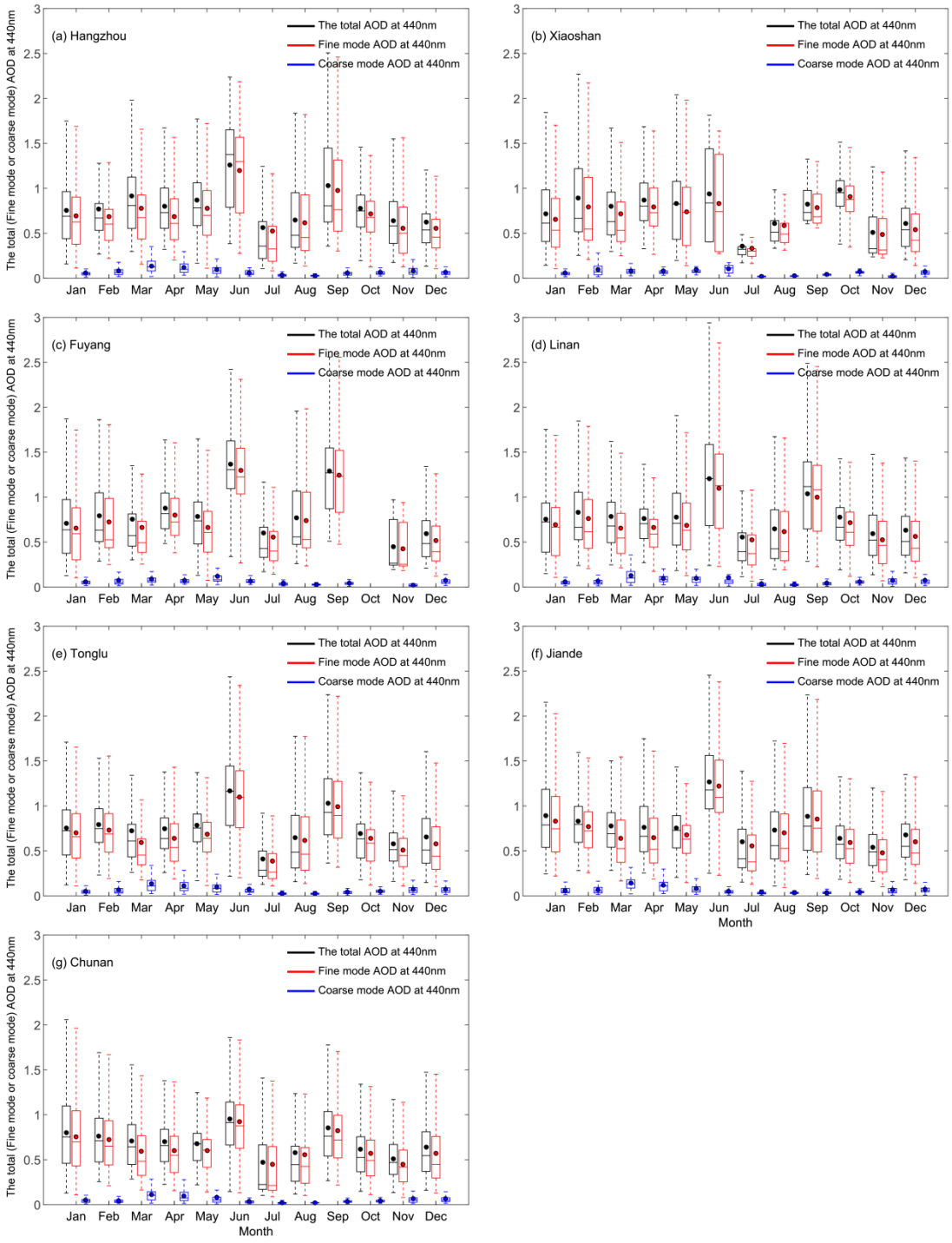

Fig. ~~2~~3. Variation in the total, fine- and coarse-mode $AOD_{440\ nm}$ over (a) Hangzhou, (b) Xiaoshan, (c) Fuyang, (d) LinAn, (e) Tonglu, (f) Jiande and (g) ChunAn. The boxes represent the 25th to 75th percentile distribution, while the dots and solid lines within each box represent the mean and median, respectively.

~~Figure3shows that the annual extinction Angström exponent(EAE) atHangzhou,~~

~~Xiaoshan, Fuyang, LinAn, Tonglu, Jiande and ChunAnwasabout 1.29±0.26, 1.37±0.24, 1.32±0.24, 1.29±0.27, 1.30±0.26, 1.32±0.28 and 1.22±0.25, respectively.Values of EAE >1.20were found in all monthsthroughoutthe year,indicatingthat smallparticlesize distributions were favored in the YRD region.The monthly average valueof the EAEin Hangzhou was higher in January (~1.40±0.23) and September (~1.43±0.24).This indicatedthe dominance of small particles fromanthropogenic emissions and agricultural activity in autumn and winter (Tan et al.,2009).The EAE was lower in March (~1.16±0.24) and April (~1.13±0.22), which reflectstheeffect ofmineraldustaerosols (Gong et al., 2003). However, this effectis not as obvious in the YRD region as other regions in north or northeast China.~~

~~Moreover, we alsodiscussest~~The monthly and diurnal cycle of AOD at 500nm has also been discussed in Fig.4 and Fig.5. The annual values of AOD500nm over the seven urban, suburban and rural sites in this study varied from 0.53~~68~~ (ChunAn) to 0.~~76~~68 (Hangzhou).The results show that two peaks of AOD at 500nm occurs in June and September ~~in the seven megacity of eastern China. The higher AOD500nmoccurs inJune and September~~with values of ~~0.10~~1.25~~±0.59~~10 and ~~0.23~~1.00~~±0.34~~42 –in the urban site of Hangzhou, respectively which has the similar pattern as~~as~~ the other sites. The increase of AOD at 500nm in June is not corresponding to the same increase pattern of EAE (about 1.5) which indicates the aerosols types may be relatively constant in this region. The Fig.4~~5~~2~~2~~ depicts the diurnal patterns of AOD at 500nm in this megacity area of eastern China. We can see that there are two types of diurnal patterns in this region. The daily AOD has been found increased in early morning (08:00 hr to 09:00 hr) ~~about —~~and afternoon (12:00 hr to 14:00 hr) about the value of 0.60 to 0.70~~has been found~~ in Hangzhou, Xiaoshan, Fuyang and Linan, while the decreasing of daily AOD has been observed from 0.70 to 0.50 during the daytime (from 07:00 hr to 16:00 hr) in Tonglu, Jiande and ChunAn. The high AOD during 07:00～09:00 in the urban area may be due to the anthropogenic activities and aerosol emissions from the morning rush hour. The decreased AOD with the value of 0.37±0.36 occurred in the suburban cities of Tonglu, Jiande and ChunAn may be due to the meteorological conditions more than anthropogenic effects~~,—~~. During the day, the aerosols in the near-surface may spread into vertical as a result of turbulence due to the more and more unstable atmosphere by the continuous strengthening of

solar radiation.

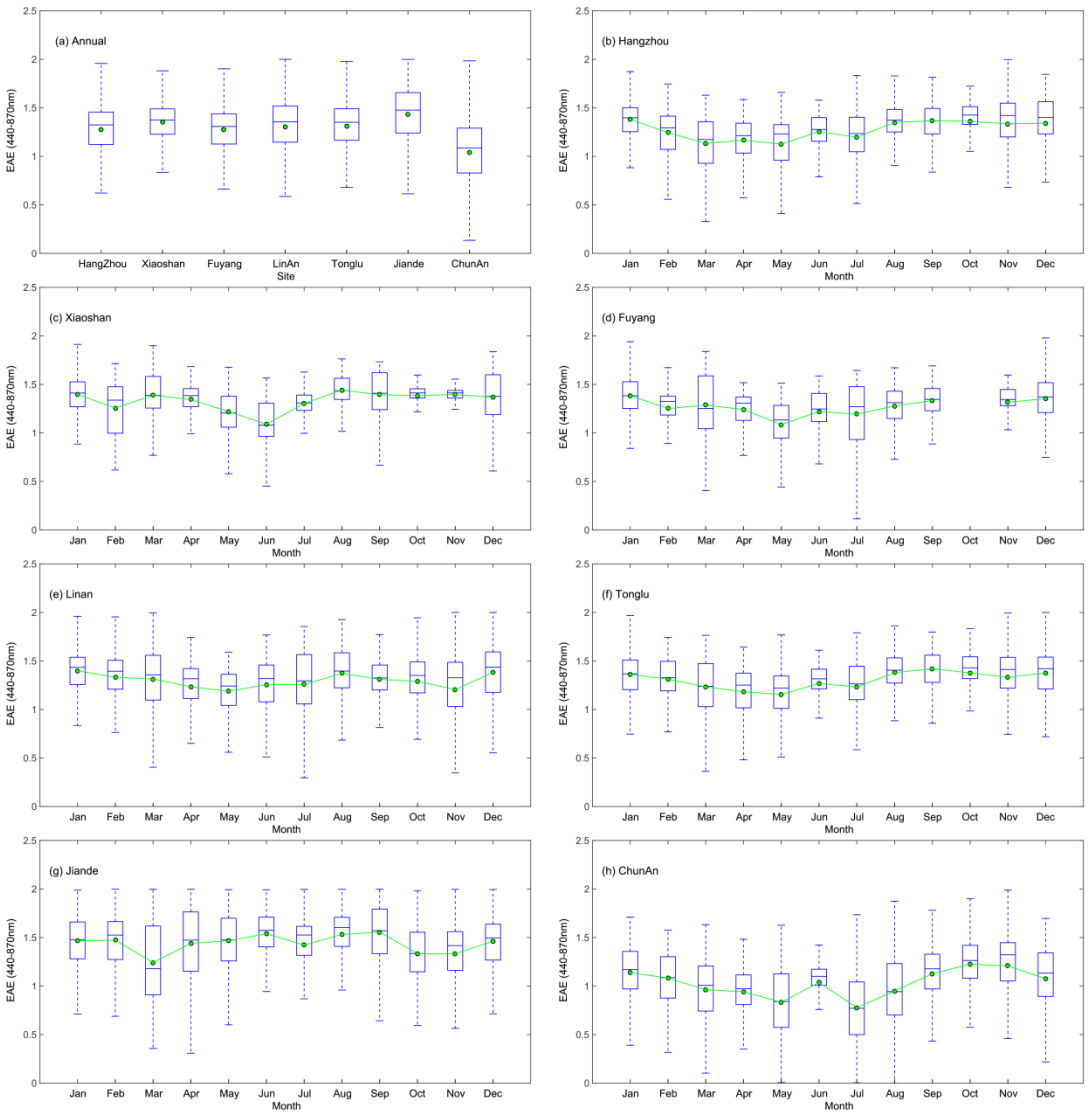

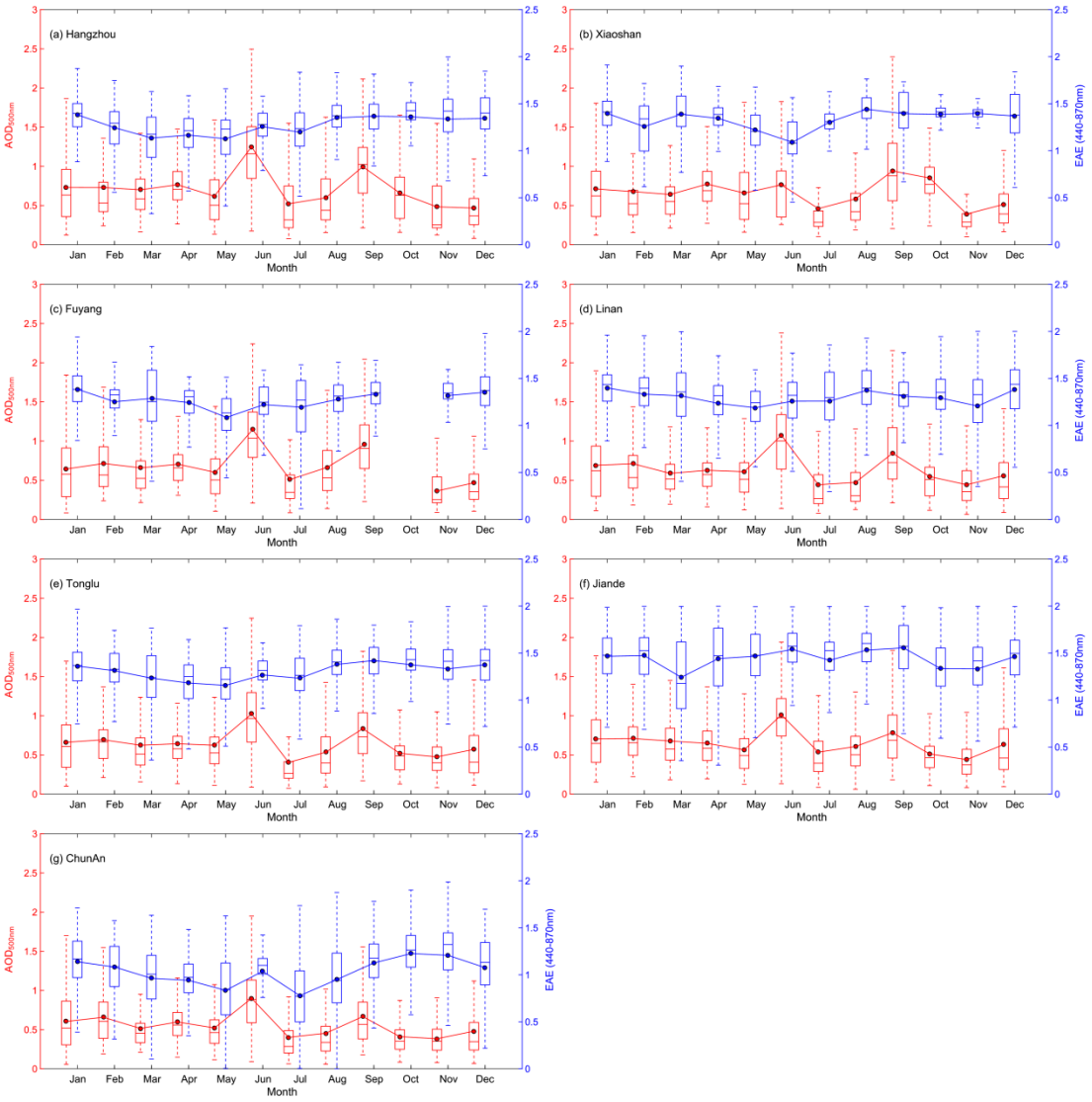

Fig.~~34~~.~~(a) Annual variation in the EAE at 440–870 nm.~~ Variation in the AOD at 500nm & EAE at 440–870 nm over (~~b~~a) Hangzhou, (~~c~~b) Xiaoshan, (~~d~~c) Fuyang, (~~e~~d) LinAn, (~~f~~e) Tonglu, (~~g~~f) Jiande and (~~h~~g) ChunAn. The boxes represent the 25th to 75th percentile distribution, while the dots and solid lines within each box represent the mean and median, respectively.

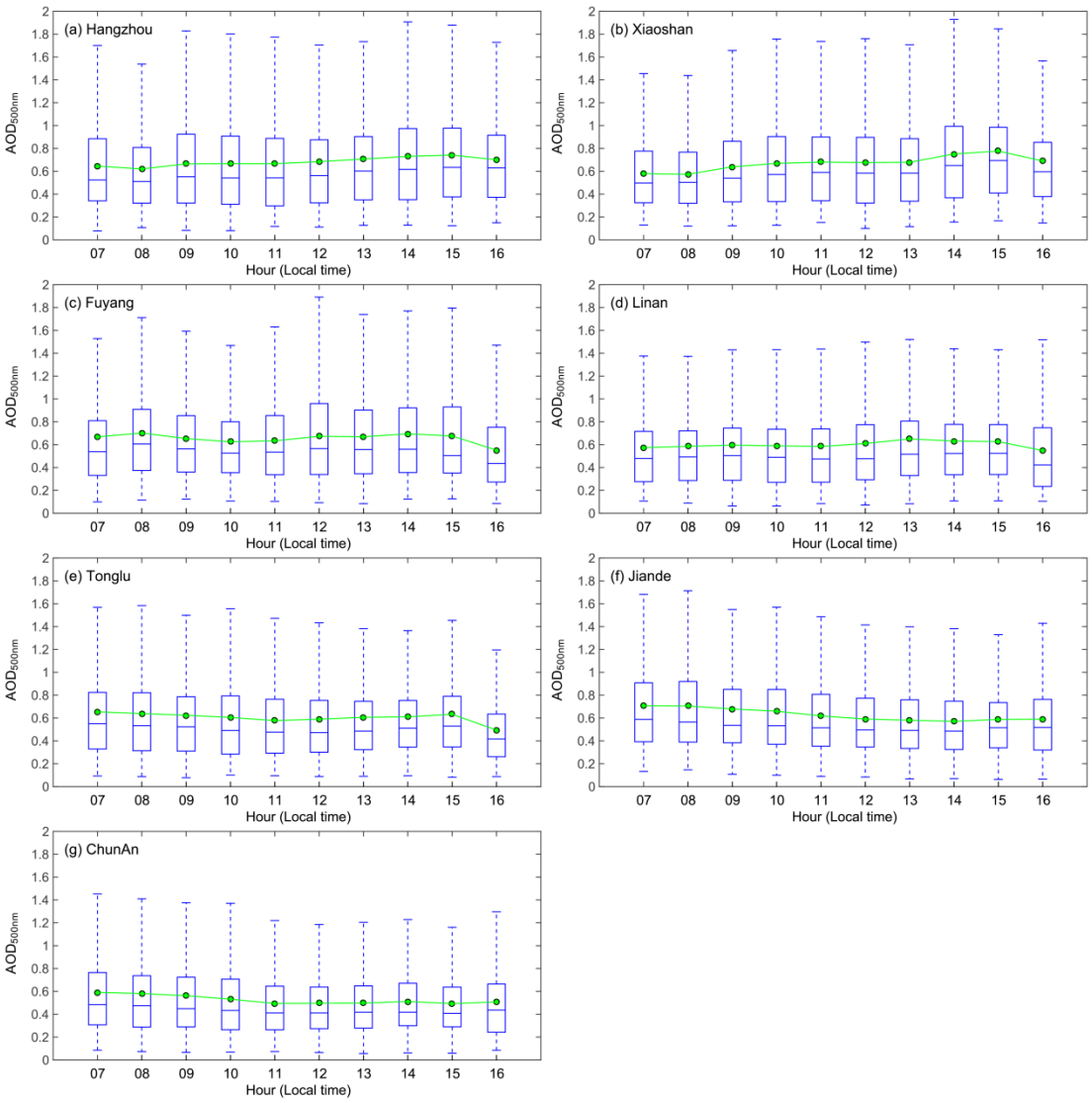

Fig.5. Variation of diurnal cycle in the AOD at 500 nm over (a) Hangzhou, (b) Xiaoshan, (c) Fuyang, (d) LinAn, (e) Tonglu, (f) Jiande and (g) ChunAn. The boxes represent the 25th to 75th percentile distribution, while the dots and solid lines within each box represent the mean and median, respectively.

~~Validation of the MODIS C6 retrieval AOD values was carried out by comparisonwith ground-based observations (Figure 4).~~The product of ~~Terra-~~MODIS/Terra and ~~Aqua-~~MODIS/Aqua with Deep Blue (at 10km) and Dark Target (at 3km and 10km) methods ~~at 3km and 10km~~ has been evaluated against by ground-based observations separately in Fig~~ure~~. 6~~5~~4-8~~02~~. We use the better estimated data of Quality flag = 3 and Quality flag=2, 3 for DT and TB methods, respectively. The systematic performance of the ~~Terra-~~MODIS/Terra~~MODIS~~ C6

retrieval AOD values was generally more stable in the YRD region compared with the ~~Aqua-~~MODIS/Aqua product with the two Deep Blue and Dark Target methods, ~~with~~ which most of the plots scattered around the 1:1 regression line. ~~The correlation coefficients (R^2)fitting relations between the Terra-MODIS and sun photometer AOD (550 nm) values by the Deep Blue methods at 10km were better than that of by the Dark Target methods.~~

~~about 0.73, 0.83, 0.77, 0.89, 0.85, 0.81 and 0.86 at Hangzhou, Xiaoshan, Fuyang, LinAn, Tonglu, Jiande and ChunAn, respectively.~~The correlation coefficients (R) ~~of~~ between the ~~Aqua-~~MODIS/Aqua and ~~Terra -~~MODIS/Terra between by the Dark Target methods at 3km and sun photometer AOD (550 nm) values ~~by the Dark Target methods at 3km~~ were about 0.~~70~~84 to 0.~~84~~92 and 0.~~73~~85 to 0.~~89~~94 in the YRD region, respectively. The linear regression fitting performed better at the suburban sites of LinAn and Jiande according to the product of MODIS/Terra~~Terra-MODIS~~ by the Dark Target methods at 3km. The fitting curve was almost consistent with the 1:1 reference line, which suggests that the aerosol properties were well defined for the MODIS C6 products. A large part of the MODIS retrieval AOD value was outside the expected error envelope of ± $(0.05 + 20\%\tau_{CARSNET})$, especially for AOD values<0.80 in Hangzhou and Xiaoshan. This indicates that the MODIS retrieval algorithm could still be improved, especially in urban areas. The MODIS retrieval AOD performed better at the other five sites (Fuyang, LinAn, Tonglu, Jiande and ChunAn) in the YRD; most of the retrieved AOD values for these sites fell within the expected error envelope. The MODIS/Aqua~~MODIS~~ retrievals with Dark Target methods at 3km were ~~overestimated~~ underestimated while the MODIS/Terra retrievals with Dark Target methods at 3km were overestimated except ~~at~~ Hangzhou, ~~Xiaoshan~~ Tonglu and ~~ChunAn~~Jiande. ~~This could be because the MODIS SSA was underestimated at and near to urban sites (Tao et al., 2015).~~ The small deviation at the suburban sites suggested that the MODIS C6 retrieval using the DT method was suitable for capturing the optical properties of aerosols in suburban areas with dense vegetation coverage of the YRD. However, this method may have larger difference in the urban areas with less vegetation such as Hangzhou. The correlation coefficients (R) of the MODIS/Aqua and MODIS/Terra~~Aqua-MODIS and Terra-MODIS~~ between sun photometer AOD (550 nm) values by the Deep Blue and Dark Target methods at 10km were about 0.~~65~~81 to

0.9081, 0.8573 to 0.9081, 0.6948 to 0.9182 and 0.8572 to 0.9386 in the YRD region, respectively. The MODIS/Aqua and MODIS/Terra retrievals with Deep Blue and Dark Target methods at 10km were underestimated except Hangzhou and Xiaoshan. In particular, the biases of the correlation coefficients (R) occurred in LinAn and Jiande –has decreased from 0.94 and 0.90 to 0.87 and 0.88. The validation results ~~correlation~~ indicates~~is not as better as the MODIS product at 3km which indicate~~ a good MODIS/Terra~~MODIS~~ matching with better fitting correlation at 3km rather than 10km products.

The AOD overestimation retrieved using Dark Target (DT) and Deep Blue (DB) methods are more influenced by the SSA and the phase function of aerosol in eastern China with AOD >0.4 (Tao et al. 2015). Therefore, the detailed ground-based observation in this work is more helpful to the calibration of MODIS retrievals in eastern China.

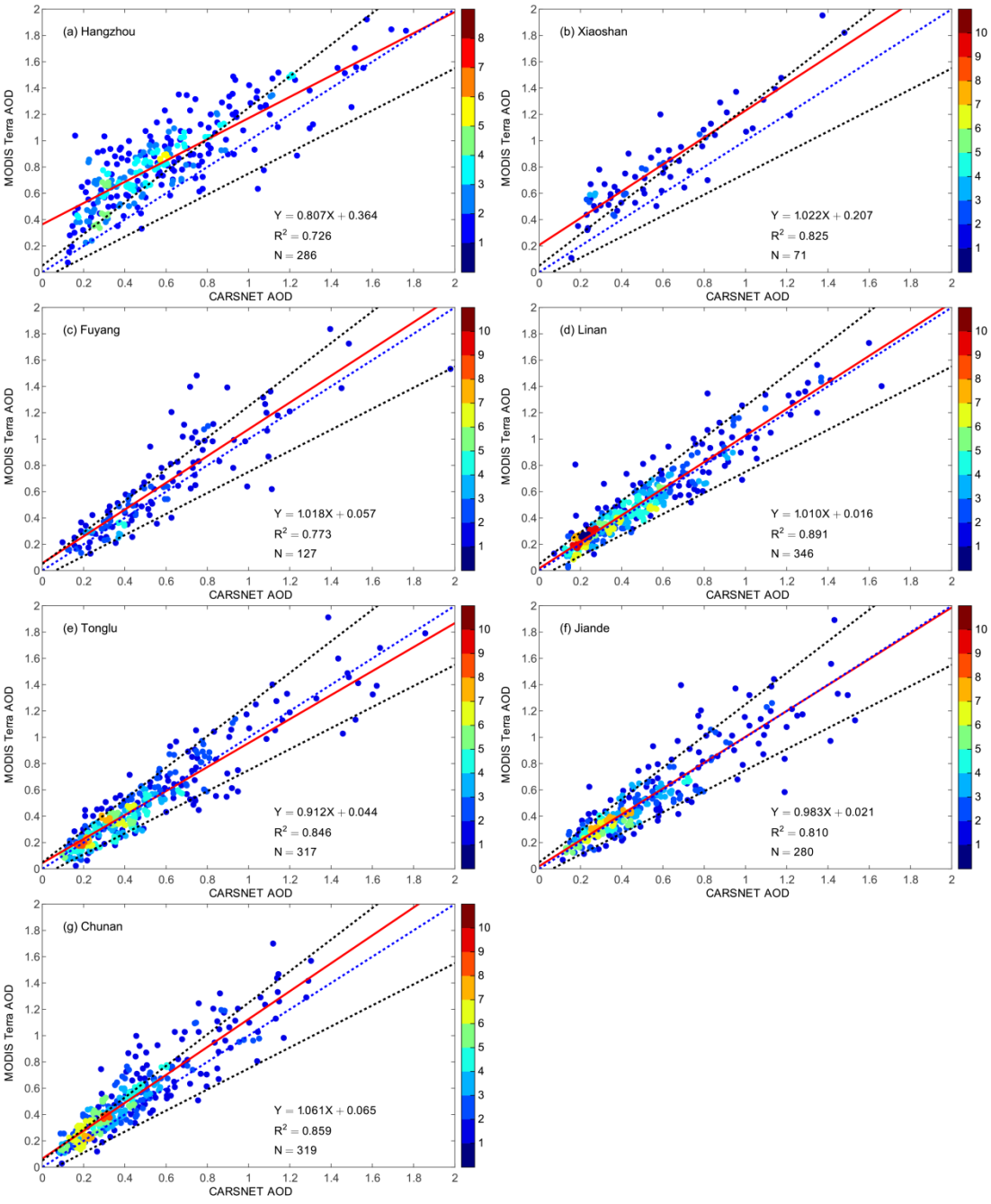
(a) Hangzhou
Y = 0.807X + 0.364
R² = 0.726
N = 286
(b) Xiaoshan
Y = 1.022X + 0.207
R² = 0.825
N = 71
(c) Fuyang
Y = 1.018X + 0.057
R² = 0.773
N = 127
(d) Linan
Y = 1.010X + 0.016
R² = 0.891
N = 346
(e) Tonglu
Y = 0.912X + 0.044
R² = 0.846
N = 317
(f) Jiande
Y = 0.983X + 0.021
R² = 0.810
N = 280
(g) Chunan
Y = 1.061X + 0.065
R² = 0.859
N = 319
MODIS Terra AOD
CARSNET AOD

448

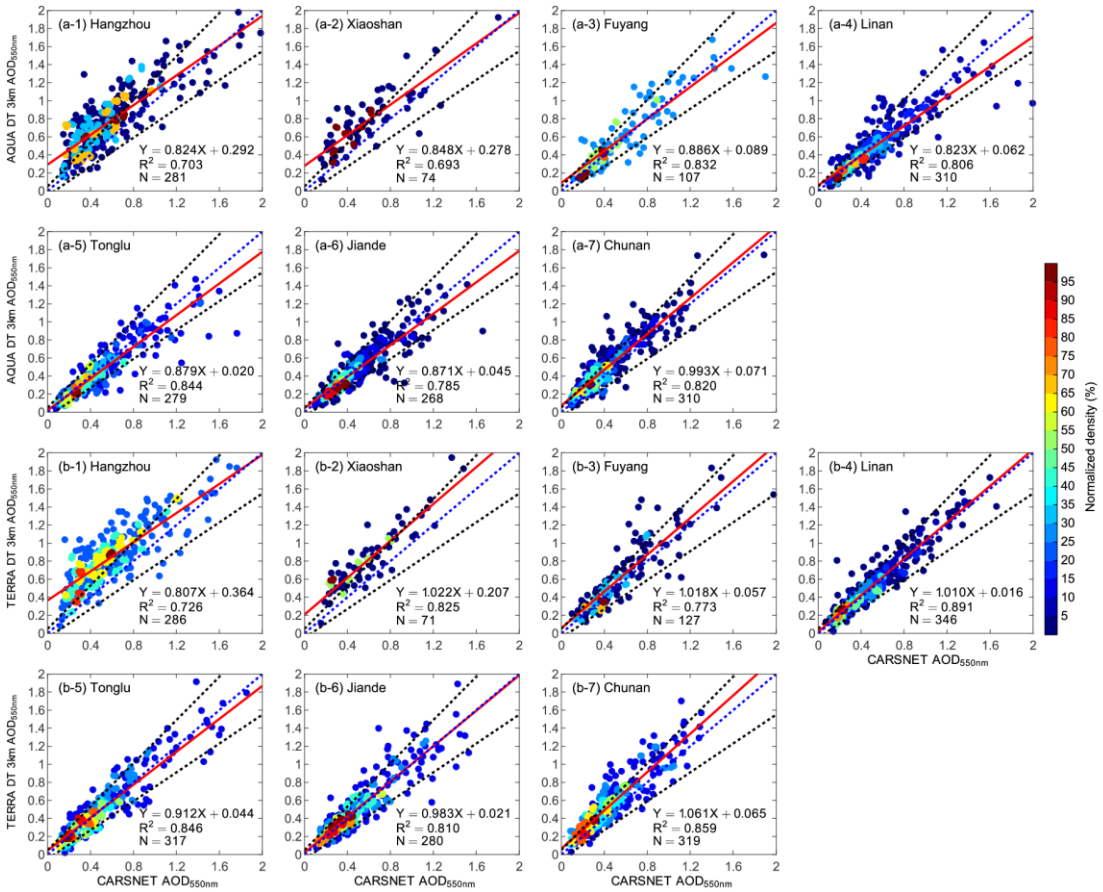

Fig.~~5~~64. Comparison of ~~C6~~ MODIS/Aqua Dark Target (DT)~~MODIS~~ AOD at 550 nm with the CARSNET AOD ~~by the Dark Target methods~~ at 3km in (a-1) Hangzhou, (a-2) Xiaoshan, (a-3) Fuyang, (a-4) LinAn, (a-5) Tonglu, (a-6) Jiande, (a-7) ChunAn and MODIS/Terra~~Terra-MODIS~~ DT AOD at 550 nm with the CARSNET AOD ~~by the Dark Target methods~~ at 3km in (b-1) Hangzhou, (b-2) Xiaoshan, (b-3) Fuyang, (b-4) LinAn, (b-5) Tonglu, (b-6) Jiande, (b-7) ChunAn. The red solid line represents the linear regression. The two black dotted lines represent the expected errors in the MODIS retrievals.

~~6Terra at 3km~~

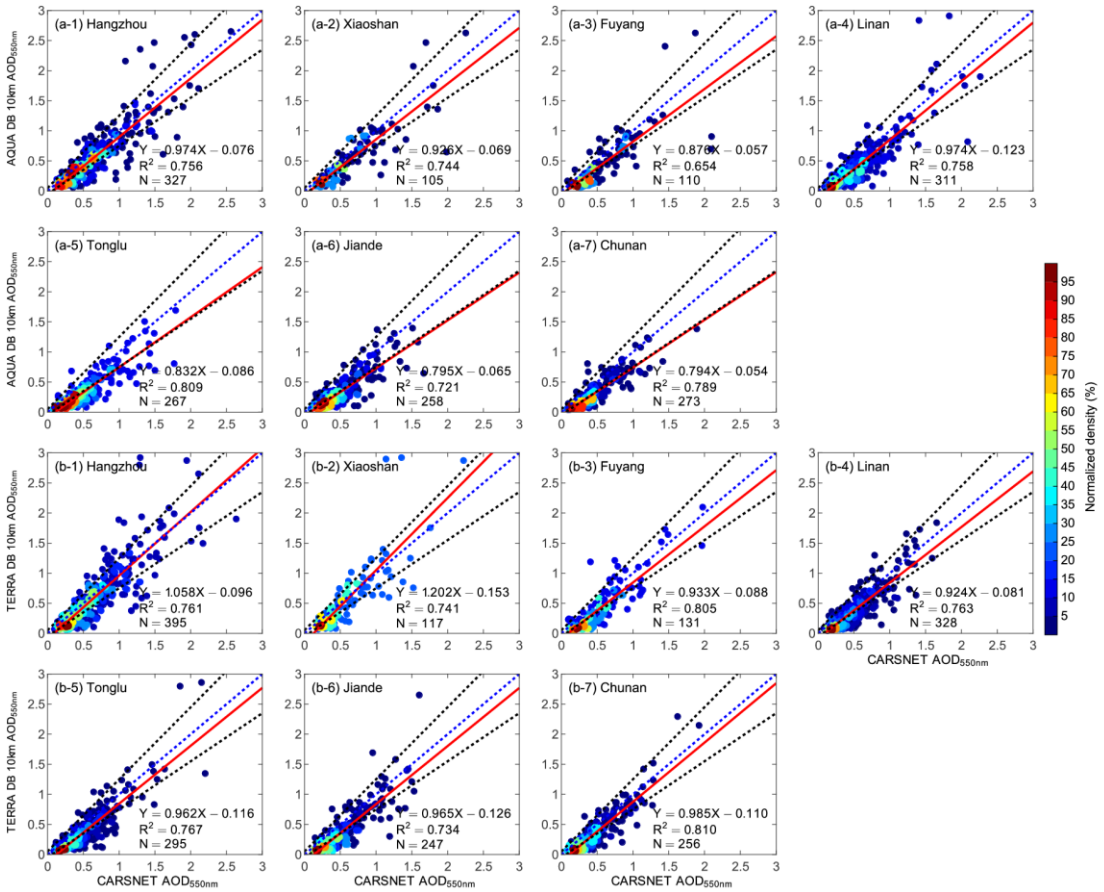

Fig. ~~4~~7. Comparison of ~~C6~~ MODIS/Aqua~~S~~ Deep Blue (DB) AOD at 550 nm with the CARSNET AOD ~~by the Deep Blue methods~~ at 10km in (a-1) Hangzhou, (a-2~~b~~) Xiaoshan, (a-3~~c~~) Fuyang, (a-4~~d~~) LinAn, (a-5~~e~~) Tonglu, (a-6~~f~~) Jiande ~~and~~, (a-7~~g~~) ChunAn~~.~~ and ~~Terra-~~MODIS/Terra AOD DB at 550 nm with the CARSNET AOD ~~by the Deep Blue methods~~ at 10km in (b-1) Hangzhou, (b-2) Xiaoshan, (b-3) Fuyang, (b-4) LinAn, (b-5) Tonglu, (b-6) Jiande, (b-7) ChunAn. The red solid line represents the linear regression. The two black dotted lines represent the expected errors in the MODIS retrievals.

~~8Terra at 10km~~

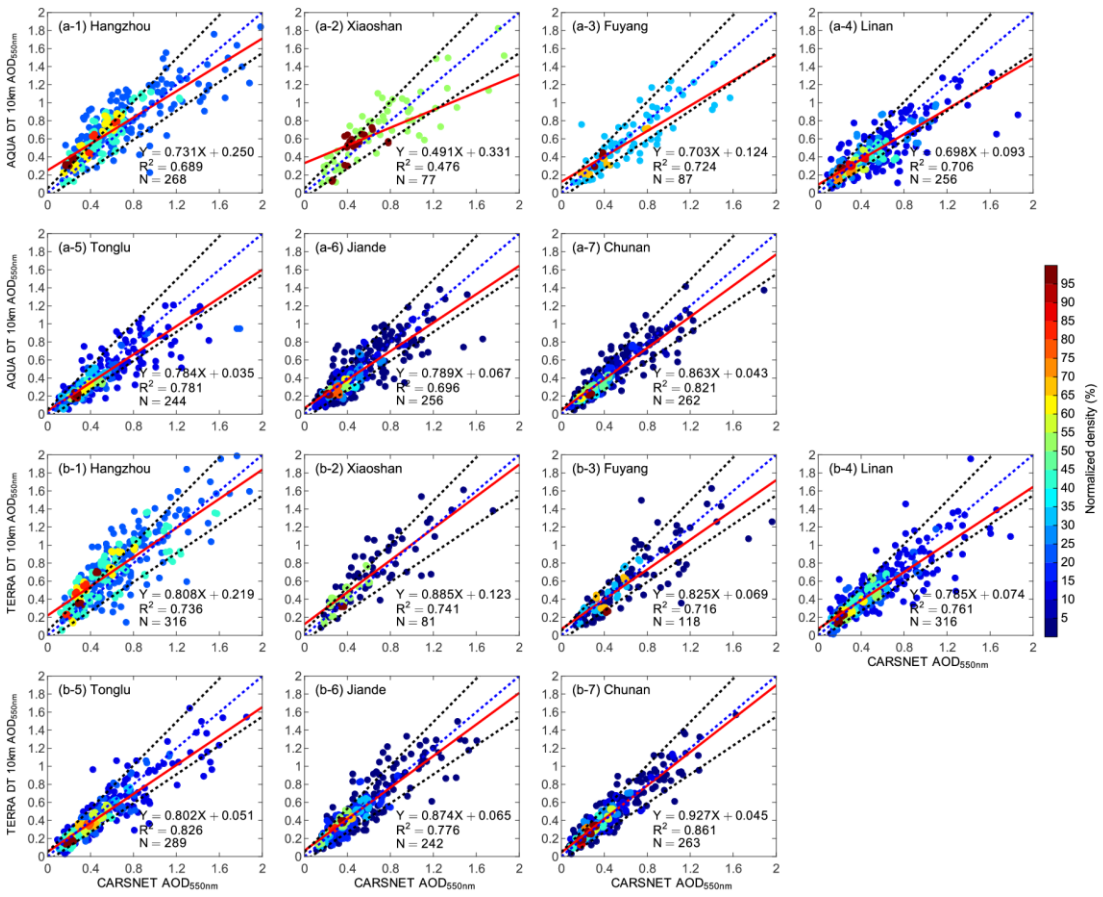

Fig.8. Comparison of ~~Aqua-~~MODIS/Aqua AOD DT at 550 nm with the CARSNET AOD ~~by the Dark Target methods~~ at 10km in (a-1) Hangzhou, (a-2) Xiaoshan, (a-3) Fuyang, (a-4) LinAn, (a-5) Tonglu, (a-6) Jiande, (a-7) ChunAn and ~~Terra-~~MODIS/Terra DT AOD at 550 nm with the CARSNET AOD ~~by the Dark Target methods~~ at 10km in (b-1) Hangzhou, (b-2) Xiaoshan, (b-3) Fuyang, (b-4) LinAn, (b-5) Tonglu, (b-6) Jiande, (b-7) ChunAn. The red solid line represents the linear regression. The two black dotted lines represent the expected errors in the MODIS retrievals.

~~9Aqua- at 10km~~ ~~10Terra- at 10km~~

The relationship between the EAE and the spectral difference in the EAE ($\delta EAE = EAE_{440–675nm} - EAE_{675–870nm}$) was analyzed to investigate the contribution of fine particles (R_f) and their fraction (η) to the total extinction (EAOD) at 440 nm (Gobbi et al., 2007). In this framework, values of AOD>0.15 are represented by different colors to avoid errors in the δEAE. The lines indicate contribution of the fixed radius (R_f) and fraction (η) of the

fine-mode particles to the total extinction. Gobbi et al. (2007) used the difference in the EAE and AOD data to determine the growth of fine-mode particles or contamination by coarse-mode particles at eight AERONET stations: Beijing (China), Rome (Italy), Kanpur (India), Ispra (Italy), Mexico City (Mexico), NASA Goddard Space Flight Center (GSFC, USA), Mongu (Zambia) and Alta Floresta (Brazil).

Fig. 5shows 911 shows that the high EAOD values (>1.00) cluster in the plots for all seven urban, suburban and rural sites, which is attributed to fine-mode particles with δEAE<0 and η ~50–90%. This variation in the fine-mode particles is similar to the results from Beijing and Kanpur (η ~70–90%). However, there were very few coarse-mode particles (δEAE~0, η~0–10%) in this study, suggesting that the dominance of dust is not significant in eastern China. These results showed a different pattern from that of other regions in north/northeast China (Wang et al., 2010; Zhu et al., 2014). For δEAE~0 and 10%<η<30%, high extinction was associated with a mixture dominated by fine-mode particles and less persistent coarse-mode particles. Clustering concentrated in the region α~1.5, δα ~−0.5 with high AOD values at all sites, which may be linked to an increase in size of the fine-mode particles by coagulation as the aged and hygroscopic events, as seen at other locations (e.g. Ispra, Italy; Mexico City, Mexico; GSFC, USA).

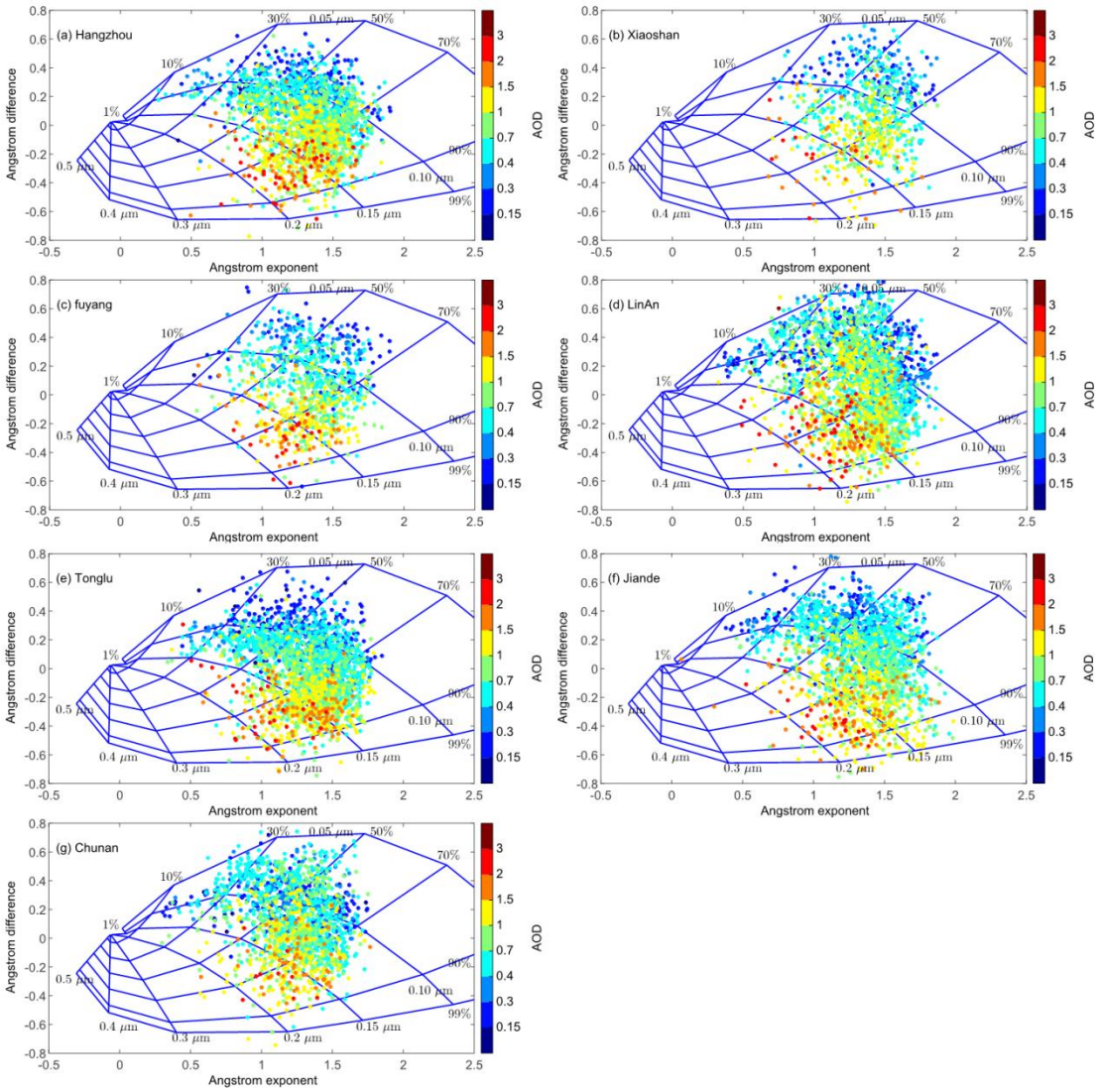

Fig.5119. Angström exponent difference as a function of $\alpha_{440–870\ nm}$ and the $AOD_{440\ nm}$ over (a) Hangzhou, (b) Xiaoshan, (c) Fuyang, (d), LinAn, (e) Tonglu, (f) Jiande and (g) ChunAn.

3.2 3 Aerosol optical properties of Singlesingle-scattering albedo and aerosol complex refractive index

The distribution of the total, fine- and coarse-mode SSAs at the wavelengths of 440nm, 670nm, 870nm and 1020nm over the seven sites in the YRD are shown in Fig..61210.. The total SSA varied from 0.91 to 0.94, which is similar to the range seen in other regions of China, such as Wuhan (0.92), Beijing (0.89) and Xinglong (0.92) (Wang et al., 2015; Xin et al., 2014; Zhu et al., 2014). This indicated that scattering aerosol particles in eastern China resulting from high levels of industrial and anthropogenic activity were dominant. The characteristics of

the SSA at these seven sites gradually increased from the east coast (0.91±0.06 at Hangzhou) inland toward the west (0.94±0.03 at ChunAn). The seven observation sites may always controlled by the same weather system that indicates a weak effect of meteorological elements in each site to the change of aerosol optical characteristics. These results indicate the emissions caused by human activity affect the absorption of aerosols in urban areas. The SSA was higher at LinAn and ChunAn than at the other sites, which may reflect the presence of a larger number of scattering aerosols (e.g. particles from urban/industrial activities) over the clean rural sites than over urban or suburban sites.

~~The range of variation inthe SSAof fine particles (SSA_f)was0.93–0.95, whereasthe SSA for coarse-mode particles (SSA_c)was 0.81—0.84at the seven sites (Fig. 6).The absorption/scattering properties of fine- and coarse-mode particles determine the total SSA in the YRD.The SSA was higher atLinAn and ChunAn than at the other sites, which may reflect the presence of a larger number of scattering aerosols (e.g.particles from urban/industrial activities) over the regional background/ruralsites than over urban or suburban sites.~~The SSA over urban and suburban sites showed the largest monthly variation. The monthly average values of SSA_T were high in February (~0.94±0.05) and June (~0.92±0.06), but low in March (~0.90±0.06) and August (~0.89±0.09) in Hangzhou. However, the monthly SSA values at the rural site of ChunAn only varied from 0.92 to 0.95. We concluded that the type of aerosol at urban/suburban sites was more complex than at rural sites. –The increased level of scattering aerosols with higher SSA in June may be influenced by the hygroscopic growth in favor of the interaction between ~~aerosol~~aerosols from different emissions sources (Xia et al., 2007). The existence of light-absorbing dust aerosols may contribute to the weaker lower SSA in spring while the aerosols from biomass burning were probably due to the strong decreased in SSA values in August (Yang et al., 2009).

~~The lower SSA of coarse mode particles in spring has been found in March/April (~0.79±0.08/~0.81±0.07) which may reflect the existence of light-absorbing dust aerosols in the dominace,andthe lower fine-mode SSA values in August(~0.90±0.08) were probably a result of aerosols from biomass burningin Hangzhouwhich has a larger contribution to the total~~

SSA (Yang et al., 200 The wavelength dependence of SSA present specific absorption/scattering properties of different type aerosol seasons (Sokolik and Toon, 1999; Eck et al., 2010). The SSA of dust in spring shown a weakdependence on the spectrum from 440nm to 1020nm in general (Cheng et al., 2006; Dubovik et al., 2002). EEspecially in the March, theof SSA at 440nm in Hangzhou, LinAn, Jiande and ChunAn was obviously lower at short wavelength than that in the longer wavelength. This resultsThis shownresult has shown a strong absorption of dust in the short wavelength in the YRD region over eastern China. It's worth noting that there is an obvious and strongly decreasing of SSA in the longer wavelength wavelength dependence of SSA by the type of aerosol from biomass burning or industrial emissions in August(Alam et al., 2011; Janjai et al., 2012). The wavelength dependence of SSA in YRD could be used to simply describe included to examine the aerosol types absorbing aerosol type, as different absorbing particles (including dust or the andbiomass burning smoke) appear different spectral contrast of SSA.

.

However, the monthly SSA values at therural site of ChunAnonly varied from 0.92 to 0.95. We concluded thatthe type of aerosol at urban/suburban sites wasmore complex than at rural sites.Fig.6shows a significant decrease in the fine-mode SSA in July/Augustand in the coarse-mode SSA in March/April.At Hangzhou, the lower fine-mode SSA values in July/August(~0.92±0.08/~0.90±0.08) were probably a result of aerosols from biomass burning and thelower coarse-mode SSA values in March/April (~0.79±0.08/~0.81±0.07) may reflect the existence of light-absorbing dust aerosols (Yang et al., 2009). The SSA depends on the wavelength and dust particles absorbstronglyat short wavelengths,resulting in a lower SSA at 440nm (Eck et al., 2010).

The range of variation inthe SSAof fine particles (SSA_f)was0.93–0.95, whereasthe SSA for coarse-mode particles (SSA_c)was 0.81–0.84at the seven sites (Fig. 6).Thefine- and coarse-mode particles displayedsignificant scattering and absorptionabilities in the urban,

~~suburban and rural areas of the YRD region.Fig.6shows a significant decrease in the fine-mode SSA in July/Augustand in the coarse-mode SSA in March/April.At Hangzhou, the lower fine-mode SSA values in July/August(~0.92±0.08/~0.90±0.08) were probably a result of aerosols from biomass burning and thelower coarse-mode SSA values in March/April (~0.79±0.08/~0.81±0.07) may reflect the existence of light-absorbing dust aerosols (Yang et al., 2009). The SSA depends on the wavelength and dust particles absorbstronglyat short wavelengths,resulting in a lower SSA at 440nm (Eck et al., 2010).The absorption/scattering properties of fine- and coarse-mode particles determine the total SSA in the YRD. These differences in the SSA were mostly dependent on the type of aerosol and theratio of absorbing and non-absorbing components in the aerosols.~~

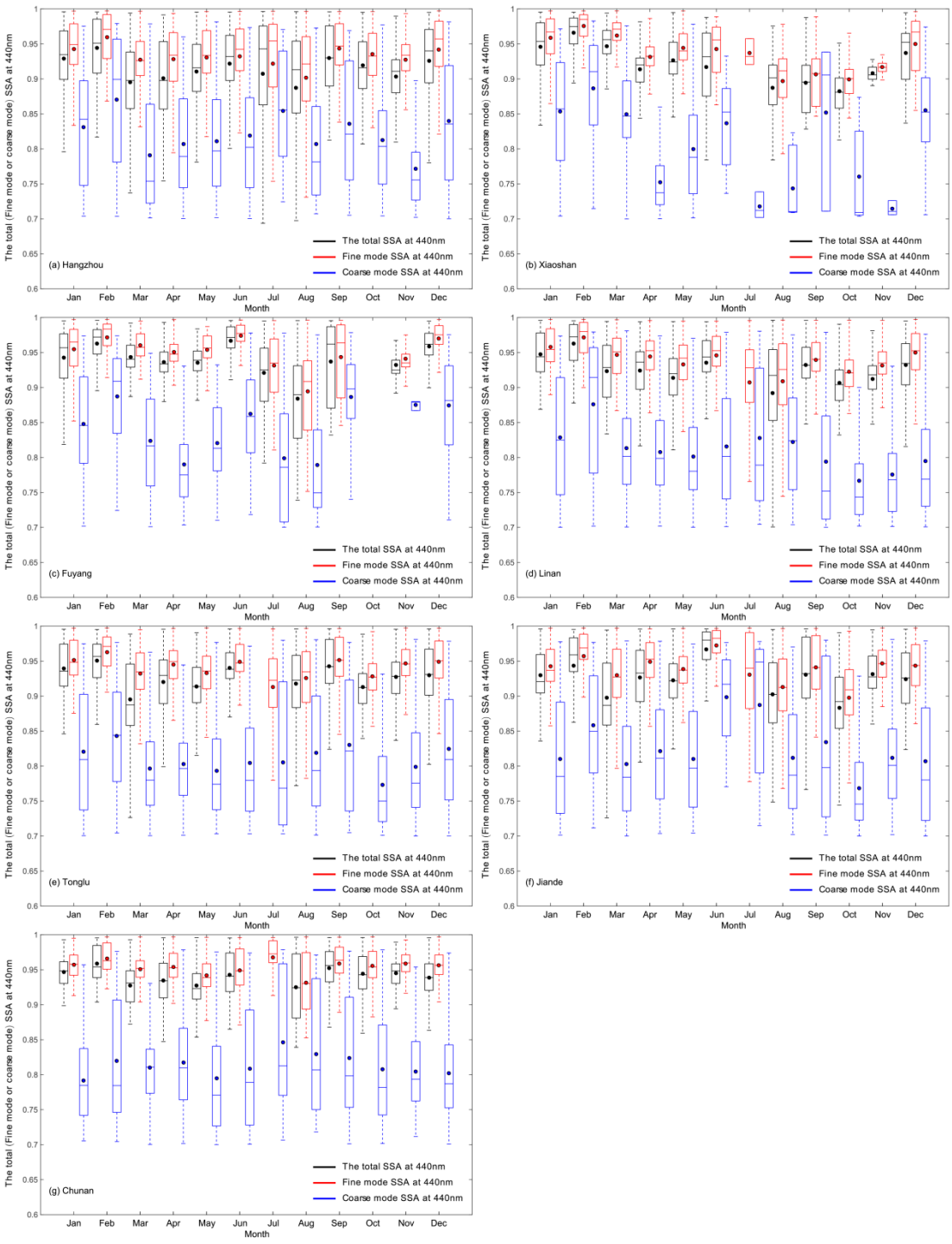
(a) Hangzhou
(b) Xiaoshan
(c) Fuyang
(d) Linan
(e) Tonglu
(f) Jiande
(g) Chunan
The total SSA at 440nm
Fine mode SSA at 440nm
Coarse mode SSA at 440nm
The total (Fine mode or coarse mode) SSA at 440nm
Month
Jan
Feb
Mar
Apr
May
Jun
Jul
Aug
Sep
Oct
Nov
Dec

577

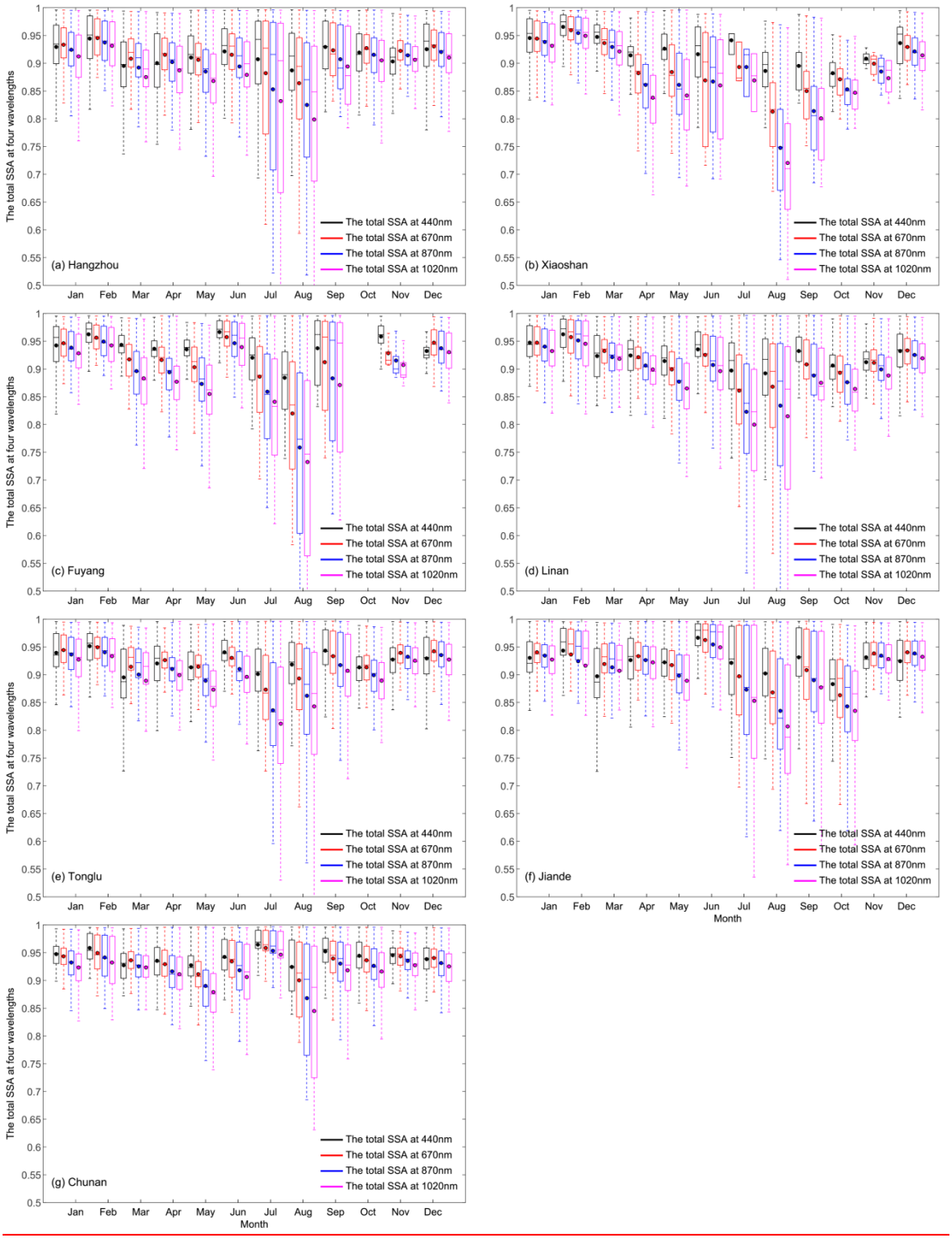

Fig.6~~12~~10. Variation in the ~~total, fine- and coarse-mode~~ SSA at 440nm, 670nm 870nm and 1020nm$_{440\ nm}$over (a) Hangzhou, (b) Xiaoshan, (c) Fuyang, (d) LinAn, (e) Tonglu, (f) Jiande and (g) ChunAn. The boxes represent the 25th to 75th percentile distribution, while the dots and solid lines within each box represent the mean and median, respectively.

The real and imaginary parts of the refractive index represent the scattering and

absorption capacity of particles, respectively. The refractive index is determined by the hygroscopic conditions and the chemical composition of the aerosols (Dubovikand King, 2000). There was no significant difference between the real parts of the refractive index among the seven urban, suburban and rural sites in this study (range 1.41–1.43). The real parts of the refractive index in this study were smaller than the real parts of ammonium sulfate and ammonium nitrate (1.55), which may be due to the hygroscopic conditions or the mixture of dust particles. The real part of the refractive index was highest in March (~1.46±0.06) and November (~1.45±0.06) and lowest in July (~1.42±0.06) and August (~1.41±0.07) at the urban sites.~~A higher level ofdust aerosols with weak scattering in spring and autumn could contribute to a higher value of the real part of the refractive index; this was reduced or eliminated by rainfall during the summer months.~~

The imaginary part of the refractive index was higher at the urban site of Hangzhou (~0.0112 ± 0.0104) as a result of the high loading of absorption aerosols in this region and was consistent with the lower SSA. High imaginary parts of the refractive index occurred in August at all urban, suburban and rural sites in the YRD, which may be due to the higher emission of absorptive particles by the post-harvest burning of crop residues~~.~~ with more spectral dependence. The burning of crop residues may cause a large deterioration in the regional air quality in the YRD region. A higher level of spring dust aerosols with absorption could contribute to a higher value of the imaginary part of the refractive index.

~~3.3 Radius and aerosol volume size distributions~~

~~Fig.7shows~~ 13 shows ~~the monthly aerosol size distribution (d*V*/dln*r*) in the YRD for all sites. The volumes of fine-mode aerosols were obviously higher than those of coarse-mode aerosols over all sites. The fine-mode radii were ~0.2–0.3 μm in the YRD with a volume of~~

~~0.10–0.12 μm^3 and the coarse-mode radii were ~2.0 μm with a volume close to 0.07 μm^3. The amount of fine-mode aerosols was higher in June and September than in other months at almost sites, except for Xiaoshan. This could be caused by aerosol humidification (Eck et al., 2012; Li et al., 2010, 2014; Huang et al., 2016).This phenomenon is also found over Bejing and Shenyang in north/northeast China, suggesting that hygroscopic growth occurs over many regions of China (Li et al., 2011; Che et al., 2015c).~~

~~The coarse-mode radius in spring at all sites was smaller than in other cities in north and northeast China affected by frequent dust transport events in spring (Kong et al., 2011; Zhao et al., 2015). The coarse-mode particles showed a larger effective radius at all seven urban, suburban and rural sites in the summer, which may due to the adhesion of new particles onto larger particles (such as fly ash).~~

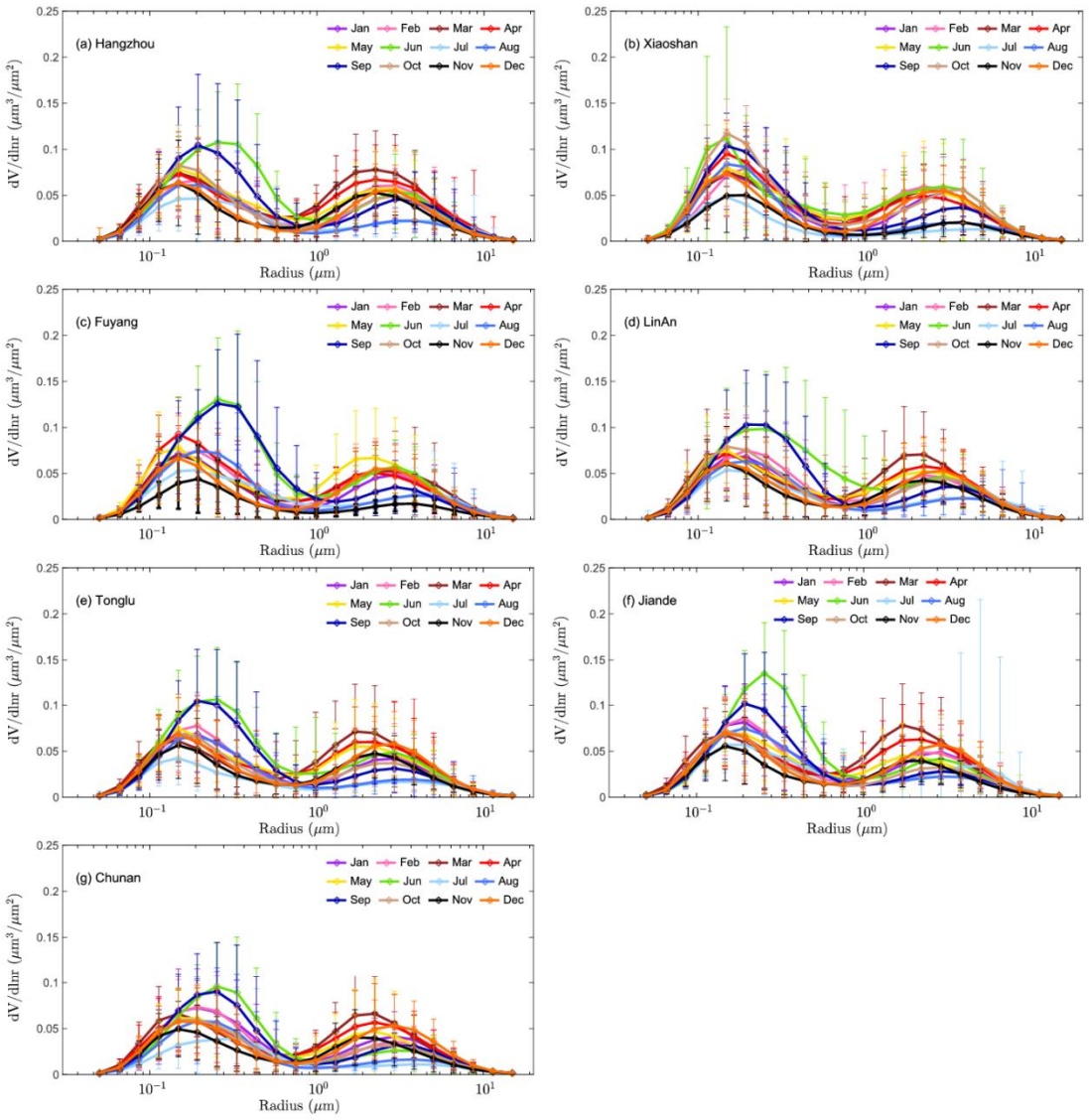

621

622 ~~Fig.137.Variation in the annual volume size distribution over (a) Hangzhou, (b) Xiaoshan, (c)~~

623 ~~Fuyang, (d) LinAn, (e) Tonglu, (f) Jiande and (g) ChunAn.~~

624 **3.4 Aerosol optical properties of ~~Absorption~~ absorption aerosol optical depth and**

625 **absorption Angström exponent**

626 The annual AAODs at Hangzhou, Xiaoshan, Fuyang, LinAn, Tonglu, Jiande and ChunAn

627 were about 0.06±0.05, 0.05±0.04, 0.04±0.04, 0.05±0.04, 0.05±0.04, 0.06±0.04 and 0.04±0.03,

628 respectively (Fig. ~~8~~11). ~~Thehigher annualvalues of the AAOD in Hangzhou and~~

629 ~~Jiandeindicatethat there are more absorbing aerosol particlesat these sites.~~The similar AAOD

630 level at the seven sites (0.04-0.06) suggests that absorbing aerosols are distributed

homogeneously in the YRD region. The AAOD values may have very large ~~uncertainties~~an uncertainty because of the dataset is including all the values in one month~~.~~. Nevertheless, there is also some varies in AAOD according to the changes of the SSA in section 3.3. These differences in the AAOD were mostly dependent on the type of aerosol and the ratio of absorbing and non-absorbing components in the aerosols.

~~These differences in the SSA were mostly dependent on the type of aerosol and theratio of absorbing and non-absorbing components in the aerosols.~~

The monthly AAOD at the urban site of Hangzhou was 0.09±0.06 in March as a result of the presence of absorbing dust particles. The AAOD of about 0.07±0.04 in August is related to the burning of crop residues. The AAODs in the winter season at all the sites in the YRD region were <0.05, which suggests that absorbing aerosol emissions did not frequently occur at these sites, unlike in the northern regions of China. As fig.1~~5~~2 shown, t~~T~~he AAE was<1.00 in June and August at all urban, suburban and rural sites of the YRD, which suggested the presence aerosols coated with absorbing or non-absorbing material in summer season. This process is favored by high temperatures and high humidity under conditions of strong solar radiation (Shen et al., 2015, Zhang et al., 2015). The particles coagulate and grow rapidly in the presence of sufficient water vapor (Li et al., 2016). The AAE became increasingly close to, or larger than, 1.00 at all seven sites from September, which is consistent with decreasing amounts of precipitation. This increase in the AAE was related to the emission of black carbon from biomass burning (Soni et al., 2010; Russell et al., 2010). According to the corresponding annual mean values for the AAE at Hangzhou, Xiaoshan, Fuyang, LinAn, Tonglu, Jiande and ChunAn (1.13±0.46, 0.88±0.42, 0.85±0.43, 0.98±0.35, 1.11±0.49, 1.16±0.44 and 0.93±0.31) in Fig. 12, the seven sites has been attributed to three categories with AAE levels. The mean values of the AAE at Xiaoshan and Fuyang were <1.00, suggesting the presence of absorbing or non-absorbing materials coating black carbon at these suburban and rural sites (Bergstrom et al., 2007; Lack and Cappa et al., 2010; Gyawali et al., 2009). The AAE values were close to 1.00 at LinAn and ChunAn, indicating that the absorptive aerosols were dominated by particles of black carbon (Zhang et al., 2012; Li et al., 2016). By contrast, the AAE values at Hangzhou,

Tonglu and Jiande were >1.00, indicating the presence of absorptive aerosols from the burning of biomass. This difference in the AAE distribution indicates the absorbing aerosols have different characteristics resulting from the different emission sources at urban, suburban and rural sites in the YRD.~~The AAEwas<1.00in June – August at all urban, suburban and rural sites of the YRD, which suggestedthe presenceaerosols coated with absorbing or non-absorbing material in summer season. This process is favored by high temperatures and high humidity under conditions of strong solar radiation (Shen et al., 2015, Zhang et al., 2015). The particles coagulate and grow rapidlyin the presence of sufficient water vapor (Li et al., 2016).The AAEbecame increasingly close to, or larger than, 1.00 at all seven sites from September, which is consistent with decreasing amounts of precipitation. This increase in the AAE was related tothe emissionof black carbon from biomass burning (Soni et al., 2010; Russell et al., 2010).~~

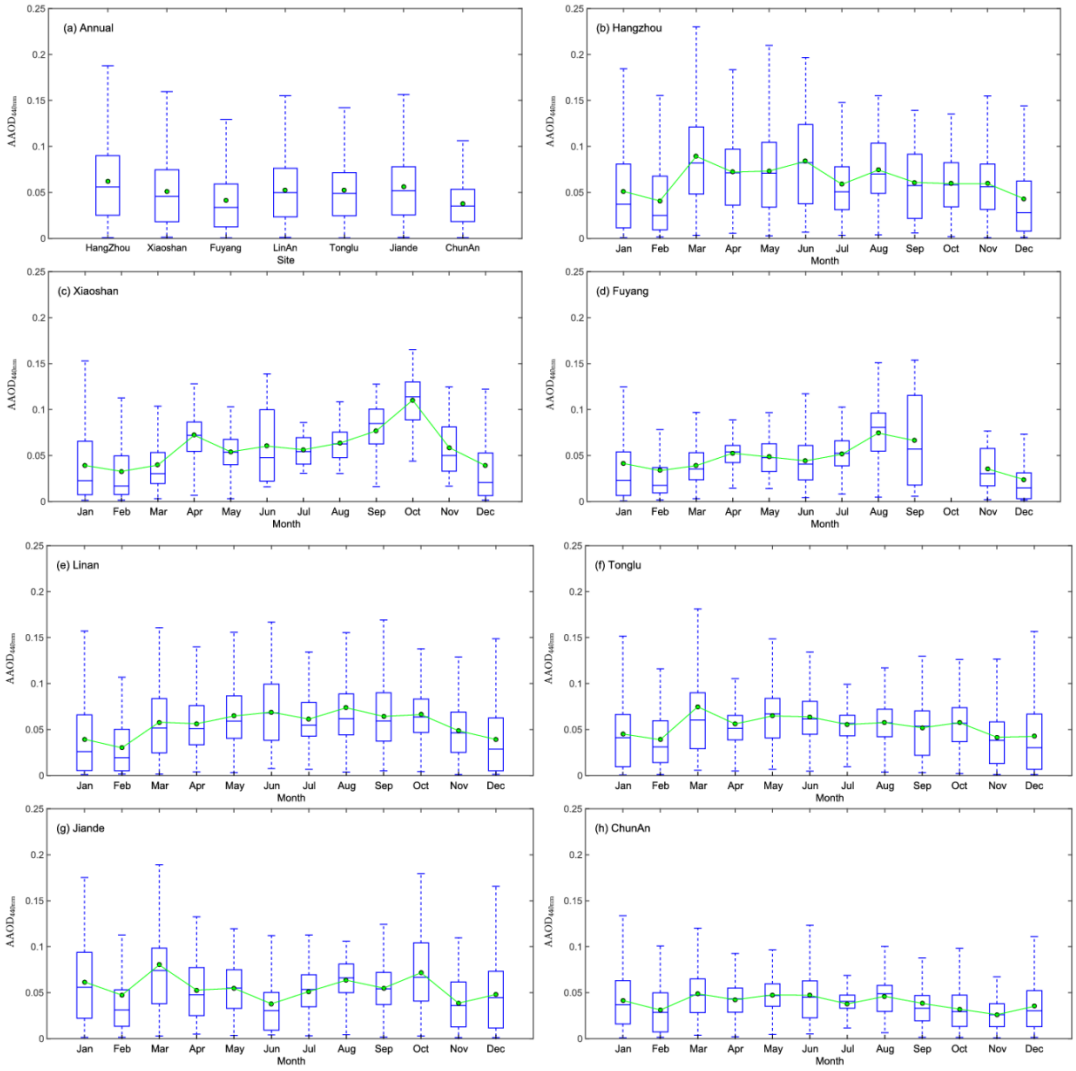

Fig. ~~8~~1~~4~~1. (a) Annual variation in the absorption aerosol optical depth at 440 nm ($AAOD_{440\ nm}$) over (b) Hangzhou, (c) Xiaoshan, (d) Fuyang, (e) LinAn, (f) Tonglu, (g) Jiande and (h) ChunAn. The boxes represent the 25th to 75th percentile distribution, while the dots and solid lines within each box represent the mean and median, respectively.

~~The annual mean values for the AAE at Hangzhou, Xiaoshan, Fuyang, LinAn, Tonglu, Jiande and ChunAn were about 1.13±0.46, 0.88±0.42, 0.85±0.43, 0.98±0.35, 1.11±0.49, 1.16±0.44 and 0.93±0.31, respectively(Fig. 9). The meanvalues of the AAE at Xiaoshan and Fuyangwere <1.00, suggesting the presence of absorbing or non-absorbing materialscoating black carbonat these suburban and rural sites(Bergstrom et al., 2007; Lack and Cappa et al., 2010; Gyawali et al., 2009).The AAE valueswere close to 1.00 at LinAn and ChunAn,~~

~~indicating thatthe absorptiveaerosolswere dominated by particlesof black carbon(Zhang et al., 2012; Li et al., 2016). By contrast, the AAE values at Hangzhou, Tonglu and Jiande were>1.00, indicating the presence of absorptive aerosols from the burning of biomass.This difference in theAAE distributionindicates the absorbing aerosols have differentcharacteristics resulting from the different emission sources at urban, suburban and rural sitesin theYRD.The AAEwas<1.00inJune – August at all urban, suburban and rural sites of the YRD, which suggestedthe presenceaerosols coatedwith absorbing or non-absorbing material in summer season. This process is favored by high temperatures and high humidity under conditions of strong solar radiation(Shen et al., 2015, Zhang et al., 2015). The particles coagulate and grow rapidlyin the presence of sufficient water vapor (Li et al., 2016).The AAEbecameincreasinglyclose to,or larger than, 1.00 at all seven sites from September, which is consistent with decreasing amounts of precipitation. This increase in the AAEwas related tothe emissionof black carbon from biomass burning (Soni et al., 2010; Russell et al., 2010).~~The AAE can be used to indicate the major types (urban/industrial, biomass burning, dust/mixed dust) or optical mixtures of absorbing aerosol particles (Schnaiter et al., 2006; Russellet al., 2010; Giles et al., 2011; 2012; Mishra and Shibata, 2012). Giles et al., (2011) examined AAE/EAE data from Kanpur to classify the categories of absorbing aerosols. The "mostly dust" category has been defined as having an EAE value ≤0.50 and sphericity fraction <0.20 with an AAE value>2.00. The "mostly black carbon" category has been defined as having an EAE value>0.80 and a sphericity fraction ≥0.20 with 1.00<AAE≤2.00. Values of EAE>0.80 and AAE>2.00 indicate a concentration of organic carbon (Arola et al., 2011). The "mixed black carbon and dust" category was centered at EAE~0.50 with AAE~1.50and used to represent an optical mixture with black carbon and mineral dust particles as the dominant absorbers.

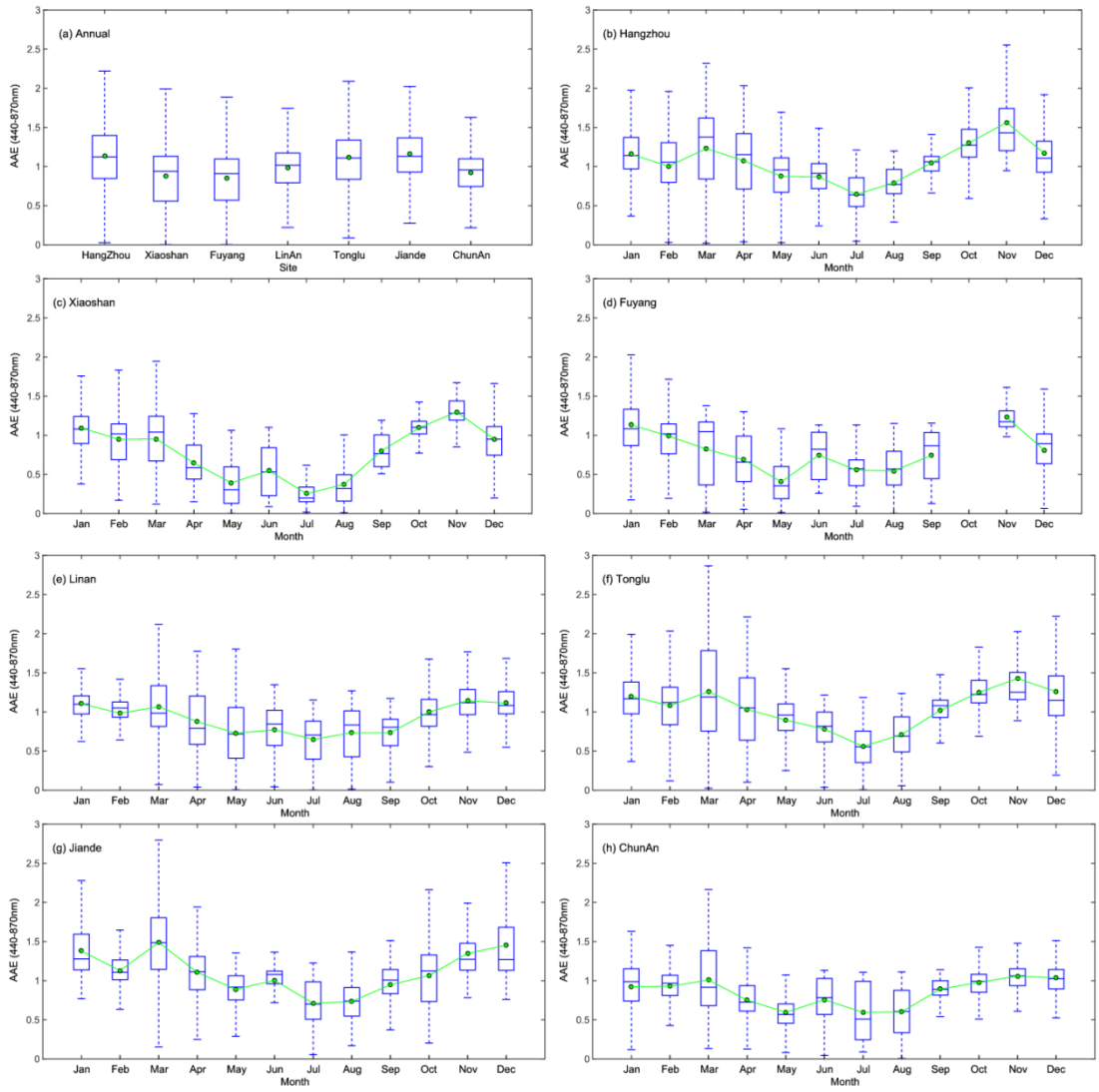

Fig. 9152. (a) Annual variation in the absorption Angström exponent at 440 nm ($AAE_{440\ nm}$) over (b) Hangzhou, (c) Xiaoshan, (d) Fuyang, (e) LinAn, (f) Tonglu, (g) Jiande and (h) ChunAn. The boxes represent the 25th to 75th percentile distribution, while the dots and solid lines within each box represent the mean and median, respectively.

~~The AAE canbe used to indicatethe majortypes (urban/industrial, biomassburning, dust/mixed dust)or optical mixtures of absorbing aerosolparticles(Schnaiter et al., 2006; Russellet al., 2010; Giles et al., 2011; 2012; Mishra and Shibata, 2012).Giles et al., (2011) examined AAE/EAE data fromKanpurto classify the categories of absorbing aerosols. The "mostly dust" category has been defined as having an EAE value ≤0.50 and sphericity fraction <0.20 with an AAE value>2.00.The "mostly black carbon" category has been defined as having~~

~~an EAE value>0.80 and a sphericity fraction ≥0.20 with 1.00<AAE≤2.00. Values ofEAE>0.80 and AAE>2.00 indicate a concentration of organic carbon (Arola et al., 2011). The "mixed black carbon and dust" category was centered at EAE ~ 0.50 with AAE ~ 1.50and used to represent an optical mixture with black carbon and mineral dust particles as the dominant absorbers.~~

We used the instantaneous AAE and EAE values to classify the dominant absorbing aerosol types in urban, suburban and rural areas of the YRD (Fig. ~~10~~16~~3~~; ~~Table 2~~). Fig. 13~~Table 2~~ shows that the "mostly dust" category was very low at both suburban and rural sites (<0.01%) and just ~0.24% at the urban site of Hangzhou. This indicates ~~that dust does notdominatethe absorbing aerosol particlesin~~the YRD region ~~of eastern China, which~~ is completely different from other ~~regions of~~ north/northeast region in China where the dust particles could contribute to the ~~-~~aerosol loading substantially. The "mostly black carbon" category dominates the absorbing aerosols in the urban, suburban and rural areas in the YRD region. The percentage "mostly black carbon" varied from ~20 to 40% depending on each site, indicating the mixing of black carbon as well as brown and soot carbon species from biomass burning and urban/industrial activities. Because of the long-distance transportation and local fugitive dust effect, the "mixed black carbon and dust" category contributed~5% of the absorbing aerosol particles in the YRD region. There was also ~1-4% of the "organic carbon" category identified as absorbing aerosol particles in this region.

The non-absorption particles are account for ~50 to 80% in the YRD region. There is higher contribution of non-absorption particles about 78.17% in Fuyang and less non-absorption particles about 50.01% in Jiande. The result is consistent with the level of total SSA at 440nm of Fuyang (0.94) with more scattering particles ~~and~~than Jiande (0.92).

Particles with EAE values of ~0.40 and ~1.25 could be regarded as "mixed large particles" greater than microns in size and submicron "mixed small particles", respectively (Giles et al. 2012). The frequency of "mixed large particles" was <0.5% at the urban, suburban and rural sites ~~(Table 2)~~. By contrast, the frequency of "mixed small particles" was ~18-36%.

The EAE (α_{ext}) and AAE (α_{abs}) values at all the urban, suburban and rural sites were

distributed mainly around 1.25 and 1.00–1.50 ~~(Fig.1016)~~, respectively (Fig.14). In contrast with the results of Giles et al. (2011), the sphericity fraction did not show an obvious transition from non-spherical to spherical particles from the urban, suburban and rural sites in YRD. The sphericity fraction showed a dispersed distribution of spherical particles, indicating a mixture of fine-mode particles derived from anthropogenic sources and coarse-mode particles, such as dust events transported from north/northwest China or local fugitive dust emissions.

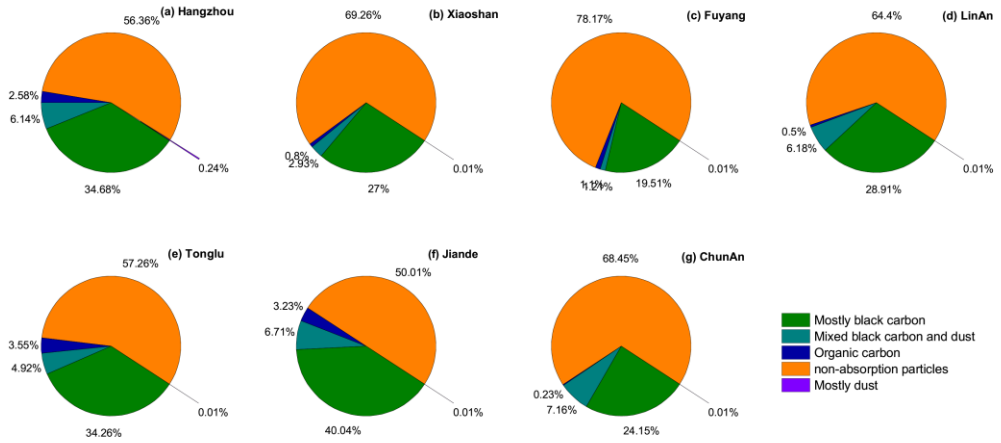

Fig.13.Types of aerosol over (a) Hangzhou, (b) Xiaoshan, (c) Fuyang, (d), LinAn, (e) Tonglu, (f) Jiande and (g) ChunAn.

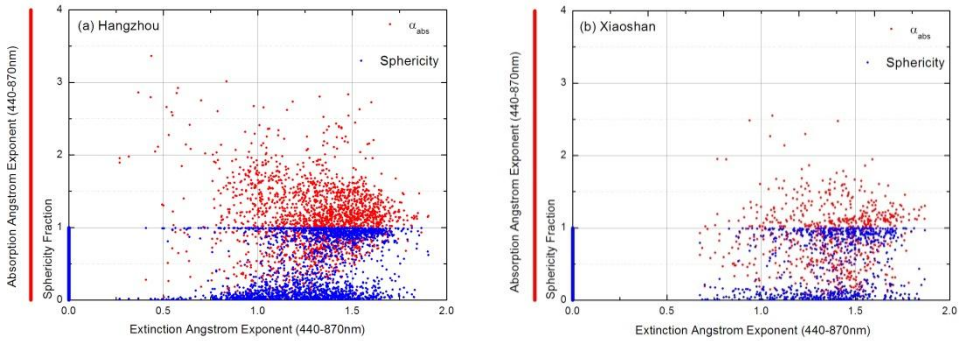

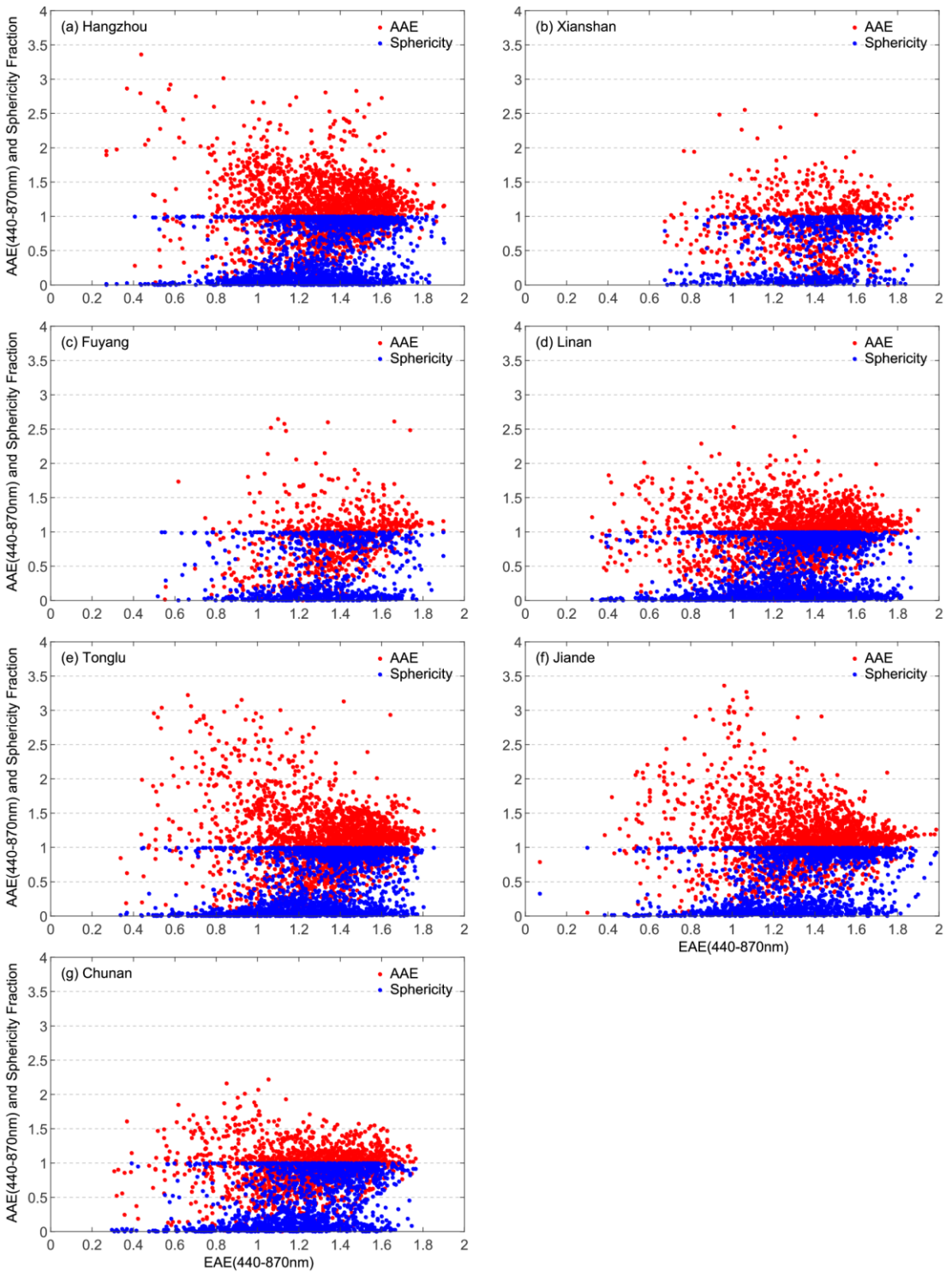
(a) Hangzhou
(b) Xianshan
(c) Fuyang
(d) Linan
(e) Tonglu
(f) Jiande
(g) Chunan
AAE
Sphericity
AAE(440-870nm) and Sphericity Fraction
EAE(440-870nm)

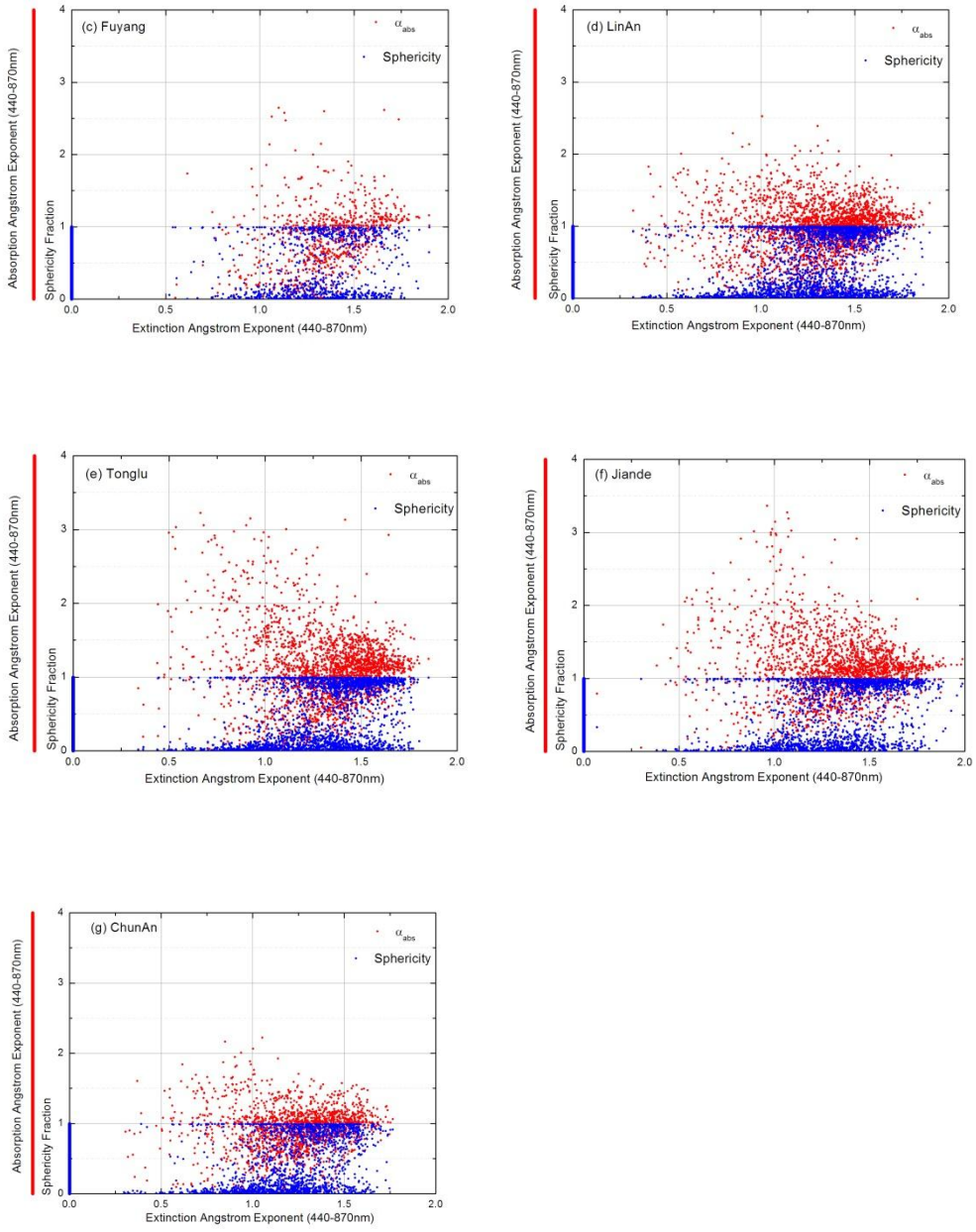

Fig.~~10~~16~~4~~.The AAE (red dot) and the sphericity fraction (blue dot) as a function of the EAE at 440–870 nm over (a) Hangzhou, (b) Xiaoshan, (c) Fuyang, (d), LinAn, (e) Tonglu, (f) Jiande and (g) ChunAn.

~~Table 2.Types of aerosol at the seven sites in the Yangtze River Delta.~~

~~Mostly~~	~~Mixed~~	~~Mostly~~	~~Organic~~	~~Mixed large~~	~~Mixed small~~

	dust (%)	black carbon and dust(%)	black carbon (%)	carbon (%)	particles (%)	particles (%)
Hangzhou	0.24	6.14	34.68	2.58	0.19	36.34
Xiaoshan	<0.01	2.93	27.00	0.80	<0.01	23.40
Fuyang	<0.01	1.21	19.51	1.10	<0.01	18.63
LinAn	<0.01	6.18	28.91	0.50	0.37	28.04
Tonglu	<0.01	4.92	34.26	3.55	0.18	33.33
Jiande	<0.01	6.71	40.04	3.23	0.26	35.28
ChunAn	<0.01	7.16	24.15	0.23	0.12	26.75

3.5 Aerosol optical properties of Aerosol aerosol radiative forcing at the Earth's surface and top of the atmosphere

Figures11and Figures 1715 and 18612 show the variations in ARF at the surface (ARF-BOA) and at the top of the atmosphere (ARF-TOA) at the urban, suburban and rural sites in the YRD region.

The annual ARF-BOA values for Hangzhou, Xiaoshan, Fuyang, LinAn, Tonglu, Jiande and ChunAn were about −93±44, −84±40, −80±40, −81±39, −79±39, −82±40 and −74±34W/m^2, respectively. The higher ARF-BOA values in Hangzhou indicate that there was high aerosol loading at this site, which scattered and absorbed more radiation and caused a significant cooling effect at the surface. The monthly value of the ARF-BOA in Hangzhou was higher in June (about −132±48 W/m^2) and September (about −106±48 W/m^2), which is consistent with the timing of burning biomass from crop residues. Ding et al. (2016) found that black carbon emitted from biomass burning can modify the meteorology of the planetary boundary layer and substantially decrease the surface heat flux. Hygroscopic grow that the same time enhances the aerosol optical extinction (Yan et al., 2009; Zhang et al., 2015); this was also an important factor in the large ARF-BOA values in June and September at the urban, suburban and rural sites in the YRD.

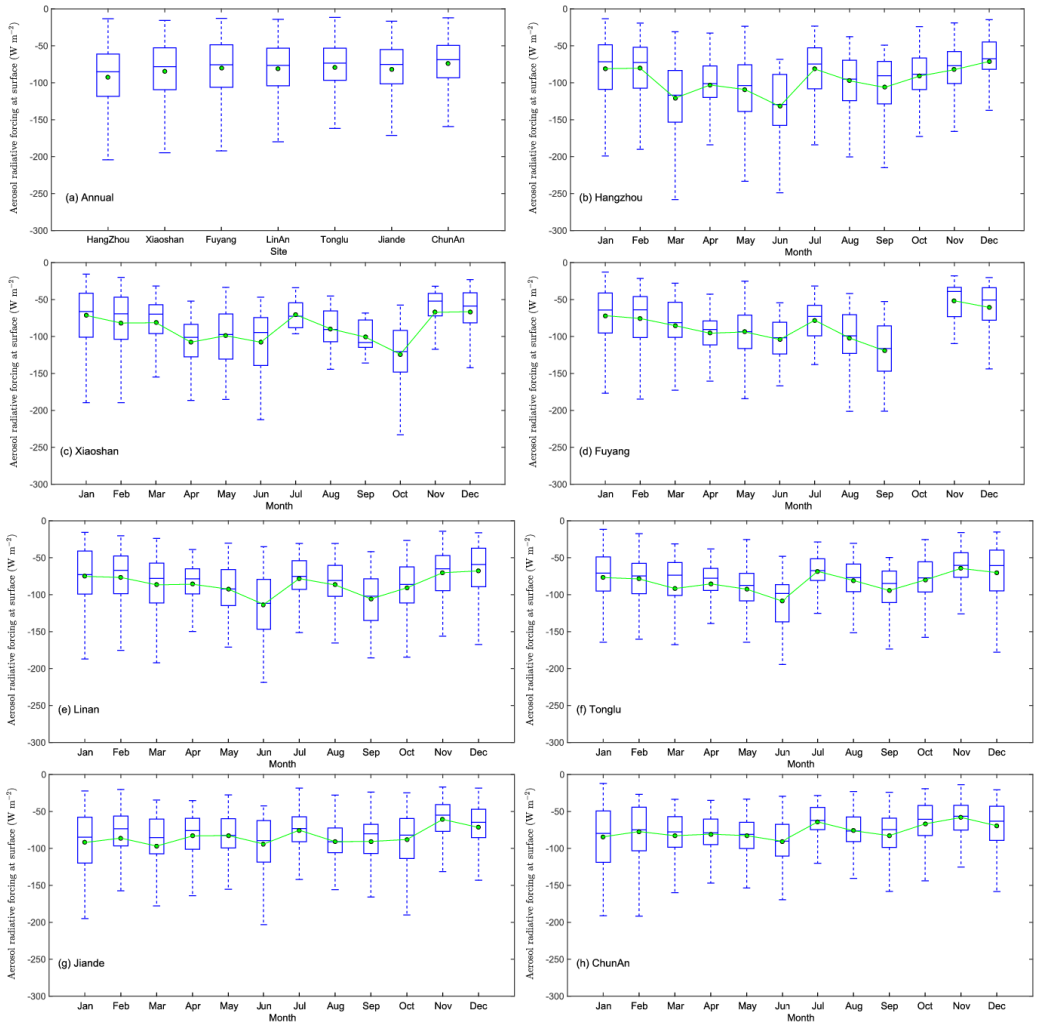

Fig.~~17~~15~~11~~.(a) Annual variation of the ARF at the surface over (b) Hangzhou, (c) Xiaoshan, (d) Fuyang, (e) LinAn, (f) Tonglu, (g) Jiande and (h) ChunAn. The boxes represent the 25th to 75th percentile distribution, while the dots and solid lines within each box represent the mean and median, respectively.

The ARF-TOA values were less than−40 W/m^2 at the urban, suburban and rural sites in the YRD. The AFR-TOA values were negative all year, which suggests that the aerosols caused a cooling effect at the TOA as well as at surface in the YRD. This is different from the north/northeast regions of China, where the instantaneous AFR-TOA value can be positive in the winter season as a result of the large surface reflectance ~~areareflecting~~on short wavelength radiation and heating caused by absorbing aerosols (Che et al., 2014). The surface albedo in the YRD region is lower than in north/northeast China as a result of better

vegetation. At the same time, there is also a low level of absorbing aerosol emissions in winter. This caused obvious negative AFR at the TOA at the urban, suburban and rural sites in the YRD.

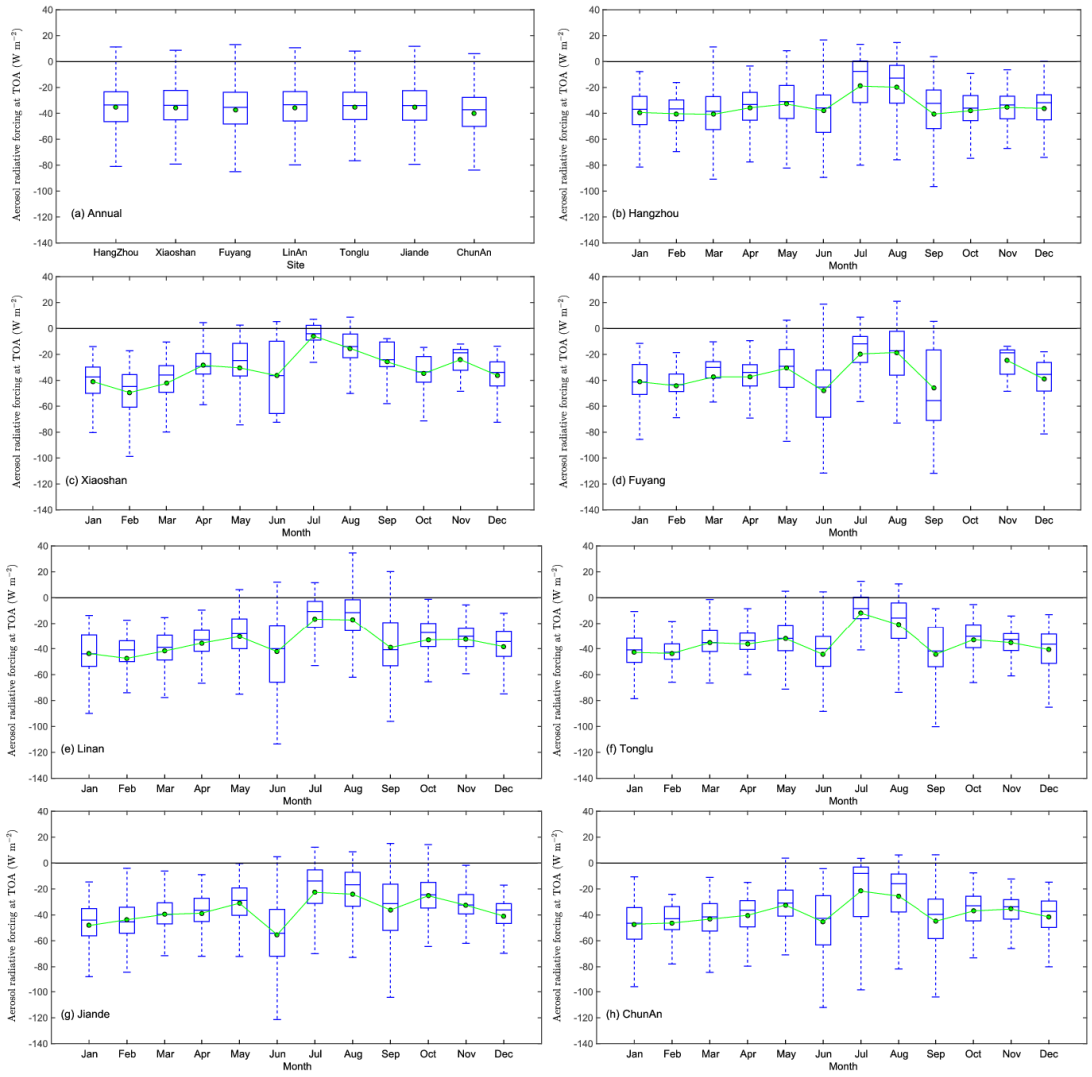

Fig.~~18~~16~~12~~. (a) Annual variation in the aerosol radiative forcing at the top of the atmosphere (TOA) in (b) Hangzhou, (c) Xiaoshan, (d) Fuyang, (e) LinAn, (f) Tonglu, (g) Jiande and (h) ChunAn. The boxes represent the 25th to 75th percentile distribution, while the dots and solid lines within each box represent the mean and median, respectively.

4. Discussion and Summary

In this paper, the aerosol optical properties, including the AOD, EAE,SSA, complex refractive index, volume size distribution, and the absorption properties of the AAOD and AAE

were retrieved from ground-based measurements data over the YRD in eastern China for the period 2011–2015. The AOD in Hangzhou in urban eastern China was similar to that in Shenyang (0.75) in urban northeast China (Zhao et al., 2013), and in Beijing (0.76) and Tianjin (0.74) in urban north China (Che et al., 2015b), indicating that the aerosol extinction is both common and at a similar level throughout most urban areas of China. The AOD values at the urban and suburban sites of Hangzhou were ~~a little bit higher~~slightly higher than at Pudong (0.70) and Hefei (0.69), other urban areas in eastern China, suggesting that higher aerosol extinction ability were observed here (He et al., 2012; Liu et al., 2017). However, the AOD at all seven sites was lower than that obtained at Wuhan (1.05), Nanjing (0.88), Dongtan (0.85), Taihu(0.77) and Xuzhou (0.92) in previous studies in eastern China (Wang et al., 2015; Li et al., 2015; Pan sphericity et al., 2010; Xia et al., 2007; Wu et al., 2016). This indicates that the aerosol loading caused by anthropogenic activities is very high in both urban and suburban areas in eastern China. The site at LinAn is regarded as the clean suburban site in eastern China with an average AOD about 0.73±0.44, which is higher than that at the other regional background stations of China, such as Longfengshan (0.35; northeastern China), Mt Waliguan (0.14, inland Asia), Xinglong (0.28, northern China), Akedala (0.20, northwestern China) and Shangri-La (0.11, southwestern China) (Wang et al., 2010; Che et al., 2011; Zhu et al., 2014; Che et al., 2015b). The aerosol loading in eastern China (especially in the YRD region) is at least twice as high as in other regions of China which indicate the strong aerosol extinction. Moreover, aerosol extinction ~~loading~~ was at a high level over both urban and suburban sites and even over the rural sites in the YRD which suggests large regional scale aerosol loading ~~extinction~~ over eastern China in recent years. ~~In this paper, t~~The ~~aerosol optical properties, including the AOD, EAE,SSA, complex refractive index, volume size distribution, and the absorption properties of the AAOD and AAE were retrieved from ground-based measurementssatellite data over the YRD in eastern China for the period 2011–2015.~~

~~Aerosol loading was at a high level over both urban and suburban sites and even over the rural sites in the YRD, which suggests that pollution from aerosolsis not justlocal, but has occurred at a regional scale aerosol extinction over eastern China in recent years. The AOD showed a decreasing trend from the east coast inland to the west as a result of contributions~~

from anthropogenicactivity. Hygroscopic growth and the burning of biomassfrom crop residuesin the summer season could cause this obvious increase in the AOD. The ratios of AOD_f/AOD_t fine mode fraction of AOD was(>0.90) and coarse mode fraction of AOD (~0.10) consistently >0.90, indicating that fine-mode particles made a major contribution to the total AOD in the YRD.Theas well as the relationship between the EAE and the spectral difference in the EAE suggested thatthe dominance of fine mode fraction to the AOD and the subordinate position of coarse mode fraction in the YRD. dustis not importantin eastern China. The validation results indicates a good Terra-MODIS matching with better fitting correlation at 3km rather than 10km products with the The MODIS C6 AOD retrievals performed better in suburban than in urban and rural areas, but were systematically over estimated in rural and urban areas and their immediate surroundings.A large part of the MODIS retrieval AOD was outside the expected error,especially atAOD values <0.80 in urban areasand their immediate surroundings.

The range of variationof the total, fine- and coarse-mode SSA at 440nmvalues was about 0.91–0.94, 0.93–0.95and 0.81–0.84, respectively, in the YRD region which ,suggesting the presence of mainly scattering aerosol particles in eastern China as a result of high industrial and anthropogenic activity. The fine- and coarse-mode particles showed significant scattering and absorptionin the urban, suburban and rural areas of the YRD region. The SSA of dust was weakly lower at short wavelength while the SSA of aerosol from biomass burning has the strong wavelength dependence in the longer wavelength. The imaginary part of the refractive index was larger aturban sitesas a result of the high loading of absorption aerosols.The large imaginary parts occurring in August may be due to the higher emission of absorptive particles from the post-harvest burning of biomass.

The similar AAOD levels at the seven sites indicated that absorbing aerosols were homogeneously distributed in the YRD region. The low AAODs in the winter season suggest fewer absorbing aerosol emissionsat the urban, suburban and rural sites. The difference in the distribution of the AAE suggests that the absorbing aerosols have different characteristics depending on the emission source.Hygroscopic growthnot only contributed to the high aerosol

~~extinction values, but also increasedthe size of the fine-mode particles in the summer in theYRD region.~~ The “mostly black carbon” category was the dominant contributor of absorbing aerosols at the urban, suburban and rural sites in the YRD region. The submicron “mixed small particle” category had a significant effect on the aerosol optical properties over the YRD region. The sphericity fraction showed a dispersed distribution of spherical particles, indicating a mixture of both fine- and coarse-mode particles from anthropogenic and natural sources.

The large ARF-BOA indicated a high aerosol loading that scattered and absorbed more radiation~~.It also showedthat~~ with the stronger ~~the~~ aerosol cooling effect ~~of the aerosols~~ at the surface ~~was stronger~~in the YRD region. Both the burning of biomass from crop residues and the hygroscopic growth of particles could make important contributions to the ARF-BOA in summer over the YRD region. The AFR-TOA values were negative all year ~~, suggesting that the aerosols had~~with ~~a~~an aerosol cooling effect at the TOA~~.~~ while the instantaneous positive in AFR-TOA value in the winter by the large surface reflectance of better vegetation has been found different from the north/northeast China.

The column aerosol optical properties over urban, suburban and rural areas of YRD region of China were investigated and the results will increase our understanding of the characteristics and sources of aerosol emissions over eastern China. Future research should consider the vertical distribution of aerosols by Lidar, the validation of the aerosol optical results of other satellite products such as VIIRS and GOCI, and a comprehensive analysis of the physical and chemical properties of aerosols and meteorological factors.

Acknowledgments

This work was supported by grant from National Key R & D Program Pilot Projects of China (2016YFA0601901), National Natural Science Foundation of China (41590874 &41375153), Natural Science Foundation of Zhejiang Province (LY16010006), the CAMS Basis Research Project (2016Z001 & 2014R17), the Climate Change Special Fund of CMA (CCSF201504), CAMS Basic Research Project (2014R17),the Special Project of Doctoral

Research supported by Liaoning Provincial Meteorological Bureau (D201501), Hangzhou Science and Technology Innovative project (20150533B17)and the European Union Seventh Framework Programme (FP7/2007-2013) under grant agreement no. 262254.

Reference

Ackerman, P., and Toon, O.B.: Absorption of visible radiation in atmosphere containing mixtures of absorbing and nonabsorbing particles, Appl. Opt., 20, 3661-3668, 1981.

Albrecht, B.: Aerosols, cloud microphysics, and fractional cloudiness, Science, 245, 1227-1230, 1989.

Arola, A., Schuster, G.,Myhre, G.,Kazadzis, S.,Dey, S., and Tripathi, S. N.: Inferring absorbing organic carbon content from AERONETdata, Atmos. Chem. Phys., 11, 215–225, doi:10.5194/acp-11-215-2011, 2011.

Bergstrom, R.W., Pilewskie, P., Russell, P.B., Redemann, J., Bond, T.C., Quinn, P.K., and Sierau, B.: Spectral absorption properties of atmospheric aerosols, Atmos. Chem. Phys., 7, 5937–5943, doi: 10.5194/ acp-7-5937-2007, 2007.

Charlson, R.J., Schwartz, S.E., Hales, J.M., Cess, D., Coakley, J.A., and Hansen, J.E.: Climate forcing by anthropogenic aerosols, Science, 255, 423–430, 1992.

Che, H.Z., Xia, X.A., Zhu, J., Wang, H., Wang, Y.Q., Sun, J.Y., Zhang, X.C., Zhang, X.Y., and Shi, G.Y.: Aerosol optical properties under the condition of heavy haze over an urban site of Beijing, China, Environ. Sci. Pollut. Res., 22, 1043–1053, 2015a.

Che, H. Z., Zhang, X. Y., Alfraro, S., Chatenet, B., Gomes, L., and Zhao, J. Q.: Aerosol optical properties and its radiative forcing over Yulin, China in 2001 and 2002, Adv. Atmos. Sci., 26, 564–576, doi:10.1007/s00376-009-0564-4, 2009b.

Che, H., Zhang, X., Chen, H., Damiri, B., Goloub, P., Li, Z., Zhang, X., Wei, Y., Zhou, H., Dong, F., Li, D., and Zhou, T.: Instrument calibration and aerosol optical depth (AOD) validation of the China Aerosol Remote Sensing Network (CARSNET), J. Geophys. Res., 114, doi: org/10.1029/2008JD011030, 2009a.

Che, H., Yang, Z., Zhang, X., Zhu, C., Ma, Q., Zhou, H., and Wang, P.: Study on the aerosol optical properties and their relationship with aerosol chemical compositions over three regional background stations in China, Atmos. Environ., 43, 1093–1099,

doi:10.1016/j.atmosenv.2008.11.010, 2009c.

Che, H., Wang, Y., Sun, J., and Zhang, X.: Assessment of In-situ Langley Calibration of CE-318 Sunphotometer Mt. Waliguan Observatory, China, SOLA, 7, 089-092, doi: 10.2151/sola.2011-023, 2011

Che, H., Wang, Y., and Sun, J.: Aerosol optical properties at Mt.Waliguan observatory, China, Atmos. Environ., 45, 6004–6009, 2011.

Che, H.Z., Zhang, X.Y., Xia, X.A., Goloub, P., Holben, B., Zhao, H., Wang, Y., Zhang, X.C., Wang, H., and Blarel, L. et al.: Ground-based aerosol climatology of China: Aerosol optical depths from the China Aerosol Remote Sensing Network (CARSNET) 2002–2013, Atmos. Chem. Phys., 15, 7619–7652, 2015b.

Che, H.Z., Zhao, H.J., Xia, X.A., Wu, Y.F., Zhu, J., Ma, Y.J., Wang, Y.F., Wang, H., Wang, Y.Q., Zhang, X.Y., and Shi, G.Y.: Fine Mode Aerosol Optical Properties Related to Cloud and Fog Processing over a Cluster of Cities in Northeast China, Aerosol. Air. Quality Research., 15, 2065–2081, 2015c.

Che, H.Z., Xia, X.A., Zhu, J., Wang, H., Wang, Y.Q., Sun, J.Y., Zhang, X.C., Zhang, X.Y., and Shi, G.Y.: Aerosol optical properties under the condition of heavy haze over anurban site of Beijing, China, Environ. Sci. Pollut. Res.,http://dx.doi.org/10.1007/s11356-014-3415-5, 2014.

Cheng, T., Liu, Y., Lu, D., Xu, Y., Li, H.,2006. Aerosol properties and radiative forcing in Hunshan Dake desert, northern China, Atmospheric Environment, 40, 2169-2179.

Cheng, T.T., Xu, C., Duan, J.Y., Wang, Y.F., Leng, C.P., Tao, J., Che, H.Z., He, Q.S., Wu, Y.F., Zhang, R.J., Li, X., Chen, J.M., Kong, L.D., and Yu, X.N.: Seasonal variation and difference of aerosol optical properties in columnar and surface atmospheres over Shanghai, Atmos. Environ., 123, 315-326, 2015.

Chu, D.A., Kaufman, Y.J., Ichoku, C.: Validation of MODIS aerosol optical depth retrieval over land, Geophysics Research Letters, 29 (12), 8007, 2002.

Ding, A. J., Fu, C. B., Yang, X. Q., Sun, J. N., Zheng, L. F., Xie, Y. N., Herrmann, E., Nie, W., Petäjä, T., Kerminen, V.-M., and Kulmala, M.: Ozone and fine particle in the western Yangtze River Delta: an overview of 1 yr data at the SORPES station, Atmos. Chem. Phys., 13, 5813–5830, doi:10.5194/acp-13-5813-2013, 2013a.

948 Ding, A. J., Fu, C. B., Yang, X. Q., Sun, J. N., Petäjä, T., Kerminen, V.-M., Wang, T., Xie, Y.,
949 Herrmann, E., Zheng, L. F., Nie, W., Liu, Q., Wei, X. L., and Kulmala, M.: Intense
950 atmospheric pollution modifies weather: a case of mixed biomass burning with fossil fuel
951 combustion pollution in eastern China, Atmos. Chem. Phys., 13, 10545-10554,
952 doi:10.5194/acp-13-10545-2013, 2013b.
953 Ding, A. J., Huang, X., Nie, W., Sun, J. N., Kerminen, V.M., Petäjä, T., Su, H., Cheng, Y. F.,
954 Yang, X.Q., and Wang, M.H. et al.: Enhanced haze pollution by black carbon in megacities
955 in China, Geophys. Res. Lett., 43, 2873–2879, doi: 10.1002/2016GL067745, 2016.
956 Duan, J., Mao, J.: Study on the distribution and variation trends of atmospheric aerosol optical
957 depth over the Yangtze River Delta, Acta Scientiae Circumstantiae, 27 (4), 537-543, 2007.
958 Dubovik, O., Holben, B.N., Eck, T.F., Smirnov, A., Kaufman, Y.J., King, M.D., Tanre, D.,
959 Slutsker, I.: Variability of absorption and optical properties of key aerosol types observed
960 in worldwide locations, J. Atmos. Sci., 59, 590–608, 2002.
961 Dubovik, O., King, M.D.: A flexible inversion algorithm for retrieval of aerosol optical properties
962 from Sun and sky radiance measurements, J. Geophys. Res., 105 (D16), 20673, 2000.
963 Dubovik, O., Sinyuk, A., Lapyonok, T., Holben, B.N., Mishchenko, M., Yang, P., Eck, T.F.,
964 Volten, H., Munoz, O., Veihelmann, B., van der Zande, W.J., Leon, J.F., Sorokin, M., and
965 Slutsker, I.: Application of spheroid models to account for aerosol particle
966 nonsphericitysphericity in remote sensing of desert dust, J. Geophys. Res.-Atmos., 111
967 (D11), 2006.
968 Dubuisson, P., Buriez, J.C., and Fouquart, Y.: High spectral resolution solar radiative transfer
969 in absorbing and scattering media, application to the satellite simulations, J. Quant.
970 Spectrosc. Radiat.Transf., 55, 103–126, 1996.
971 Dubuisson, P., Roger, J.C., Mallet, M., and Dubovik, O.: A code to compute the direct solar
972 radiative forcing: application to anthropogenic aerosols during the ESCOMPTE
973 experiment. In: Fischer, H. (Ed.), Proceedings of the International Radiation Symposium:
974 Current Problems in Atmospheric Radiation. A. Deepak Publishing, Busan, Korea, 2006.
975 Eck, T.F., Holben, B.N., Dubovik, O., Smirnov, A., Goloub, P., Chen, H.B., Chatenet, B., Gomes,
976 L., Zhang, X.Y., and Tsay, S.C. et al.: Columnar aerosol optical properties at AERONET
977 sites in central eastern Asia and aerosol transport to the tropical Mid-Pacific, J. Geophys.

978 Res., 110, 2005.
979 Eck, T.F., Holben, B.N., Reid, J.S., Giles, D.M., Rivas, M.A., Singh, R.P., Tripathi, S.N.,
980 Bruegge, C.J., Platnick, S., Arnold, G.T., Krotkov, N.A., Carn, S.A., Sinyuk, A., Dubovik, O.,
981 Arola, A., Schafer, J.S., Artaxo, P., Smirnov, A., Chen, H. and Goloub, P.: Fog- and
982 Cloudinduced Aerosol Modification Observed by the Aerosol Robotic Network
983 (AERONET), J. Geophys. Res., 117, 2012. D07206, doi: 10.1029/2011JD016839.
984 Eck, T. F., Holben, B. N., Sinyuk, A., Pinker, R. T., Goloub, P., Chen, H., Chatenet, B., Li, Z.,
985 Singh, R. P., and Tripathi, S. N.: Climatological aspects of the optical properties of
986 fine/coarse mode aerosol mixtures, Journal of Geophysical Research: Atmospheres
987 (1984–2012), 115, 19205, 2010.
988 Estellés, V., Campanelli, M., Utrillas, M. P., Expósito, F., and Martínezlozano, J. A.:
989 Comparison of AERONET and SKYRAD4.2 inversion products retrieved from a Cimel
990 CE318 sunphotometer, Atmospheric Measurement Techniques, 4, 569-579, 2012.
991 Fu, Q., Zhuang, G., Wang, J., Xu, C., Huang, K., Li, J., Hou, B., Lu, T., and Streets, D. G.:
992 Mechanism of formation of the heaviest pollution episode ever recorded in the Yangtze
993 River Delta, China, Atmospheric Environment, 42, 2023-2036, 2008.
994 García, O. E., Díaz, J. P., Expósito, F. J., Díaz, A. M., Dubovik, O., and Derimian, Y.: Aerosol
995 Radiative Forcing: AERONET Based Estimates, Climate Models, edited by: Druyan, L.,
996 ISBN: 978-953-51-0135-2, InTech, 2012.
997 Giles, D. M., Holben, B. N., Tripathi, S. N., Eck, T. F., Newcomb, W. W., Slutsker, I., Dickerson,
998 R. R., Thompson, A. M., Mattoo, S., and Wang, S. H.: Aerosol properties over the
999 Indo-Gangetic Plain: A mesoscale perspective from the TIGERZ experiment, Journal of
1000 Geophysical Research Atmospheres, 116, 10--1029, 2011.
1001 Giles, D. M., Holben, B. N., Eck, T. F., Sinyuk, A., Smirnov, A., Slutsker, I., Dickerson, R. R.,
1002 Thompson, A. M., and Schafer, J. S.: An analysis of AERONET aerosol absorption
1003 properties and classifications representative of aerosol source regions, Journal of
1004 Geophysical Research Atmospheres, 117, 127-135, 2012.
1005 Gobbi, G. P., Kaufman, Y. J., Koren, I., and Eck, T. F.: Classification of aerosol properties
1006 derived from AERONET direct sun data, Atmospheric Chemistry & Physics, 6, 8713-8726,
1007 2007.

1008 Goloub, P., Li, Z., Dubovik, O., Blarel, L., Podvin, T., Jankowiak, I., Lecoq, R., Deroo, C.,
1009 Chatenet, B., and Morel, J. P.: PHOTONS/AERONET sunphotometer network overview:
1010 description, activities, results, Fourteenth International Symposium on Atmospheric and
1011 Ocean Optics/Atmospheric Physics, 69360V-69360V-69315, 2007.
1012 Gong, S.L., Zhang, X.Y., Zhao, T.L., Mckendry, I.G., Jaffe, D.A., and Lu, N.M.: Characterization
1013 of soil dust aerosol in China and its transport/distribution during 2001 ACEAsia, 2. Model
1014 simulation and validation, J. Geophys. Res., 108,
1015 4262.http://dx.doi.org/10.1029/2002JD002633, 2003.
1016 Gyawali, M., Arnott, W. P., Lewis, K., and Moosmüller, H.: In situ aerosol optics in Reno, NV,
1017 USA during and after the summer 2008 California wildfires and the influence of absorbing
1018 and non-absorbing organic coatings on spectral light absorption, Atmospheric Chemistry
1019 & Physics, 9, 8007-8015, 2009.
1020 Hansen, J., Sato, M., Ruedy, R., Lacis, A., and Oinas, V.: Global warming in the twenty-first
1021 century: an alternative scenario, Proceedings of the National Academy of Sciences of the
1022 United States of America, 97, 9875-9880, 2000.
1023 He, Q., Li, C., Geng, F., Yang, H., Li, P., Li, T., Liu, D., and Pei, Z.: Aerosol optical properties
1024 retrieved from Sun photometer measurements over Shanghai, China, Journal of
1025 Geophysical Research Atmospheres, 117, 81-81, 2012.
1026 Holben, B. N., Eck, T. F., Slutsker, I., Tanré, D., Buis, J. P., Setzer, A., Vermote, E., Reagan, J.
1027 A., Kaufman, Y. J., Nakajima, T., Lavenu, F., Jankowiak, I., and Smirnov, A.:
1028 AERONET—A Federated Instrument Network and Data Archive for Aerosol
1029 Characterization, Remote Sensing of Environment, 66, 1-16,
1030 https://doi.org/10.1016/S0034-4257(98)00031-5, 1998.
1031 Holben, B. N., Tanré, D., Smirnov, A., Eck, T. F., Slutsker, I., Abuhassan, N., Newcomb, W. W.,
1032 Schafer, J. S., Chatenet, B., and Lavenu, F.: An emerging ground-based aerosol
1033 climatology: Aerosol optical depth from AERONET, Journal of Geophysical Research
1034 Atmospheres, 106, 12067–12097, 2001.
1035 Holben, B. N., Kim, J., Sano, I., Mukai, S., Eck, T. F., Giles, D. M., Schafer, J. S., Sinyuk, A.,
1036 Slutsker, I., Smirnov, A., Sorokin, M., Anderson, B. E., Che, H., Choi, M., Crawford, J. E.,
1037 Ferrare, R. A., Garay, M. J., Jeong, U., Kim, M., Kim, W., Knox, N., Li, Z., Lim, H. S., Liu,

1038 Y., Maring, H., Nakata, M., Pickering, K. E., Piketh, S., Redemenn, J., Reid, J. S., Salinas,
1039 S., Seo, S., Tan, F., Tripathi, S. N., Toon, O. B., and Xiao, Q.: An overview of meso-scale
1040 aerosol processes, comparison and validation studies from DRAGON networks, Atmos.
1041 Chem. Phys. Discuss., https://doi.org/10.5194/acp-2016-1182, in review, 2017.
1042 Huang, X., Ding, A., Liu, L., Liu, Q., Ding, K., Niu, X., Nie, W., Xu, Z., Chi, X., Wang, M., Sun, J.,
1043 Guo, W., and Fu, C.: Effects of aerosol–radiation interaction on precipitation during
1044 biomass-burning season in East China, Atmos. Chem. Phys., 16, 10063-10082,
1045 doi:10.5194/acp-16-10063-2016, 2016.
1046 Hsu, N. C., Jeong, M. J., Bettenhausen, C., Sayer, A. M., Hansell, R., Seftor, C. S., Huang, J.,
1047 and Tsay, S. C.: Enhanced Deep Blue aerosol retrieval algorithm: The second generation,
1048 Journal of Geophysical Research-atmospheres, 118, 9296-9315, 2013.
1049 Ichoku, C., Chu, D. A., Mattoo, S., Kaufman, Y. J., Remer, L. A., Tanré, D., Slutsker, I., and
1050 Holben, B. N.: A spatio‐temporal approach for global validation and analysis of MODIS
1051 aerosol products, Geophysical Research Letters, 29, MOD1-1–MOD1-4, 2002.
1052 Intergovernmental Panel on Climate Change (IPCC).Climate Change 2013. The Scientific
1053 Basis; Cambridge University Press: New York, NY, USA, 2013.
1054 Kaufman, Y. J., Tanré, D., and Boucher, O. A.: satellite view of aerosols in the climate system,
1055 nature, 419, 215–223, 2002.
1056 Kaufman, Y.J., Tanré, D., Remer, L.A., Vermote, E., Chu, A., and Holben, B.N.: Operational
1057 remote sensing of tropospheric aerosol over land from EOS moderate resolution imaging
1058 spectroradiometer, J. Geophys. Res., 102, 17051-17067, 1997.
1059 Kong, S.F., Ji, Y.Q., Lu, B., Chen, L., Han, B., Li, Z.Y., and Bai, Z.P.: Characterization of
1060 PM10source profiles for fugitive dust in Fushun—a city famous for coal, Atmos. Environ.,
1061 45,5351–5365, 2011.
1062 Lack, D. A., and Cappa, C. D.: Impact of brown and clear carbon on light absorption
1063 enhancement, single scatter albedo and absorption wavelength dependence of black
1064 carbon, Atmos. Chem. Phys., 10(9), 4207-4220, 2010.
1065 Lee, K. H., Li, Z., Cribb, M. C., Liu, J., Wang, L., Zheng, Y., Xia, X., Chen, H., and Li, B.:
1066 Aerosol optical depth measurements in eastern China and a new calibration method, J.
1067 Geophys. Res., 115, 4038-4044, doi: 10.1029/2009JD012812, 2010.

Levy, R.C., Remer, L.A., Kleidman, R.G., Mattoo, S., Ichoku, C., Kahn, R., and Eck, T.F.: Global evaluation of the collection 5 MODIS dark-target aerosol products over land, Atmos. Chem. Phys., 10, 10399-10420, 2010.

Levy, R. C., S. Mattoo, L. A. Munchak, L. A. Remer, A. M. Sayer, F. Patadia, and Hsu, N. C.: The Collection 6 MODIS aerosol products over land and ocean, Atmos. Meas. Tech., 6(11), 2989–3034, 2013.

Li S., Wang T., Xie M., Han Y., and Zhuang B.: Observed aerosol optical depth and angstrom exponent in urban area of Nanjing, China, Atmos. Environ., 123, 350–356, 2015.

Li, W.J., Shao, L.Y., and Buseck, P.R.: Haze types in Beijing and the influence of agriculturalbiomass burning, Atmos. Chem. Phys. 10, 8119–8130, 2010.

Li, W., Li, P., Sun, G., Zhou, S., Yuan, Q. and Wang, W.: Cloud Residues and Interstitial Aerosols from Non-precipitating Clouds over an Industrial and Urban Area in Northern China, Atmos. Environ., 45, 2488–2495, doi: 10.1016/j.atmosenv.2011.02.044, 2011.

Li, W.J., Sun, J.X., Xu, L., Shi, Z.B., Riemer, N., Sun, Y.L., Fu, P.Q., Zhang, J.C., Lin, Y.T., Wang, X.F., Shao, L.Y., Chen, J.M., Zhang, X.Y., Wang, Z. F. and Wang, W.X.: A conceptual framework for mixing structures in individual aerosol particles, J. Geophys. Res., 121, 13205-13798, doi:10.1002/2016JD025252, 2016.

Li, Z., Niu, F., Lee, K., and Xin, J.: Validation and understanding of moderate resolution imaging spectroradiometer aerosol products (C5) using ground-based measurements from the handheld sun photometer network in China, J. Geophys. Res., 112,1-6, 2007.

Li, Z.Q., Eck,T., Zhang, Y., Zhang, Y.H., Li, D.H., Li, L., Xu, H., Hou, W.Z., Lv, Y., Goloub, P. and Gu, X.F.: Observations of Residual Submicron Fine Aerosol Particles Related to Cloud and Fog Processing during a Major Pollution Event in Beijing, Atmos. Environ., 86, 187–192, 2014.

Li Z., Lau, W.K.-M., Ramanathan,V., Wu,G., Ding,Y., Manoj,M.G., Liu,J., Qian,Y., Li,J., Zhou,T., Fan,J., Rosenfeld,D., Ming,Y., Wang,Y., Huang,J., Wang,B., Xu,X., Lee,S.-S., Cribb,M., Zhang,F., Yang,X.,Takemura, Wang,K., Xia,X., Yin,Y., Zhang,H.,Guo,J.,Zhai,P.M., Sugimoto,N.,Babu,S. S., and Brasseur,G.P.: Aerosol and Monsoon Climate Interactions over Asia, Rev. Geophys., doi:10.1002/2015RG000500, 2016.

Liu, Q.,Ding, W.D.,Xie, L.,Zhang, J.Q.,Zhu, J.,Xia, X.A.,Liu, D.Y.,Yuan, R.M., and Fu, Y.F.:

1098 AerosolpropertiesoveranurbansiteincentralEastChinaderivedfromgroundsun-photometer
1099 measurements, ScienceChinaEarthSciences,60, 297–314,doi:
1100 10.1007/s11430-016-0104-3, 2017.
1101 Lyapustin, A., Wang, Y., Xiong, X., Meister, G., Platnick, S., Levy, R., Franz, B., Korkin, S.,
1102 Hilker, T., Tucker, J., Hall, F., Sellers, P., Wu, A., and Angal, A.: Scientific impact of MODIS
1103 C5 calibration degradation and C6+ improvements, Atmos. Meas. Tech., 7(12), 4353–
1104 4365, 2014.
1105 Mishra, A.K., and Shibata, T.: Synergistic analyses of optical and microphysical propertiesof
1106 agricultural crop residue burning aerosols over the Indo-Gangetic Basin (IGB), Atmos.
1107 Environ., 57, 205–218, 2012.
1108 Myhre, G.: Consistency between satellite-derived and modeled estimates of the direct aerosol
1109 effect, Science, 325, 187–190, 2009
1110 Pan, L., Che, H., Geng, F., Xia, X., Wang, Y., Zhu, C., Chen,M., Gao,W., and Guo, J.: Aerosol
1111 optical properties based on ground measurements over the Chinese Yangtze Delta
1112 Region, Atmos. Environ., 44(21), 2587-2596, 2010.
1113 Panicker, A.S., Lee, D.I., Kumkar, Y.V., Kim, D., Maki, M., Uyeda, H.: Decadal climatological
1114 trends of aerosoloptical parameters over three different environments in South Korea., Int.
1115 J. Climatol., 33, 1909–1916, 2013.
1116 Pappalardo, G., Amodeo, A., Apituley, A., Comeron, A., Freudenthaler, V., Linné, H., Ansmann,
1117 A., Bösenberg, J., D'Amico, G., Mattis, I. Mona, L., Wandinger, U., Amiridis,V.,
1118 Alados-Arboledas, L., Nicolae, D., and Wiegner, W.: EARLINET: Towards an advanced
1119 sustainable Europeanaerosol Lidar network, Atmos. Meas. Tech., 7, 2389–2409, 2014.
1120 Remer, L.A., Kaufman, Y.J., Tanre, D., Mattoo, S., Chu, D.A., Martins, J.V., Li, R.R., Ichoku, C.,
1121 Levy, R.C., Kleidman, R.G., Eck, T.F., Vermote, E., and Holben, B.N.: The MODIS aerosol
1122 algorithm, products and validation, J. Atmos. Sci., 62, 947-973, 2005.
1123 Roger, J.-C., Mallet, M., Dubuisson, P., Cachier, H., Vermote, E., Dubovik, O., and Despiau, S.:
1124 A synergetic approach for estimating the local direct aerosol forcing:applications to an
1125 urban zone during the ESCOMPTE experiment, J. Geophys. Res., 111, D13208,
1126 http://dx.doi.org/10.1029/2005JD006361, 2006.
1127 Russell, P.B., Bergstrom, R.W., Shinozuka, Y., Clarke, A.D., DeCarlo, P.F., Jimenez, J.L.,

Livingston, J.M., Redemann, J., Dubovik, O., and Strawa, A.: Absorption Angstrom Exponent in AERONET and related data as an indicator of aerosol composition, Atmos.Chem. Phys., 10, 1155–1169, http://dx.doi.org/10.5194/acp-10-1155-2010, 2010.

Sanap, S.D., and Pandithurai, G.: Inter-annual variability of aerosols and its relationship with regional climate over Indian subcontinent, Int. J. Climatol., 35, 1041–1053, http://dx.doi.org/10.1002/joc.4037, 2014.

Schnaiter, M., Gimmler, M., Llamas, I., Linke, C., Jäger, C., and Mutschke, H.: Strong spectral dependence of light absorption by organic carbon particles formed by propanecombustion. Atmos. Chem. Phys. 6, 2981–2990, 2006.

Schwartz, S.E., and Andreae, M.O.: Uncertainty in climate change caused by aerosols, Science, 272, 1121–1122, 1996.

Shen X. J., Sun, J. Y., Zhang, X. Y., Zhang, Y. M., Zhang L., Che, H. C., Ma, Q. L., Yu, X. M., Yue, Y. and Zhang, Y. W.: Characterization of submicron aerosols and effect on visibility during a severe haze-fog episode in Yangtze River Delta, China, Atmospheric Environment, 120, 307-316, 2015.

Smirnov, A., Holben, B.N., Eck, T.F., Dubovik, O., and Slutsker, I.: Cloud screening and quality control algorithmsfor the AERONET data base, Remote Sens. Environ., 73, 337–349, 2000.

Sokolik, I. N., Toon, O. B.,1999. Incorporation of mineralogical composition into models of the radiative properties of mineral aerosol from UV to IR wavelengths, J. Geophys. Res., 104(D8), 9423-9444, doi:10.1029/ 1998JD200048.

Solomon, S., Qin, D., Manning, M., Chen, Z., Marquis, M., Averyt, K.B.,Tignor, M., Miller, and H.L.(Eds.): Climate change 2007: the physical science basis., Contribution of Working Group I to the FourthAssessment Report of the Intergovernmental Panel on Climate Change. Cambridge University Press, Cambridge, United Kingdom and New York, USA, 2007.

Soni, K., Singh, S., Bano, T., and Tanwar, R.S.: Variations in single scattering albedo and Angström absorption exponent during different seasons at Delhi, India. Atmos. Environ., 44, 4355-4363, 2010.

Takamura, T., and Nakajima, T.: Overview of SKYNET and its activities, Opt. Puray. Apl., 37,

3303–3308, 2004.

Tan, H., Wu, D., Deng, X., Bi, X., Li, F., and Deng, T.: Observation of aerosol optical depth over the Pearl River Delta, Acta Scientiae Circumstantiae., 29, 1146–1155, 2009 (in Chinese).

Tanré, D., Kaufman, Y.J., Herman, M., and Mattoo, S.: Remote sensing of aerosol properties over oceans using the MODIS/EOS spectral radiance, Journal of Geophysical Research., 102, 16971-16988, 1997.

Tao, M., Chen, L., Wang, Z., Tao, J., Che, H., Wang, X., and Wang Y.: Comparison and evaluation of the MODIS Collection 6 aerosol data in China, J. Geophys. Res. Atmos., 120, 6992–7005, doi:10.1002/2015JD023360, 2015.

Twomey, S.A., Piepgrass, M., and Wolfe, T.L.: An assessment of the impact of pollution on the global cloud Albedo, Tellus., 36B, 356-366, 1984.

Wang, L.C., Gong, W., Xia, X.A., Zhu, J., Li, J., and Zhu, Z.M.: Long-term observations of aerosol optical properties at Wuhan, an urban site in Central China, Atmos. Environ.,101, 94–102, 2015.

Wang, L.L., Xin, J., Wang, Y., Li, Z., Wang, P., Liu, G., and Wen, T.: Validation of MODIS aerosol products by CSHNET over China, Chinese Science Bulletin 52 (12), 1708-1718, 2007.

Wang, P., Che, H.Z., Zhang, X.C., Song, Q.L., Wang, Y.Q., Zhang, Z.H., Dai, X., and Yu, D.J.: Aerosol opticalproperties of regional background atmosphere in Northeast China, Atmos. Environ., 44, 4404–4412, 2010.

Wang, Z., Liu, D., Wang, Y., Wang, Z., and Shi, G.: Diurnal aerosol variations do affect daily averaged radiative forcing under heavy aerosol loading observed in Hefei, China, Atmos. Meas. Tech., 8, 2901, 2015.

Wehrli, C.: Calibration of filter radiometers for the GAW Aerosol Optical Depth network at Jungfraujoch and Mauna Loa. In: Proceedings of ARJ Workshop,SANW Congress, Davos, Switzerland, pp. 70-71,2002.

Wu, L.X.,Lü, X., Qin, K., Bai, Y., Li, J.L., Ren, C.B., and Zhang, Y.Y.: Analysis to Xuzhou aerosol optical characteristics with ground-based measurements by sun photometer (in Chinese), Chin Sci Bull, 61: 2287–2298, doi: 10.1360/N972015-00874, 2016.

Xia, X., Chen, H., Goloub, P., Zong, X., Zhang, W., and Wang, P.: Climatological aspects of

1188 aerosol opticalproperties in North China Plain based on ground and satellite
1189 remote-sensing data, J. Quant. Spectrosc.Radiat.Transf., 127, 12–23, 2013.
1190 Xia, X., Li, Z., Holben, B., Wang, P., Eck, T., Chen, H., Cribb, M., and Zhao, Y.: Aerosol
1191 optical properties and radiative effects in the Yangtze Delta region of China, J. Geophys.
1192 Res., 112, D22S12, doi:10.1029/2007JD008859, 2007.
1193 Xiao, Q., Zhang, H., Choi, M., Li, S., Kondragunta, S., Kim, J., Holben, B., Levy, R. C., and Liu,
1194 Y.: Evaluation of VIIRS, GOCI, and MODIS Collection 6 AOD retrievals against ground
1195 sunphotometer observations over East Asia, Atmos. Chem. Phys., 16, 1255-1269,
1196 doi:10.5194/acp-16-1255-2016, 2016.
1197 Xie, Y., Zhang, Y., Xiong, X.X, Qu, J.J., and Che, H.Z.: Validation of MODIS aerosol optical
1198 depth product over China using CARSNET measurements, Atmos. Environ., 45,
1199 5970-5978, 2011.
1200 Xin, J., Wang, Y., Li, Z., Wang, P., Hao, W., Nordgren, B., Wang, S., Liu, G., Wang, L., Wen, T.,
1201 Sun, Y., and Hu, B.: Aerosoloptical depth (AOD) and angstrom exponent of aerosols
1202 observed by the Chinese Sun Hazemeter Networkfrom August 2004 to September 2005,
1203 J. Geophys. Res., 112 (D05203), 2007.
1204 Xin, J.Y., Zhang, Q., Gong, C.S., Wang, Y.S., Du, W.P., and Zhao, Y.F.: Aerosol direct radiative
1205 forcing over Shandong Peninsula in East Asia from 2004 to 2011, Atmos. Ocean. Sci. Lett.,
1206 7, 74-79, 2014.
1207 Yan, P., Pan, X.L., Tang, J., Zhou, X.J., Zhang, R.J., and Zeng, L.M.: Hygroscopic growth
1208 ofaerosol scattering coefficient: a comparative analysis between urban and suburbansites
1209 at winter in Beijing, Particuology, 7, 52–60,2009.
1210 Yang, M., Howell, S.G., Zhuang, J., and Huebert, B.J.: Attribution of aerosol light absorption to
1211 black carbon, brown carbon, and dust in China – interpretations of atmospheric
1212 measurements during EAST-AIRE, Atmos. Chem. Phys., 9, 2035–2050,
1213 http://www.atmos-chem-phys.net/9/2035/2009/, doi:10.5194/acp-9-2035-2009, 2009.
1214 Zhang, L., Sun, J. Y., Shen, X. J., Zhang, Y. M., Che, H., Ma, Q. L., Zhang, Y. W., Zhang, X. Y.,
1215 and Ogren, J. A.: Observations of relative humidity effects on aerosol light scattering in the
1216 Yangtze River Delta of China, Atmos. Chem. Phys., 15, 8439-8454,
1217 doi:10.5194/acp-15-8439-2015, 2015.

1218 Zhang, Q., Streets, D., Carmichael, G., He, K., Huo, H., Kannari, A., Klimont, Z., Park, I.S.,
1219 Reddy, S., Fu, J., Chen, D., Duan, L., Lei, Y., Wang, L., and Yao, Z.L.: Asian emissions in
1220 2006 for the NASA INTEX-B mission, Atmos. Chem. Phys., 9,5131-5153,
1221 doi:10.5194/acp-9-5131-2009, 2009.
1222 Zhang, X., Wang, Y., Niu, T., Zhang, X., Gong, S., Zhang, Y., and Sun, J.: Atmospheric aerosol
1223 compositions in China: spatial/temporal variability, chemical signature, regional haze
1224 distribution and comparisons with global aerosols. Atmos. Chem. Phys., 12, 779–799,
1225 http://dx.doi.org/10.5194/acp-12-779-2012, 2012.
1226 Zhao, H., Che, H., Ma, Y., Xia, X., Wang, Y., Wang, P, and Wu, X.: Temporal variability of the
1227 visibility, particulate matter mass concentration and aerosol optical properties over an
1228 urban site in Northeast China. Atmos. Res., 166, 204-212, 2015.
1229 Zhao, H., Che, H., Zhang, X., Ma, Y., Wang, Y., Wang, X., Liu, C., Hou, B., and Che, H.:
1230 Aerosol optical properties over urban and industrial region of Northeast China by using
1231 ground-based sun-photometer measurement. Atmos. Environ., 75, 270–278, 2013.
1232 Zhu, J., Che, H., Xia, X., Chen, H.B, Goloub, P., and Zhang, W.: Column-integrated aerosol
1233 optical and physical properties at a regional background atmosphere in North China Plain.
1234 Atmos. Environ., 84,54–64, 2014.
1235 Zhuang, B., Wang, T., Li, S., Liu, J., Talbot, R., Mao, H., Yang, X., Fu, C., Yin, C., Zhu, J., Che,
1236 H., and Zhang, X.: Optical properties and radiative forcing of urban aerosols in Nanjing
1237 over China. Atmos. Environ., 83, 43–52, 2014.
1238
1239
1240